

INVESTIGATION OF FLOW CHARACTERISTICS OF REFRIGERANT IN  
CAPILLARY TUBES



by  
Hasan Kalkan

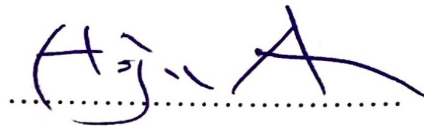
Submitted to Graduate School of Natural and Applied Sciences  
in Partial Fulfillment of the Requirements  
for the Degree of Master of Science in  
Mechanical Engineering

Yeditepe University  
2017

INVESTIGATION OF FLOW CHARACTERISTICS OF REFRIGERANT IN  
CAPILLARY TUBES

APPROVED BY:

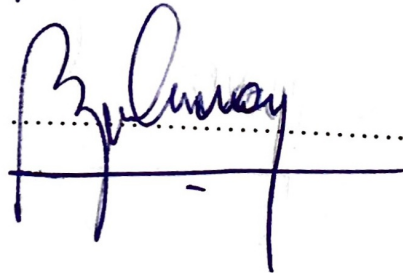
Prof. Dr. Hojin Ahn  
(Thesis Supervisor)



Assist. Prof. Dr. Ali Bahadır Olcay



Assist. Prof. Dr. Barış Yılmaz



DATE OF APPROVAL: ...../...../2017

## ACKNOWLEDGEMENTS

I would like to express my very great appreciation to my advisor Prof. Dr. Hojin Ahn. His sensible advices enable me to cope with critical points.

I would also thank to Ahmet Çağrı Develi and Can Polat Çıgay with their grateful help.

Also, I would like to thank to Yeditepe University and Department of Mechanical Engineering for education and opportunity to complete my master degree.

Lastly, I would like to thank to my family with their endless support.

## ABSTRACT

### INVESTIGATION OF FLOW CHARACTERISTICS OF REFRIGERANT IN CAPILLARY TUBES

Refrigerant flows through a capillary tube have been investigated both experimentally and numerically. A test setup is built for a vapor compression refrigeration cycle with condenser, evaporator, compressor and capillary tube. The capillary tube is 1.5 m in length and 1.3 mm in diameter, and R134a is used as the working fluid. In addition, a close-loop of air flow cycle is also built such that dry air flows through the evaporator and then through the condenser. Numerous thermocouples are located in both refrigeration and air cycles. Especially 25 thermocouples placed on the capillary tube measure the temperature change along the tube, which is aimed to provide the pressure distribution along the tube. The refrigerant flow rate was calculated in three methods: (1) using the compressor displacement volume with the volumetric efficiency, (2) energy balance over the condenser between refrigerant and air flows and (3) energy balance over the evaporator between refrigerant and air flows. The air flow rate is obtained by measuring pressure drop across the nozzle. Moreover, two numerical models are investigated. The first model does not consider metastable phenomena while the second model takes metastable regions into consideration. The discrepancy in flow rates between the two numerical models is 5 percent in general. Sensitivity studies using the second model show that the roughness of the capillary tube affects the refrigerant flow rate by 0.7 percent at most while the uncertainty of 0.01 mm in the capillary tube diameter results in 2 percent flowrate change. The comparison of the numerical models with the test results indicates that the second model appears more accurate than the first model.

## ÖZET

### KILCAL BORULARDAKİ SOĞUTKANIN AKIŞ KARAKTERİSTİĞİNİN İNCELENMESİ

Kılcal borudaki soğutucu akışkan deneysel ve sayısal olarak incelendi. İçerisinde yoğunlaştırıcı, buharlaştırıcı, kompresör ve kılcal boru barındıran test düzeneği kuruldu. İçerisinde soğutkan olarak R134a kullanılan kılcal boru 1.5 m uzunluğunda ve 1.3 mm çapındadır. Bu düzeneğe ek olarak havanın kapalı döngüde olduğu ve buharlaştırıcı ve yoğunlaştırıcı içerisinden geçen hava akış düzeneği kuruldu. Çok sayıda termokupl soğutma ve hava düzeneklerine yerleştirildi. Özellikle 25 tane termokupl, kılcal boru üzerindeki basınç dağılımını gözlemlemek için yerleştirildi. Soğutucu akışkan debisi üç farklı yöntemle hesaplandı: (1) volümetrik verim ile kompresör strok hacmi üzerinden, (2) yoğunlaştırıcı üzerindeki hava ve soğutkan arasındaki enerji korunumu üzerinden, ve (3) buharlaştırıcı üzerindeki hava ve soğutkan arasındaki enerji korunumu üzerinden. Havanın akış debisi lüle boyunca oluşan basınç düşüşünden hesaplandı. Bundan başka, iki tane sayısal model geliştirildi. İlk sayısal model akışkanın yarı kararlı davranışını göz önünde bulundurmazken ikinci sayısal model bulundurmaktadır. İki sayısal model arasındaki sonuçların farkı genel olarak yüzde beştir. İkinci sayısal model kullanılarak soğutucu akışkan debi üzerinde yapılan hassaslık incelemesi sonucu kılcal boru içerisindeki pürüzlüğün yüzde 0.7 etki ettiği ve kılcal boru çapındaki 0.01 mm'lik değişimin yüzde 2 etkilediği görülmüştür. İki sayısal model deneysel sonuçlarla karşılaştırıldığında ikinci sayısal modelin daha tutarlı olduğu sonuçlardan anlaşılmaktadır.

## TABLE OF CONTENTS

ACKNOWLEDGEMENTS.....	III
ABSTRACT.....	IV
ÖZET .....	V
LIST OF FIGURES .....	VIII
LIST OF TABLES.....	XII
1. INTRODUCTION.....	1
2. LITERATURE SURVEY .....	4
3. EXPERIMENTAL METHOD .....	6
3.1. AIR CYCLE AND SETUP .....	7
3.1.1. Flow Nozzle.....	9
3.1.2. Heaters .....	12
3.1.3. Pipes.....	13
3.1.4. Pressure Sensor .....	14
3.1.5. Fan .....	14
3.1.6. Energy Meter .....	15
3.2. VAPOR COMPRESSION REFRIGERATION CYCLE AND SETUP .....	16
3.2.1. Condenser .....	19
3.2.2. Evaporator.....	20
3.2.3. Compressor .....	21
3.2.4. Capillary Tube .....	22
3.2.5. Heater.....	25
4. NUMERICAL METHODS .....	27
4.1. NUMERICAL MODEL WITHOUT CONSIDERING METASTABLE PHENOMENON.....	28
4.2. NUMERICAL MODEL WITH CONSIDERING METASTABLE PHENOMENON.....	31
5. RESULTS AND DISCUSSION.....	34
5.1. EXPERIMENTAL RESULTS.....	34

5.2. NUMERICAL RESULTS.....	47
5.2.1. Numerical Model Without Considering Metastable Phenomenon .....	47
5.2.2. Numerical Model With Considering the Metastable Phenomenon .....	53
5.3. COMPARISION OF NUMERICAL AND EXPERIMENTAL METHODS.....	63
6. CONCLUSION .....	67
REFERENCES .....	69
APPENDIX A .....	71
APPENDIX B .....	92



## LIST OF FIGURES

Figure 1.1: Basic thermodynamic P-V cycle .....	1
Figure 1.2: Basic components of vapor compression refrigeration cycle.....	2
Figure 3.1: Air cycle system .....	8
Figure 3.2: Scheme of the whole system .....	8
Figure 3.3: Design parameters of flow nozzle according to ASME standarts.....	10
Figure 3.4: Flow measurement devices' pressure loses.....	10
Figure 3.5: 3D sketches of designed flow nozzle .....	11
Figure 3.6:ASME flow nozzle section standart .....	11
Figure 3.7: Resistance wire heater in between condenser and evaporator .....	12
Figure 3.8: PVC pipes and the system .....	13
Figure 3.9: Fan.....	14
Figure 3.10: Energy meter measured power vs error with respect to calculated power(kW) .....	15
Figure 3.11: Basic vapor compression refrigeration cycle and T-s diagram .....	16
Figure 3.12: Vapor compression refrigeration cycle .....	17



Figure 3.13: Scheme of the refrigerant cycle.....	18
Figure 3.14: Condenser.....	19
Figure 3.15: Evaporator.....	21
Figure 3.16: Compressor.....	22
Figure 3.17: Capillary Tube.....	23
Figure 3.18: Thermocoupled capillary tube.....	23
Figure 3.19: Thermocouple connection.....	24
Figure 3.20: Evaporator heater.....	25
Figure 3.21: Condenser heater.....	26
Figure 4.1: Capillary tube and flow phases.....	27
Figure 4.2: Flowchart of first numerical model.....	30
Figure 4.3: Flowchart of second numerical model.....	33
Figure 5.1: Condenser temperature distribution.....	35
Figure 5.2: Capillary tube temperature distribution.....	38
Figure 5.3: Evaporator Temperature Distribution.....	39
Figure 5.4: Mass flow rates versus pressure differences between the condenser and evaporator at given subcooling temperatures using three different methods.....	45

Figure 5.5: COP of experimental results .....	46
Figure 5.6: Mass flow rate vs pressure difference (inlet-exit) for the model without metastable condition .....	48
Figure 5.7: Pressure drops over capillary tube for different mass flowrates vs experimental results .....	50
Figure 5.8: Mass flowrate vs subcooling temperature for numerical model without consideration of metastable condition .....	52
Figure 5.9: Regions of second numerical model with metastable phenomena.....	54
Figure 5.10: Mass flowrates vs pressure differences for the model with metastable condition .....	55
Figure 5.11: Mass flowrates for diameter and roughness changes .....	57
Figure 5.12: Mass flowrates vs entrance pressure of numerical model with metastable condition .....	58
Figure 5.13: Mass flowrates of numerical model with and without consideration of metastable flow .....	60
Figure 5.14: Numerical models' pressure results .....	62
Figure 5.15: Mass flowrates comparison.....	63

Figure 5.16: Experimental and numerical pressure results ..... 64

Figure 5.17: Mixture quality calculation from two numerical models ..... 66



## LIST OF TABLES

Table 3.1: Thermocouple locations for air cycle .....	9
Table 3.2: Designed flow nozzle dimensions .....	10
Table 3.3: Thermocouple locations on condenser .....	20
Table 3.4: Thermocouple locations on evaporator .....	21
Table 3.5: Thermocouples locations on capillary tube .....	24
Table 5.1: Test conditions.....	34
Table 5.2: Condenser temperatures .....	34
Table 5.3: Subcooling temperatures .....	36
Table 5.4: Capillary tube temperatures I .....	36
Table 5.5: Capillary tube temperatures II .....	37
Table 5.6: Capillary tube temperatures III.....	37
Table 5.7: Evaporator temperatures .....	39
Table 5.8: Compressor temperatures .....	40
Table 5.9: Air temperatures I.....	40
Table 5.10: Air temperatures II.....	41

Table 5.11: Current differences of flow from flow nozzle .....	42
Table 5.12: Air cycle calculation results .....	42
Table 5.13: Enthalpy values at the evaporator .....	43
Table 5.14: Enthalpy values at the condenser .....	43
Table 5.15: Enthalpy values at the compressor .....	44
Table 5.16: Mass flow rates using three different methods .....	44
Table 5.17: Sensitivity study of thermocouples on mass flowrates .....	46
Table 5.18: Mass flow rate results of non-metastable model .....	48
Table 5.19: Capillary tube roughness affect on numerical model with non-metastable approach .....	51
Table 5.20: Capillary tube diameter affect on numerical model with non-metastable approach .....	52
Table 5.21: Mass flowrates from the model considers metastable condition .....	54
Table 5.22: Capillary tube roughness affect on mass flowrate .....	56
Table 5.23: Capillary tube diameter affect on mass flowrate .....	56
Table 5.24: Choking pressures of numerical model with metastable condition .....	59
Table 5.25: Mass flowrate results of numerical models .....	61

## LIST OF SYMBOLS/ABBREVIATIONS

COP	Coefficient of performance
d	Diameter of the capillary tube
D'	Reference length
d <sub>L</sub>	Differential tube length in numerical model
f	Friction factor
f,g,lm, ls	Liquid, gas, metastable liquid, metastable vapour
f <sub>r</sub>	Working frequency of compressor
G	Mass flowrate per area
h	Enthalpy
h <sub>L</sub>	Total head loss
I	Current
k	Boltzman constant
L	Length of the tube
N	Revolution per speed number of compressor
P	Pressure
Re	Reynolds number
s	Entropy
st, tp	Single phase, two phase
T	Temperature
T <sub>L</sub>	Total length of capillary tube
U	Capillary cross-sectional area
V	Mean velocity
V'	Volume displacement
x	Quality
y	Mass ratio of total saturated to total phase
z	Height
ΔP	Pressure drop
ρ	Density of the fluid
$\dot{m}$	Mass flowrate

$\dot{Q}$	Flowrate
$\varepsilon$	Roughness
$\mu$	Dynamic viscosity
$\sigma$	Surface tension
#	Test number



## 1. INTRODUCTION

Refrigeration, air-conditioning, or heating systems are used commonly in working or daily life and their importance is rapidly increasing day by day. Those systems are the example of thermodynamic cycles. Basically, in a thermodynamic cycle, series of thermodynamic processes as pressure and temperature change, heat rejections or injections occur due to heat removal or heat transfer to the system or from the system. An ideal cycle can be figured as below. Numbers represent the process direction of pressure and volume change through the cycle.

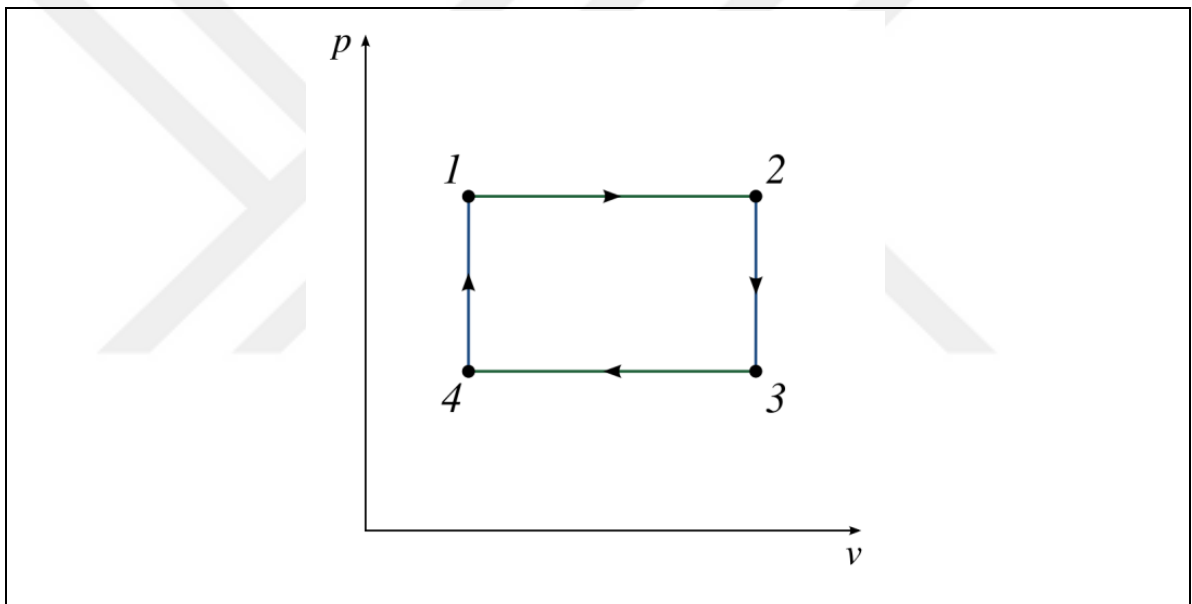


Figure 1.1: Basic thermodynamic P-V cycle

An ordinary vapor compression refrigeration cycle includes evaporator, condenser, compressor, and expansion valve. Each component has its unique importance in the cycle. Usually, condensers are used for heat rejection from system to outside air although evaporators are used for heat injection from a heat sink to system. Compressors provide necessary work to maintain the process in a cycle. Lastly, expansion valves control the pressure before evaporator.



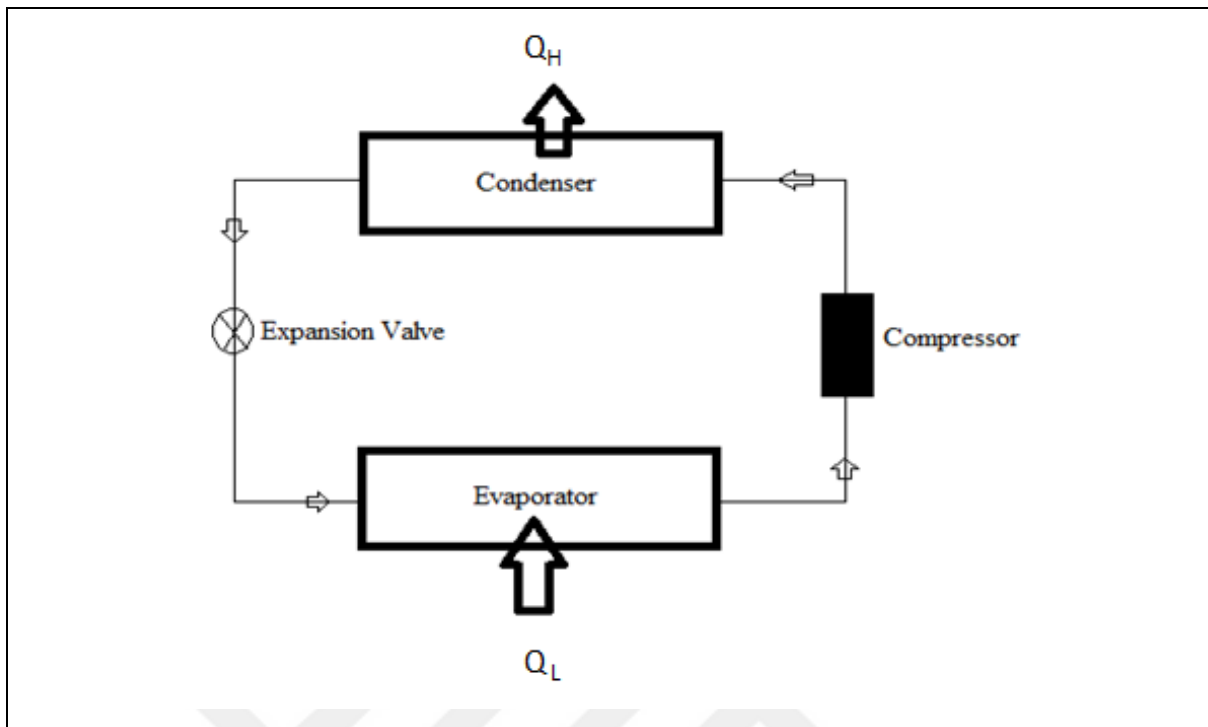


Figure 1.2: Basic components of vapor compression refrigeration cycle

The basic functions of an expansion device are to reduce pressure from condenser pressure to evaporator pressure, and to regulate the refrigerant flow from the high-pressure liquid into the evaporator. Capillary tube is one of the expansion devices. In capillary tubes, liquid flow from a condenser to evaporator, changes into two-phase flow due to rapid pressure drop. This situation may cause chocking at the exit of capillary tubes.

Flow in the capillary tube is indeed complicated. Flow characteristics can be affected by the diameter or length of the tube. Furthermore, the type of refrigerant used in the system can also have significant role in flow characteristics through the tube according to some researches[4],[7]. R134A and R404A are some examples of the fluid commonly used in the systems.

In the present study, a test setup is built to investigate characteristics of flow in the capillary tubes with given condenser and evaporator pressures and the degree of subcooling at the end of the condenser. The test setup includes a refrigerant cycle made of a compressor, a condenser, a capillary tube and an evaporator, and an air cycle with a fan and a nozzle flow meter. One capillary tube, 1.50 m in length and 1.3 mm in diameter, is employed.

In addition to the experimental study, two analytical models for flow through the capillary tube are developed. One of the models considers metastable phenomenon and the other does not. Since the metastable phenomenon delays vaporization, liquid can exist below the saturation pressure. Therefore, as subcooled liquid enters the tube from the exit of the condenser and pressure decreases along the tube and reaches the saturation pressure, liquid can stay as metastable liquid due to the vaporization delay. With further pressure decrease, some liquid changes into vapor, resulting in the mixture of metastable liquid and two-phase flow. Flow ultimately reaches the equilibrium two-phase flow of liquid-vapor mixture. The present study has employed the numerical model to examine the four regions of liquid, metastable liquid, the mixture of metastable liquid and two-phase flow, and the equilibrium two-phase flow.

## 2. LITERATURE SURVEY

There are numerous researches and journals about flow characteristics in capillary tube. Although, the flow in capillary tube is divided into two main regions, there are also some researches includes four regions in a detailed view in journals.

Somchai Wongwises and Worechet Pirompak[1] investigated refrigerant flow in two regions as liquid and gas phases in a adiabatic capillary tube. They developed a model to study flow in capillary tube with previous journals data. They take into account the acceleration term in their two-phase flow model although metastable flow is not considered. They claim that the model can be used in order to select a tube length and diameter of capillary tube or to find out mass flowrate from known tube sizes and conditions.

Zhou Guobing, Zhang Yufeng[2] investigated flow both experimental and numerically using the coiled adiabatic capillary tube, and they compared their results with those of straight capillary tubes. The model included metastable but did not consider the acceleration term in two-phase flow. They also used R134a as refrigerant and tried to find a correlation for mass flowrate with known initial pressure and temperature.

Subodh D. Deodhar, Hardik B. Kothadia, K.N. Iyer, S.V. Prabhu[3] investigated capillary tube both experimental and numerical for adiabatic and diabatic cases for R134a fluid. They used two straight and five helical coiled tube and investigated flow with visualization. They used an algorithm to predict mass flow rate, length and pressure drop beside experimental study.

S. G. Kim, M. S. Kim, S. T. Ro[4] used R22, R407C, R410A to develop dimensionless correlation for alternative fluids about the flow in capillary tubes. They developed a correlation to predict the mass flow rate with using capillary tubes in different length and diameter.

C.Melo, R.T.S Ferreira, C. Boabaid Neto, J.M. Goncalves, M. M. Mezavi[5] studied flow in capillary tube experimentally. They collected data for various capillary tubes in diameter and length and developed a correlation to predict mass flow rate.

V. Feburie, M. Gior, S. Granger, and J. M. Seynhaeve[6] developed a model to predict mass flowrate of the flow through cracks and they validated the model. The model takes into account metastable flow.

F.A.S. Fiorelli, C.A.S Silva, A.A.S Huerta[7] examined metastable flow of R410A in capillary tubes. They performed experimental study on the flow. They developed a correlation based on experimental data for predicting under pressure of vaporization. They also developed a capillary tube simulation model.

S. Chingulpitak, S. Wongwises[8] presented a numerical model to examine flow characteristics of refrigerant flow in helically coiled capillary tubes with the assumption of homogenous two-phase flow. They tried to develop a model that can be helpful for designing and optimizing capillary tubes with alternative refrigerants as working fluid.

M. K. Khan, R. Kumar, P. K. Sahoo[9] reviewed the journals and reviews about flow characteristics of refrigerant flows in capillary tubes to compare and sum up. The review includes diabatic and adiabatic cases, straight and coiled conditions and also with and without metastable conditions.

All of studies mentioned above differ from each other in their section of refrigerants, capillary tube length and diameters, and even how many regions flow is divided into. Each one tries to predict the exit pressure and mass flowrate through the tube with choking or without choking at the exit of the tube.

In the present study an experimental setup is built and temperature measurements are made at various locations with the purpose of calculating the mass flowrate of refrigerant and understanding the flow regimes. In addition, two numerical models are developed. The first model is similar to that of Somchai Wongwises and Worechet Pirompak[1] which includes the acceleration term in two-phase flow but does not consider the metastable phenomenon. The second model includes both the acceleration term and the metastable phenomenon. The results of two models are compared with each other and also with experimental results.

### 3. EXPERIMENTAL METHOD

Heat pumps or vapor compression refrigeration cycles are the main examples of thermodynamic cycles and they differ from each other by their usage. If the aim is to heat a space, system can be designed as heat pump cycle, however for cooling intentions the cycle can be designed as vapor compression refrigeration cycle. Both cycles have identical principles and same components as evaporator, condenser, compressor and expansion valve for their use reasons. In both cycles process is the same, heat is moved from a cold sink to heat sink.

Main process in the vapor compression refrigeration cycle basically is, compressed fluid heats the environment while the fluid loses its heat through condenser and moves from compressor to capillary tube. In capillary tube the pressure of fluid is decreased when the fluid reaches from condenser to evaporator. In evaporator, the fluid evaporates due to the heat transfer from environment so that phase of the fluid changes to gas. Finally, the fluid goes back to compressor and the cycle is completed.

Present test setup includes two main nested parts. One system is built for air cycle and another system is built for vapor compression refrigeration cycle. In order to cycle work, there is heat transfer from air to system and also from system to air through condenser and evaporator.

### 3.1. AIR CYCLE AND SETUP

In order to analyze the system, how a condenser and an evaporator works needs to be known. Heat transfer and rejection,  $Q_L$  and  $Q_H$ , can be obtained with temperature differences between air entrance and air exit points of evaporator and condenser from equation 3.1 and 3.2.

$$Q_H = \dot{m}_a c \Delta T = \dot{m}_a c (T_{air,cond,exit} - T_{air,cond,ent}) \quad (3.1)$$

$$Q_L = \dot{m}_a c \Delta T = \dot{m}_a c (T_{air,evap,exit} - T_{air,evap,ent}) \quad (3.2)$$

One more step needs to be calculated before finding heat injection and heat rejection, measuring flowrate which can be tricky and need to be measured carefully. For this purpose, the device to measure flowrate need to be accurate and well chosen. Flow nozzle is used to measure flowrate of air. A pressure transducer is used to obtain pressure change between two points anywhere through a tube or pipe.

Pressure transducer just gives the ampere difference between the points that it needs to be converted to pressure:

$$\Delta P = \frac{I - I_o}{Range(I)} \times Sensor\ Range(Pa) \quad (3.3)$$

Where  $I_o$  is the current reading when there is no flow,  $I$  is the current when there is flow.

Lastly air flowrate can be found with known pressure difference:

$$\dot{Q} = C_n \times A_n \times \sqrt{\frac{2\Delta P}{\rho(1 - \beta^4)}} \quad (3.4)$$

Where  $C_n$  is taken as 0.98,  $A_n$  is the area of nozzle with smaller face, and  $\rho$  is the density of air.

$$\dot{m} = \dot{Q} \times \rho \quad (3.5)$$

Mass flowrate is known. After obtaining entrance and exit temperatures of condenser and evaporator, the work on condenser and evaporator can be calculated.

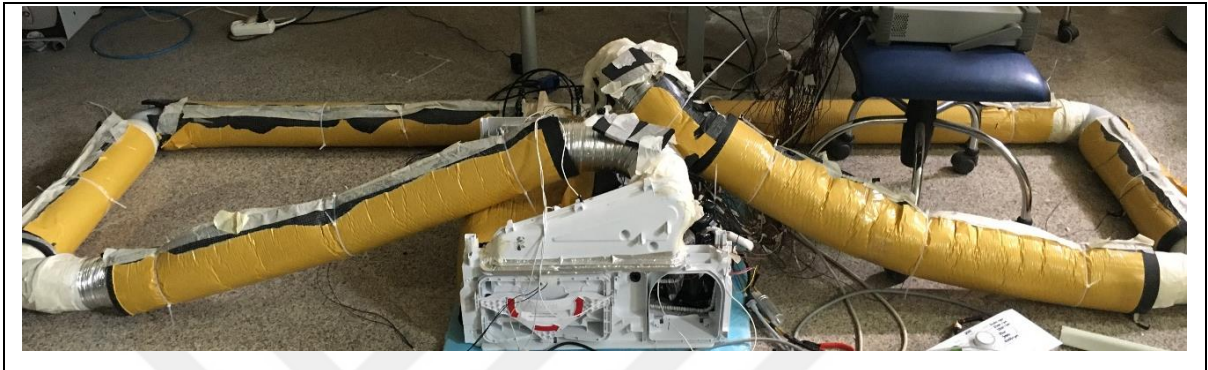


Figure 3.1: Air cycle system

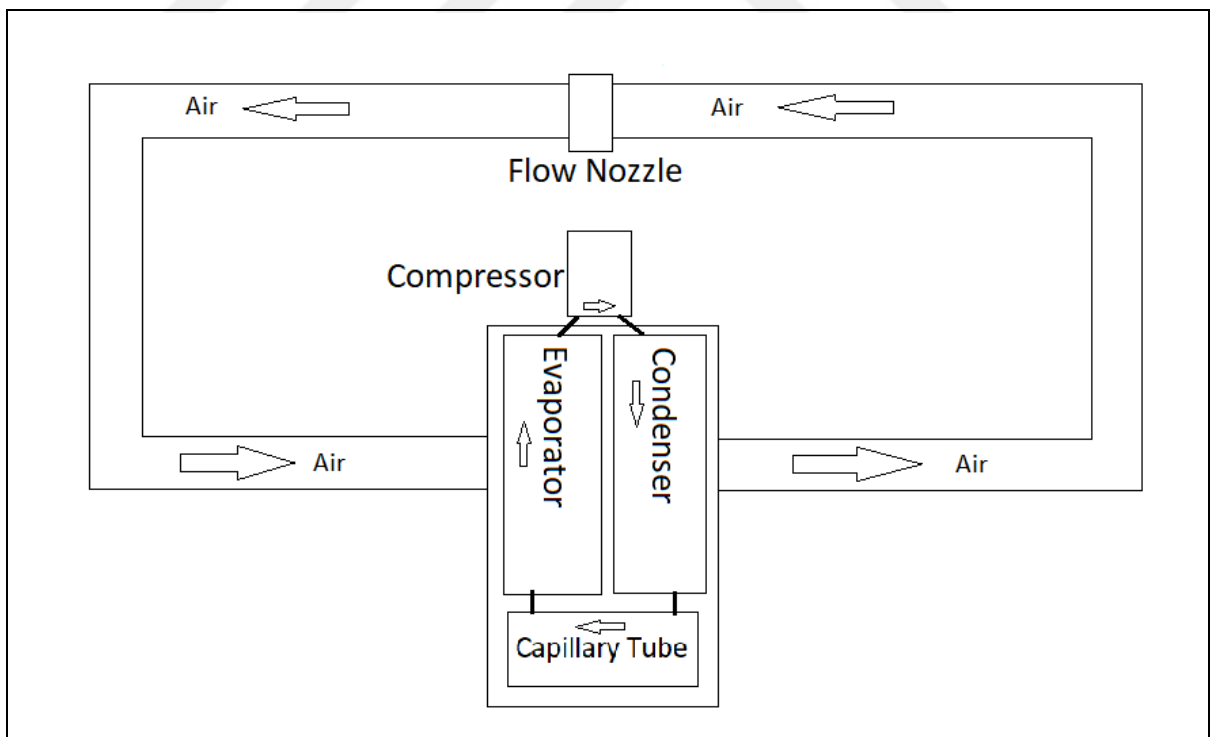


Figure 3.2: Scheme of the whole system

Thermocouples are placed at ten different points in order to measure air temperature through the system. Thermocouples at the inlet of evaporator, at the exit of condenser and in between evaporator and condenser are at different heights that averages of them are aimed to use in calculations.

Table 3.1: Thermocouple locations for air cycle

<b>Thermocouple Locations</b>	<b>Thermocouple Numbers</b>
Before Evaporator	2
Between Eva-Cond	2
After Condenser	4
Before Nozzle	1
Outside Air	1

### **3.1.1. Flow Nozzle**

Flow nozzle is one of the ways to measure flowrate. In order to measure flowrate a flow nozzle needs to be designed and produced. According to ASME standards flow nozzle design should follow the pattern in Figure 3.3:



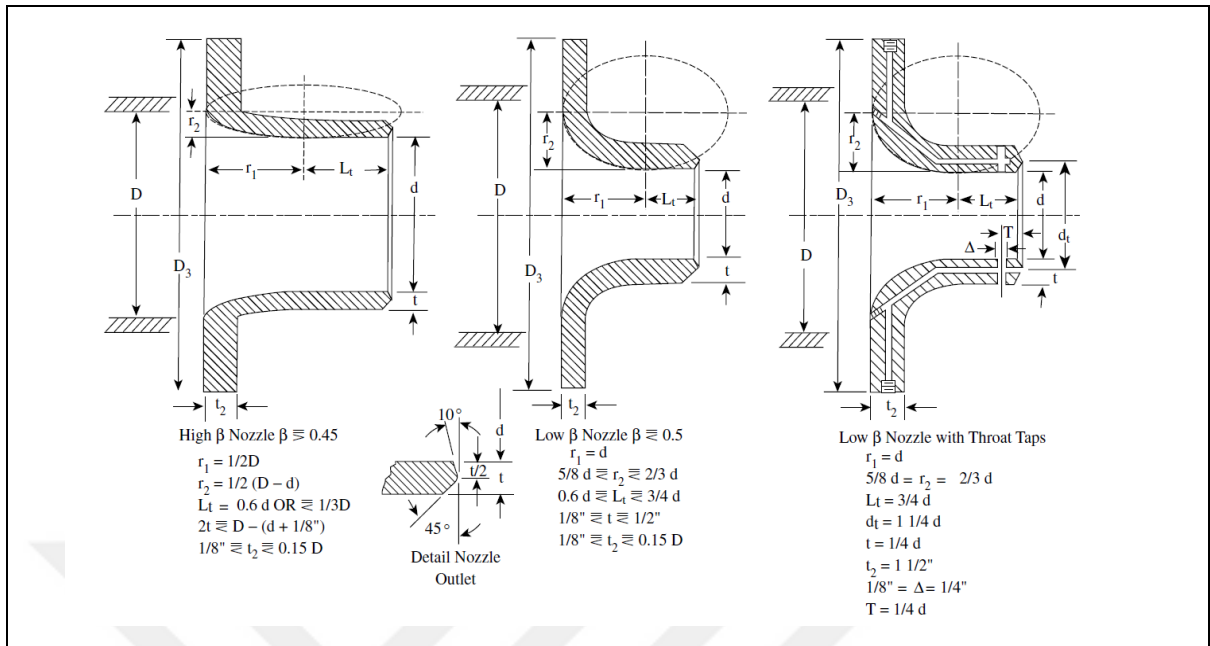


Figure 3.3: Design parameters of flow nozzle according to ASME standards

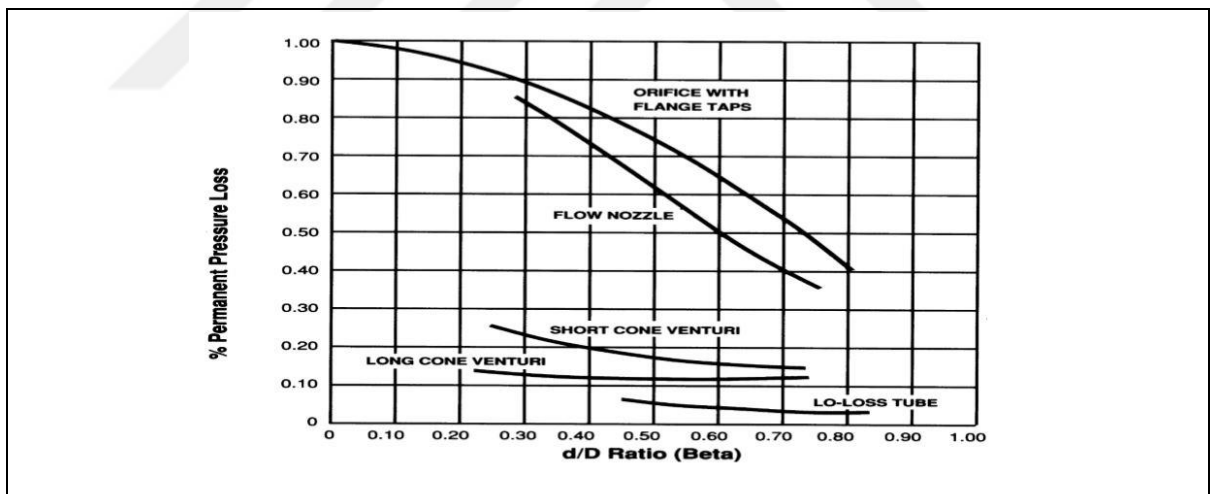


Figure 3.4: Flow measurement devices' pressure losses

Table 3.2: Designed flow nozzle dimensions

$\beta$	D(mm)	d(mm)	r1(mm)	r2(mm)	Lt(mm)	t(mm)	t2(mm)
0.7	103	72.1	51.5	15.45	43.26	13.86	3.18

A flow nozzle is designed in a solid computer-aided-design program with mentioned ASME standards to measure air flowrate with above specifications.

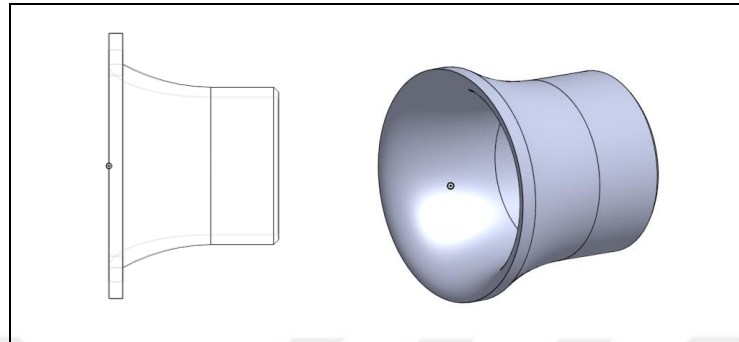


Figure 3.5: 3D sketches of designed flow nozzle

Pressure tabs are also placed according to same standards as can be seen below.

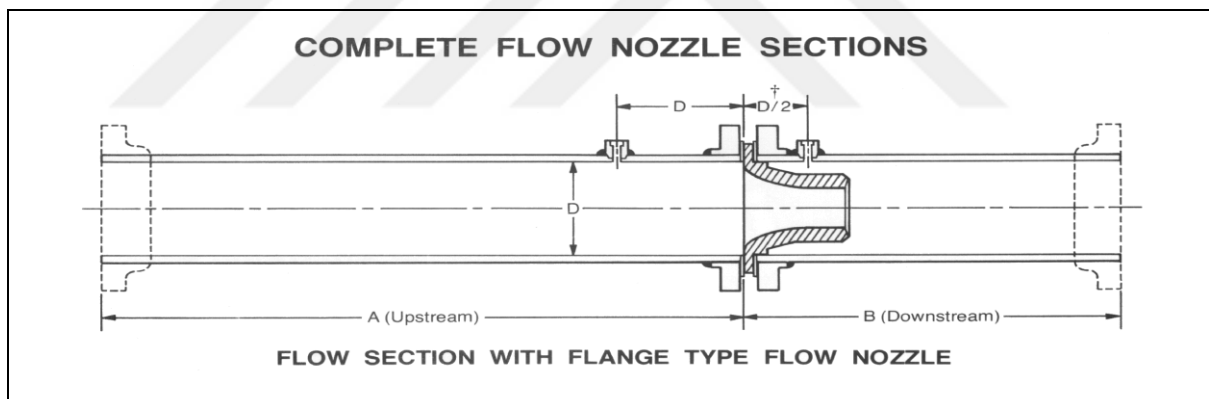


Figure 3.6:ASME flow nozzle section standart

In order to obtain pressure differences from pressure tabs, pneumatic pipes are used to connect the tabs and pressure sensor.

There are four pressure tab each before and after the flow nozzle on the PVC pipes. This makes the reading more accurate since result of the reading is the average value of those four tabs.

### 3.1.2. Heaters

A 600W capacity heater is used to heat air for some cases. Resistance wire is used to build heater with 11.2 ohm per meter resistance wire. It is placed just after flow nozzle.

Another 600 W capacity is used between condenser and compressor to heat air.

Each one is used separately during experiment, they are not used at the same time.



Figure 3.7: Resistance wire heater in between condenser and evaporator

### 3.1.3. Pipes

PVC pipes are used to measure flowrate through flow nozzle. A 1.5 m long PVC pipe is placed before flow nozzle and 1 m long PVC pipe is placed after flow nozzle to get accurate reading from flow nozzle. Pipes are isolated with isolation material through the system.

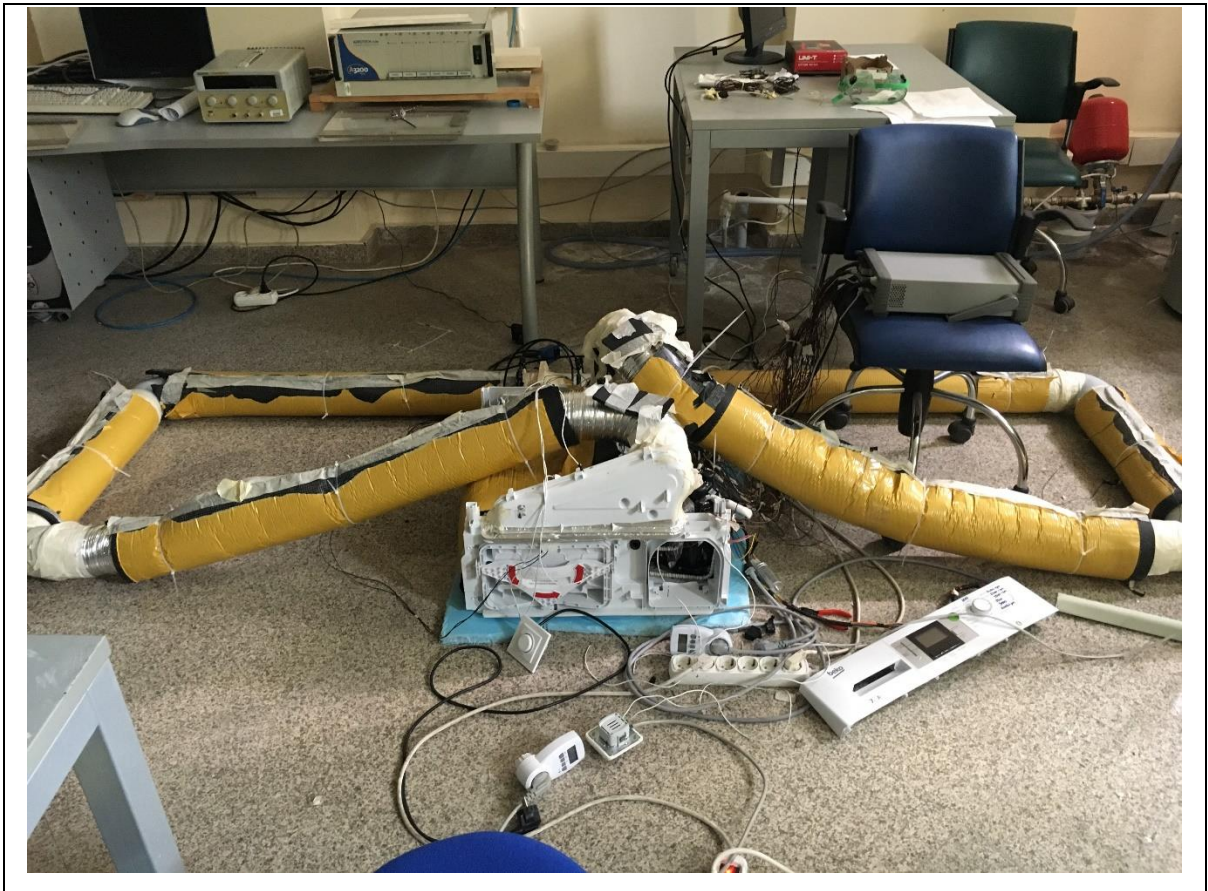


Figure 3.8: PVC pipes and the system

Between PVC pipes and entrances of condenser and evaporator flexible aluminum pipes are used to complete the loop of air.

### 3.1.4. Pressure Sensor

In order to sense pressure difference between pressure taps, pressure sensors are used. The range of the sensor is 250 Pa. Its working voltage range is 12-30V that it is supplied with a DC power supply.

### 3.1.5. Fan

Electric motor fan provides a constant air flow through the system. It is set to a constant rpm value to maintain the air flow. Two different frequencies are used as 2200 rpm and 3000 rpm for tests.



Figure 3.9: Fan

### 3.1.6. Energy Meter

Energy meters are used to measure heaters' energy consumption. In order to test its accuracy a simple test is performed.

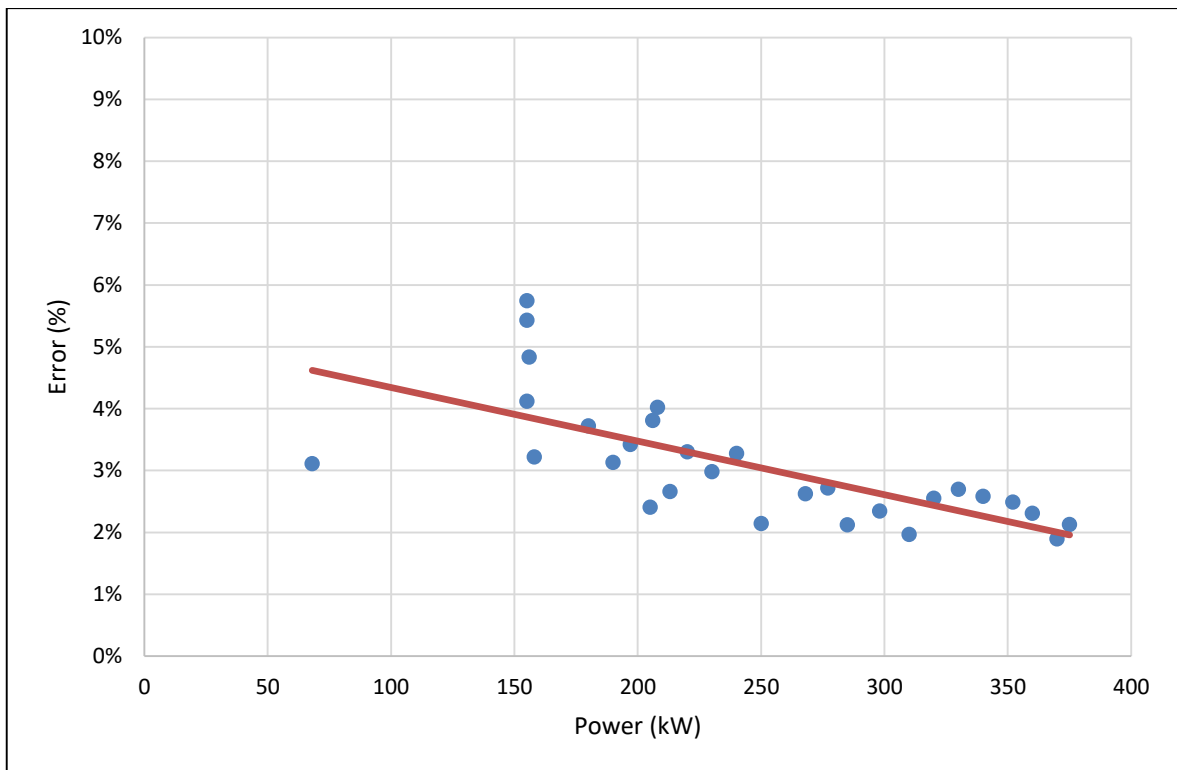


Figure 3.10: Energy meter measured power vs error with respect to calculated power(kW)

Energy meter stability is checked with the help of multimeter. The voltage output from the source is measured with multimeter and the current between energy meter poles is measured. Because energy meter creates a resistance to read power. With the measured current, voltage power is calculated and compared with reading from energy meter. The difference between them is under five percent through the working powers of the system. Also it can be seen that when the power is increased for the heaters, difference between calculated and measured power decreases. The system usually works in a range above 300 W.

### 3.2. VAPOR COMPRESSION REFRIGERATION CYCLE AND SETUP

The refrigerant cycle consists of condenser, evaporator, compressor and capillary tube as shown in Figure 3.11. Along the capillary tube, fluid changes from liquid phase to two-phase flow due to pressure drop.

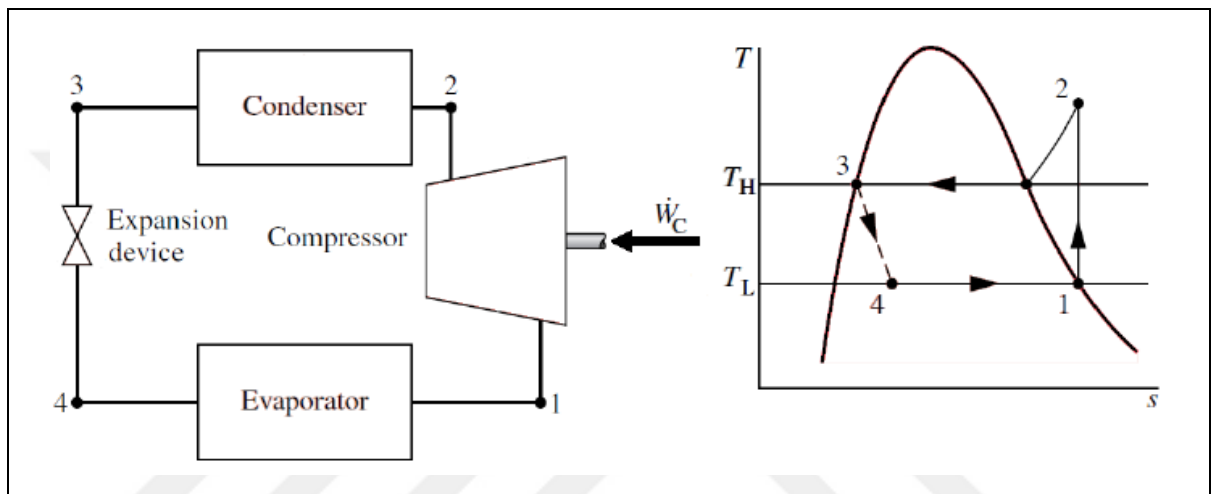


Figure 3.11: Basic vapor compression refrigeration cycle and T-s diagram

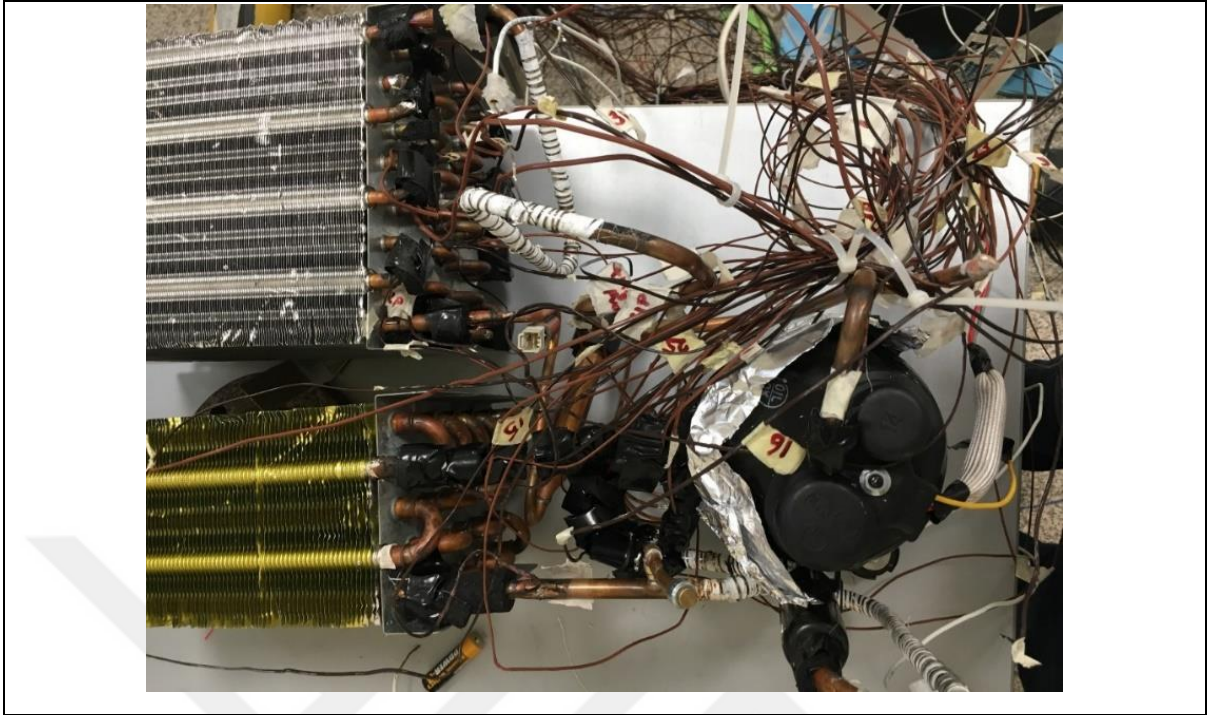


Figure 3.12: Vapor compression refrigeration cycle

In the present study, the refrigerant mass flowrate was not directly measured. Therefore, it was necessary to calculate flowrate indirectly. Three different methods to calculate flowrate indirectly are used in the present study.

The first method is to use a simple compressor model as shown in Eq. (3.6).

$$\dot{m}_{comp,vol} = \eta \times \left( \frac{V'}{N} \right) \times fr \times \rho \quad (3.6)$$

The volumetric efficiency  $\eta$  is assumed to be 0.92 in this study. The density at the compressor inlet is designated as  $\rho$ .  $V'$  is volume displacement and  $fr$  is the working frequency of compressor.

On the other hand, the energy balance between air and refrigerant cycles at the evaporator and condenser can make it possible to calculate mass flowrate as follows.



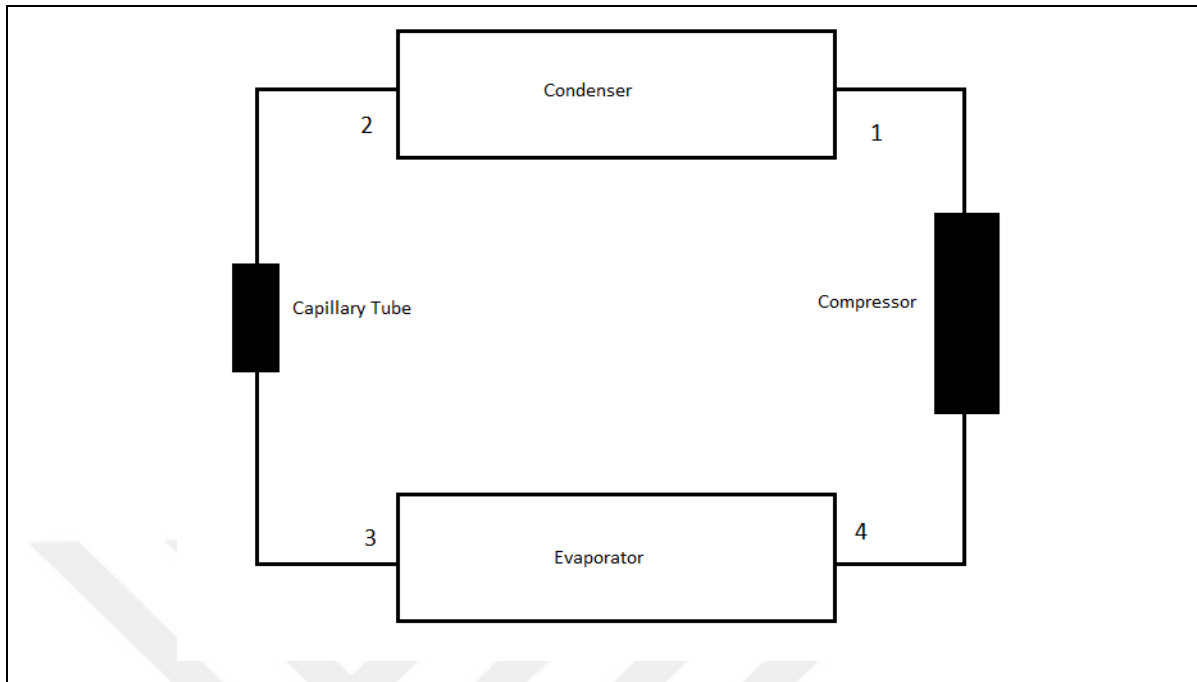


Figure 3.13: Scheme of the refrigerant cycle

At points indicated in Figure 3.13, the following assumptions are made:

At point 1:  $h_1 = \text{Superheated } h_{@ P_{sat,cond} \& T}$  and  $P_1 = P_{sat @ T_{sat,cond}}$

At point 2:  $h_2 = h_f @ P_{sat}$  and  $P_2 = P_{sat @ T_{sat,cond}}$

At point 3:  $h_3 = h_2$  and  $P_3 = P_{sat @ T_{sat,evap}}$

At point 4:  $h_4 = \text{Superheated } h_{@ P_{sat,evap} \& T}$  and  $P_4 = P_{sat @ T_{sat,evap}}$

Then the energy balances between air and refrigerant flows can be made as shown in Eqs (3.7) and (3.8).

$$Q_L = \dot{m}_{air} c \Delta T_{air,evap} = \dot{m}_{ref,evap} (h_1 - h_2) \quad (3.7)$$

$$Q_H = \dot{m}_{air} c \Delta T_{air,cond} = \dot{m}_{ref,cond} (h_4 - h_3) \quad (3.8)$$

Therefore, the mass flowrate of refrigerant at the evaporator and condenser can be calculated from the air flowrate, the heat capacity of air, air temperature change across the evaporator and condenser, respectively, and the refrigerant enthalpy change across the evaporator and condenser, respectively, from Eqs. (3.7) and (3.8). These methods will be named as the second and third methods in the present study.

### 3.2.1. Condenser

The condenser is consisting of 13.2 m long and 0.73 cm diameter tube and numerous fins which are placed every 1 mm on it. It has 23 cm x 17.5 cm x 15 cm dimensions as length, width and height respectively. Thermocouples are placed on eleven different locations on condenser surface. They are all insulated after soldering.

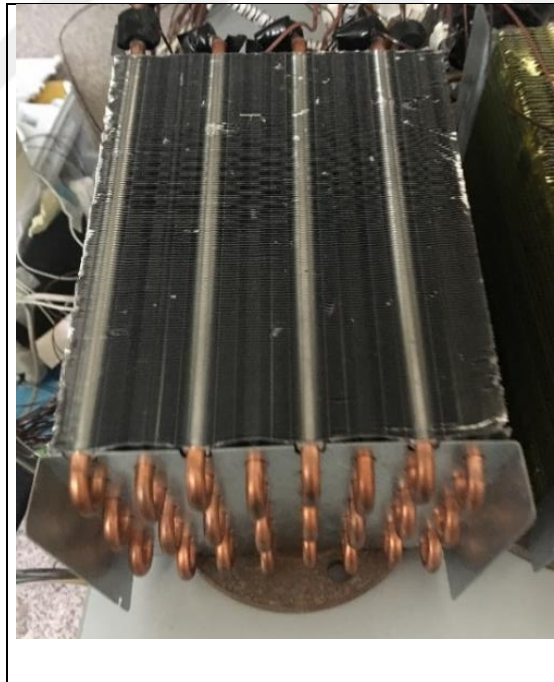


Figure 3.14: Condenser

Table 3.3: Thermocouple locations on condenser

<b>DAQ Channels</b>	<b>Condenser Length(m)</b>	<b>Condenser Passes</b>	<b>Dimensionless Location</b>
101 (C)	0	ENT	0
102 (C)	0.55	1P	0.04
103 (C)	1.65	3P	0.13
104 (C)	3.3	6P	0.25
105 (C)	4.95	9P	0.38
106 (C)	6.6	12P	0.50
107 (C)	8.25	15P	0.63
108 (C)	9.9	18P	0.75
109 (C)	11.55	21P	0.88
110 (C)	12.65	23P	0.96
111 (C)	13.2	EXIT	1

### 3.2.2. Evaporator

The evaporator is made of 8.25 m long and 1 cm diameter tube and numerous fins which are placed every 2.5 mm on it. It has 23 cm x 11 cm x 15 cm dimensions as length, width and height respectively. Thermocouples are placed on five different locations on evaporator. They are all insulated after soldering.



Figure 3.15: Evaporator

Table 3.4: Thermocouple locations on evaporator

DAQ Channels	Length (m)	Evaporator Passes	Dimensionless Location
219 (C)	0	ENT	0
220 (C)	5.500	10P	0.67
301 (C)	7.425	14P	0.90
302 (C)	7.975	15P	0.97
303 (C)	8.250	EXIT	1

### 3.2.3. Compressor

In order to compress the refrigerant fluid a RECHI PRECISION 39E0G3B model, 50 Hz rotary compressor is used. It has 220-240 V working range and 6.5 cc/rev displacement volume. The compressor has 745 W capacity and it is claimed that its COP is 2.81 Two thermocouples are placed on compressor entrance and exit.



Figure 3.16: Compressor

#### 3.2.4. Capillary Tube

The capillary tube has 1.5 m length and 1.3 mm diameter. It is coiled between evaporator and condenser. Twenty-five thermocouples are placed on capillary tube surface on different locations. Also one more thermocouple is placed just after the end of capillary tube to examine more. After 1.1 m of capillary tube, thermocouples are placed more frequent that it is placed every 2 cm until the end of tube to see the effects of two phase flow. Uncertainty of the tube diameter is 0.1 mm due to calipers.



Figure 3.17: Capillary Tube

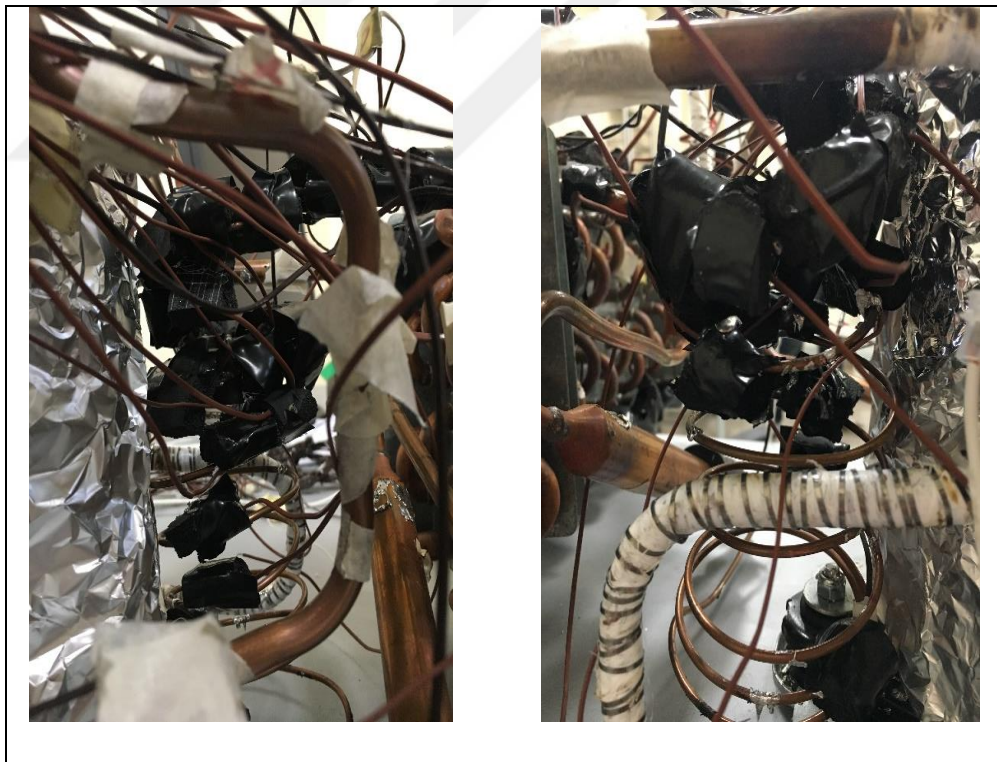


Figure 3.18: Thermocoupled capillary tube

Thermocouples are placed on tube surface with soldering. After that, it is also covered with aluminum insulated tape and moreover insulation material to decrease the mismeasurements.

Table 3.5: Thermocouples locations on capillary tube

#	DAQ Channels	Length (m)	Dimensions Location
1	112 (C)	0	0.00
2	113 (C)	0.4	0.27
3	114 (C)	0.65	0.44
4	115 (C)	0.9	0.61
5	116 (C)	1.1	0.75
6	117 (C)	1.12	0.76
7	118 (C)	1.14	0.78
8	119 (C)	1.16	0.79
9	120 (C)	1.18	0.80
10	201 (C)	1.195	0.81
11	202 (C)	1.21	0.82
12	204 (C)	1.23	0.84
13	205 (C)	1.25	0.85

#	DAQ Channels	Length (m)	Dimensions Location
14	206 (C)	1.265	0.86
15	207 (C)	1.28	0.87
16	208 (C)	1.3	0.88
17	209 (C)	1.32	0.90
18	210 (C)	1.34	0.91
19	211 (C)	1.36	0.93
20	212 (C)	1.375	0.94
21	213 (C)	1.39	0.95
22	214 (C)	1.41	0.96
23	215 (C)	1.43	0.97
24	216 (C)	1.45	0.99
25	217 (C)	1.47	1.00
26	218 (C)	1.5	1.02



Figure 3.19: Thermocouple connection

### 3.2.5. Heater

During several preliminary tests, it was discovered that refrigerant flow into the compressor is slightly two phase. In order to make it superheated, therefore, resistance wire was coiled up on the connecting tube between the evaporator and the compressor. Teflon tape was first wrapped over the tube to provide electrical insulation between the tube and the coiled heater. The power of the heater was 600 watt.

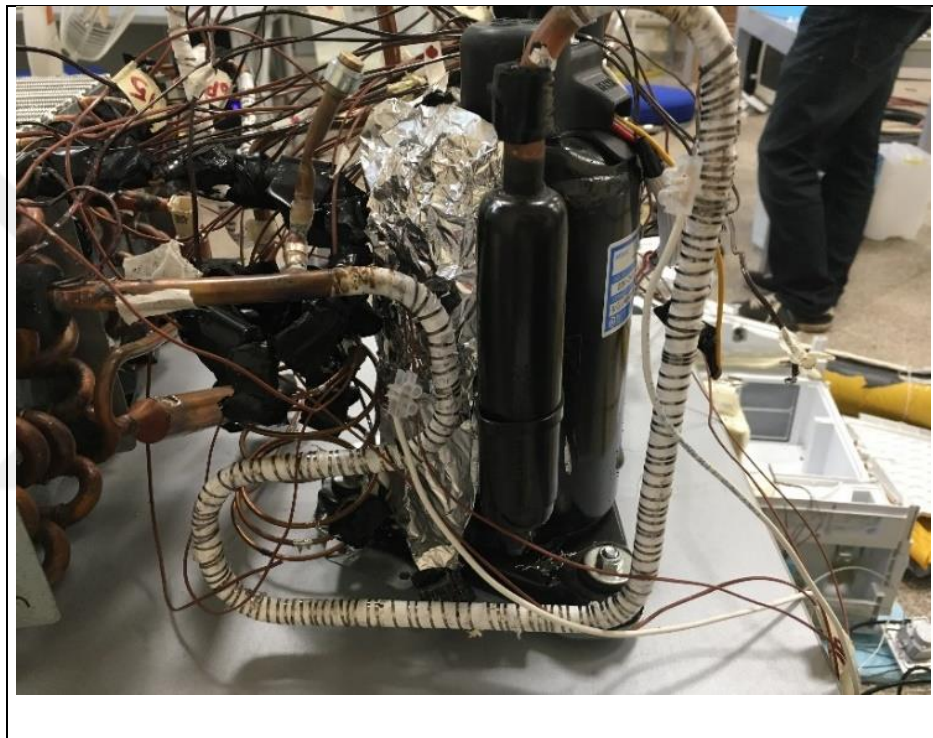


Figure 3.20: Evaporator heater

Likewise another coiled heater was placed in between the compressor and the condenser. Its purpose was supposed to control the degree of the subcooling of the refrigerant by heating the refrigerant at the inlet of the condenser.



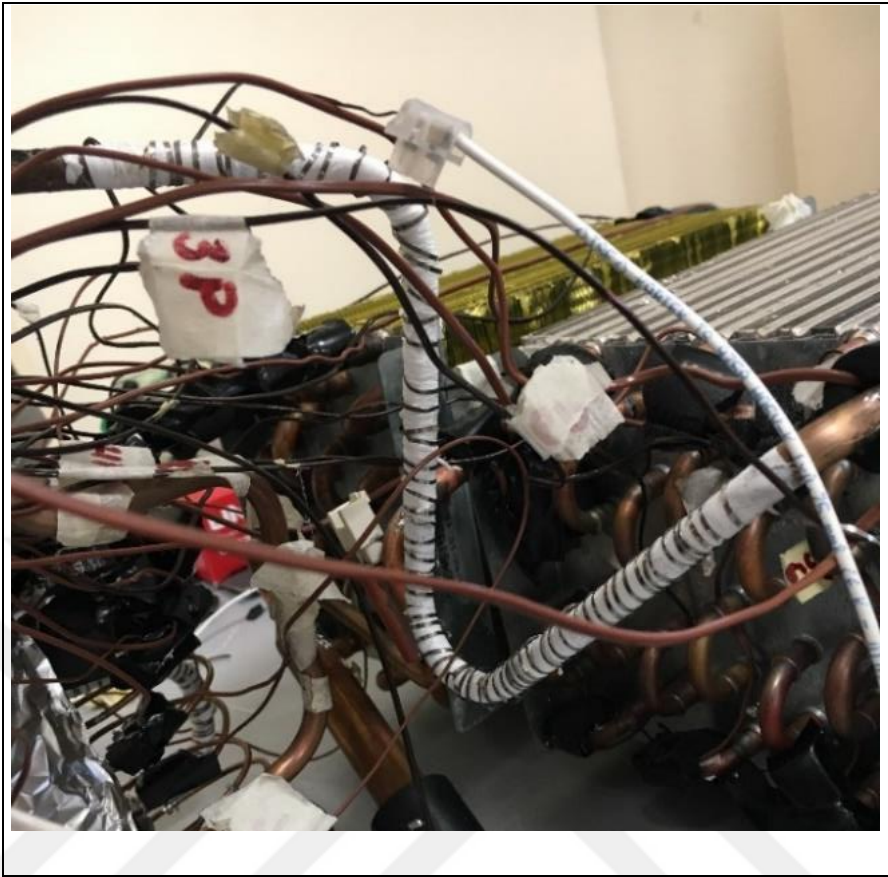


Figure 3.21: Condenser heater

## 4. NUMERICAL METHODS

Numerical model is used without and with consideration of metastable phenomenon. One of the model considers metastable phenomenon and other one does not. Basically, metastable phenomenon is delay of vaporization. If the flow is considered as single and two phase flow regions, single flow region in models is the same for both approaches.

Capillary tube can be numbered into five points as it can be seen below, condenser exit as 1, capillary inlet as 2, single phase end as 3, capillary tube exit as 4 and evaporator inlet as 5.

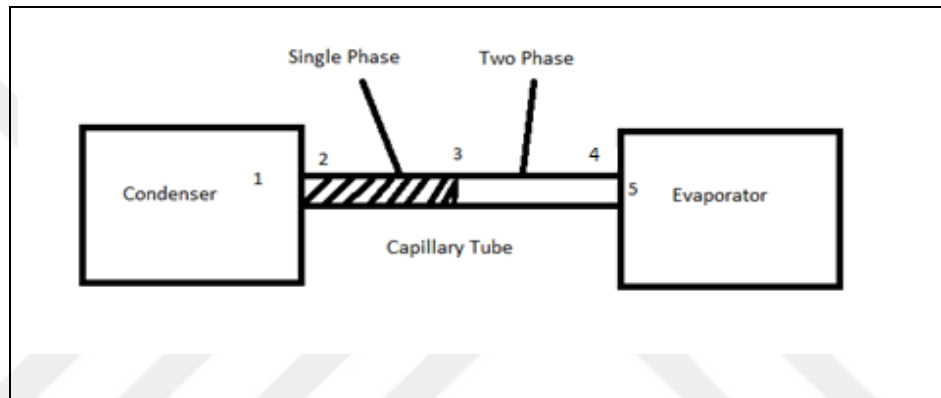


Figure 4.1: Capillary tube and flow phases

Initial pressure starts to decrease and when the pressure of the liquid is decreased to its saturation pressure it starts to change phase. This can be called liquid region. Liquid region length can be find from the equilibrium:

$$\frac{P_1}{\rho_g} + \frac{V_1^2}{2g} + z_1 = \frac{P_3}{\rho_g} + \frac{V_3^2}{2g} + z_3 + h_L \quad (4.1)$$

For an incompressible fluid, mass flowrate is constant through tube.

$$\dot{m} = \rho_1 V_1 A = \rho_3 V_3 A \quad (4.2)$$

$$h_L = k \frac{V^2}{2g} + f_{sp} \frac{L_{sp}}{D} \frac{V^2}{2g} \quad (4.3)$$

$$L = \frac{2(P_i - P_{sat})}{fvG^2} \quad (4.4)$$

Where the Haaland Equation[11] states;

$$\frac{1}{\sqrt{f}} = 1.8 \log \left( \left( \frac{\varepsilon/D}{3.7} \right)^{1.11} + \frac{6.9}{Re} \right) \quad (4.5)$$

$$G = \frac{\dot{m}}{Area} \quad (4.6)$$

$$Re = \frac{\rho u d}{\mu} \quad (4.7)$$

Through single phase region, viscosity of fluid is constant since there is no phase change during the flow. Flow is considered as one phase liquid flow up to this point. From this, there are two different approaches for flow with and without consideration of metastable phenomena. The fluid is not at its stable situation due to rapid pressure change, flow is unstable but relatively long-lived state of flow through tube. This instability can be named as metastability in flow. If the metastable flow is considered, flow is divided into four regions, first one is single flow liquid region as it is mentioned above, second region is called as metastable liquid region, third region is named as two phase metastable region and lastly fourth region is one phase vapor flow region.

#### **4.1. NUMERICAL MODEL WITHOUT CONSIDERING METASTABLE PHENOMENON**

Wongwises, S. and Pirompak, W. [1] presented a flow model through capillary tube with neglecting metastable flow as following:

For adiabatic steady-state conservation of energy is:

$$h + \frac{v^2}{2} = constant \quad (4.8)$$

At any point h, v and s are:

$$h = (1 - x)h_f + xh_g \quad (4.9)$$

$$v = (1 - x)v_f + xv_g \quad (4.10)$$

$$s = (1 - x)s_f + xs_g \quad (4.11)$$

$$V = \frac{m}{\rho A} = \frac{G}{\rho} = Gv \quad (4.12)$$

$$h_3 = \frac{V_3^2}{2} = h_f + x(h_g - h_f) + \frac{G^2}{2}(v_f(1 - x) + v_g x)^2 \quad (4.13)$$

$$\left[ (v_g - v_f)^2 \frac{G^2}{2} \right] x^2 + [G^2 v_f (v_g - v_f) + (h_g - h_f)] x + \left[ \frac{G^2 v_f^2}{2} - h_3 - \frac{V_3^2}{2} + h_f \right] = 0 \quad (4.14)$$

$$x = \frac{-h_{fg} - G^2 v_f v_{fg} + \sqrt{(G^2 v_f v_{fg} + h_{fg})^2 - (2G^2 v_{fg}^2) \left[ \frac{G^2 v_f^2}{2} - h_3 + \frac{V_3^2}{2} + h_f \right]}}{G^2 v_{fg}^2} \quad (4.15)$$

Viscosity for two-phase flow can be found from McAdams[1] formula:

$$\mu_{tp} = \frac{1}{\frac{x}{\mu_g} + \frac{1-x}{\mu_f}} \quad (4.16)$$

And also:

$$dL = \frac{2D}{f_{tp}} \left[ \frac{-\rho dP}{G^2} + \frac{dv}{\rho} \right] \quad (4.17)$$

$$\frac{d\rho}{\rho} = -\frac{dv}{v} \quad (4.18)$$

$$\begin{aligned} dv &= (1 - x) \frac{dv_f}{dp} dp - v_f \frac{dx}{dp} dp + x \frac{dv_g}{dp} dp + v_g \frac{dx}{dp} dp \\ &= \left( (1 - x) \frac{dv_f}{dp} + x \frac{dv_g}{dp} + (v_g - v_f) \frac{dx}{dp} \right) dp \end{aligned} \quad (4.19)$$

$$\begin{aligned} dL &= \frac{2D}{f_{tp}} \left[ -\frac{dp}{G^2 v} - \frac{dv}{v} \right] \\ &= -\frac{2D}{f_{tp} v} \left[ \frac{1}{G^2} + \left( (1 - x) \frac{dv_f}{dp} + x \frac{dv_g}{dp} + (v_g - v_f) \frac{dx}{dp} \right) \right] dp \end{aligned} \quad (4.20)$$

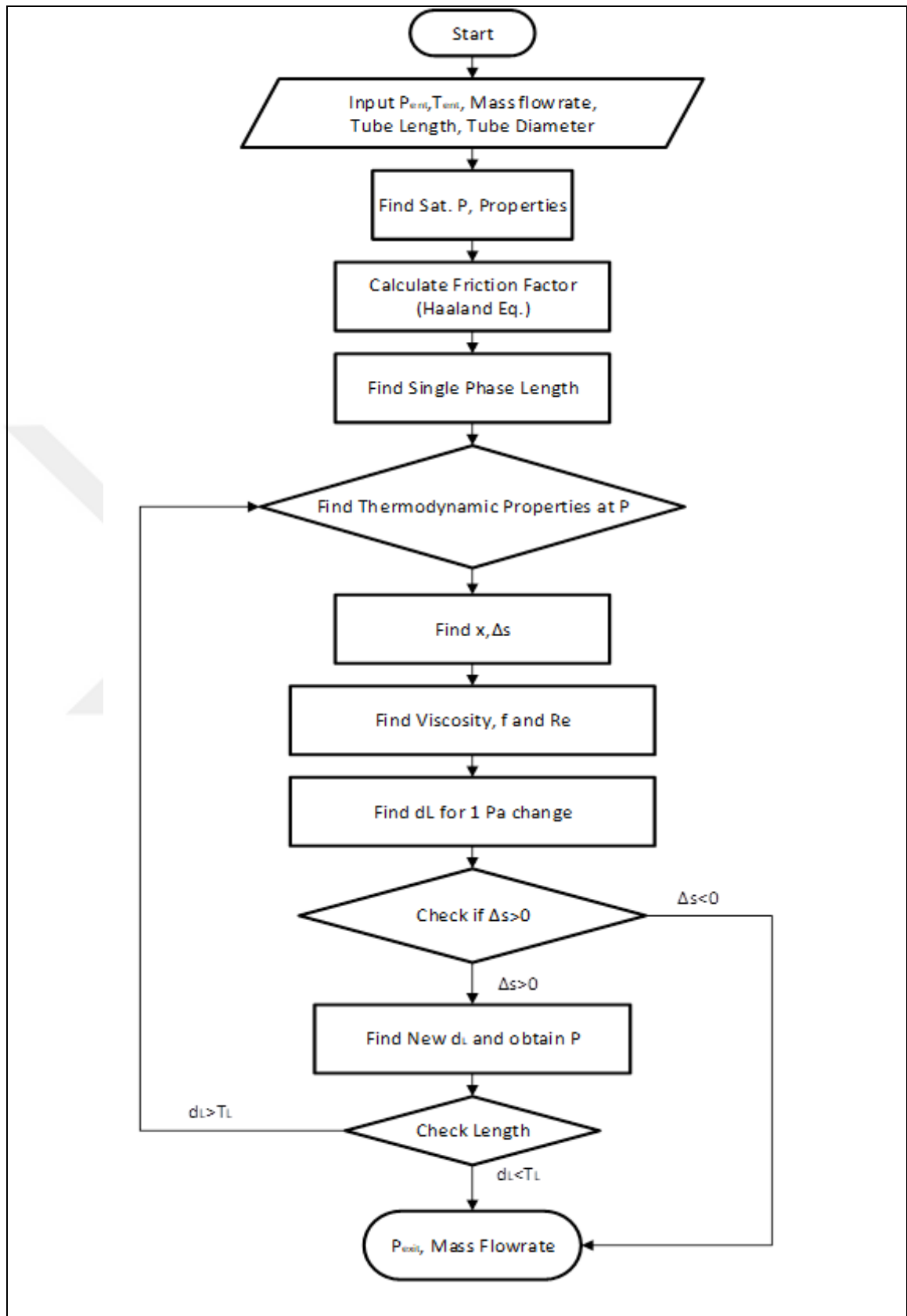


Figure 4.2: Flowchart of first numerical model

## 4.2. NUMERICAL MODEL WITH CONSIDERING METASTABLE PHENOMENON

There is a delay of vaporization that vaporization does not occur at saturation pressure but at some pressure below it. Between vaporization pressure and saturation pressure called metastable liquid region. This vaporization pressure can be obtained for two-phase flow with metastable condition from Chen[11] et al study as:

$$\frac{(P_{sat} - P_{vap})\sqrt{kT_{sat}}}{\sigma^{1.5}} \quad (4.21)$$

$$= 0.679 \left( \frac{v_g}{v_g - v_f} \right) Re^{0.914} \left( \frac{\Delta T_s}{T_c} \right)^{-0.208} \left( \frac{d}{D'} \right)^{-3.18}$$

$$D' = \sqrt{\frac{kT_{sat}}{\sigma}} \times 10^4 \quad (4.22)$$

After vaporization, fluid does not reach thermodynamic equilibrium yet. Fluid starts to change phase and includes both gases and liquid at same time at this state. This state ends when the mass fraction of gasses and liquid in the tube reaches equilibrium. Also, while phase changes, viscosity of fluid also changes. Also acceleration of two-phase flow is considered in flow as it is used in the model that does not consider metastable condition. Feburie[6] defined  $y$  to express mass fraction for saturated phase and rearrange  $h$  and  $v$  as:

$$y = \frac{m_l + m_g}{m_m + m_l + m_g} \quad (4.23)$$

$$\frac{dy}{dl} = 0.02 \left( \frac{U}{A} \right) (1 - y) \left[ \frac{P_{sat} - P}{P_c - P_{sat}} \right]^{0.25} \quad (4.24)$$

$$h = (1 - y)h_m + (y - x)h_{ls} + xh_g \quad (4.25)$$

$$v = (1 - y)v_m + (y - x)v_{ls} + xg v_g \quad (4.26)$$

$$h_{total} = h + \frac{1}{2} G^2 v^2 \quad (4.27)$$

$$\begin{aligned}
h_{total} &= (1-y)h_{lm} + yh_{ls} + x(h_g - h_{ls}) \\
&\quad + \frac{1}{2}G^2 \left( (1-y)v_{lm} + yv_{ls} + x(v_g - v_{ls}) \right)^2 \\
&= h_l + x(h_g - h_{ls}) + \frac{1}{2}G^2(v_l + x(v_g - v_{ls}))^2
\end{aligned} \tag{4.28}$$

$$\begin{aligned}
\frac{1}{2}G^2(v_g - v_{ls})^2x^2 + \left( G^2v_l(v_g - v_{ls}) + (h_g - h_{ls}) \right)x + \frac{1}{2}G^2v_l^2 + h_l \\
- h_{total} = 0
\end{aligned} \tag{4.29}$$

Mixture quality, x can be found from equation 4.29 by solving for x.

And also,

$$dL = \frac{2D}{f_{tp}} \left[ \frac{-\rho dP}{G^2} + \frac{d\rho}{\rho} \right] \tag{4.30}$$

$$\frac{d\rho}{\rho} = -\frac{dv}{v} \tag{4.31}$$

$$\begin{aligned}
dv &= (y-x) \frac{dv_f}{dp} dp - x \frac{dv_g}{dp} dp + (v_g - v_f) \frac{dx}{dp} dp \\
&= \left( (y-x) \frac{dv_f}{dp} - x \frac{dv_g}{dp} + (v_g - v_f) \frac{dx}{dp} \right) dp
\end{aligned} \tag{4.32}$$

$$\begin{aligned}
dL &= \frac{2D}{f_{tp}} \left[ -\frac{dp}{G^2v} - \frac{dv}{v} \right] \\
&= -\frac{2D}{f_{tp}v} \left[ \frac{1}{G^2} \right. \\
&\quad \left. + \left( (y-x) \frac{dv_f}{dp} + x \frac{dv_g}{dp} + (v_g - v_f) \frac{dx}{dp} \right) \right] dp
\end{aligned} \tag{4.33}$$

Reynolds number and friction factor are also a function of pressure only. Dukler[2] two-phase viscosity equation is used as:

$$\mu = \frac{(1-x_g)v_l\mu_l + x_gv_g\mu_g}{(1-x_g)v_l + x_gv_g} \tag{4.34}$$

As Feburie et al state specific volumes for metastable region:

$$v_l = \left( \frac{1-y}{1-x_g} \right) v_m + \left( \frac{y-x_g}{1-x_g} \right) v_{ls} \tag{4.35}$$

Lastly, phase change reaches its final equilibrium in the tube. From this point to end flow becomes equilibrium two phase flow that x can be found by using equation 4.15.

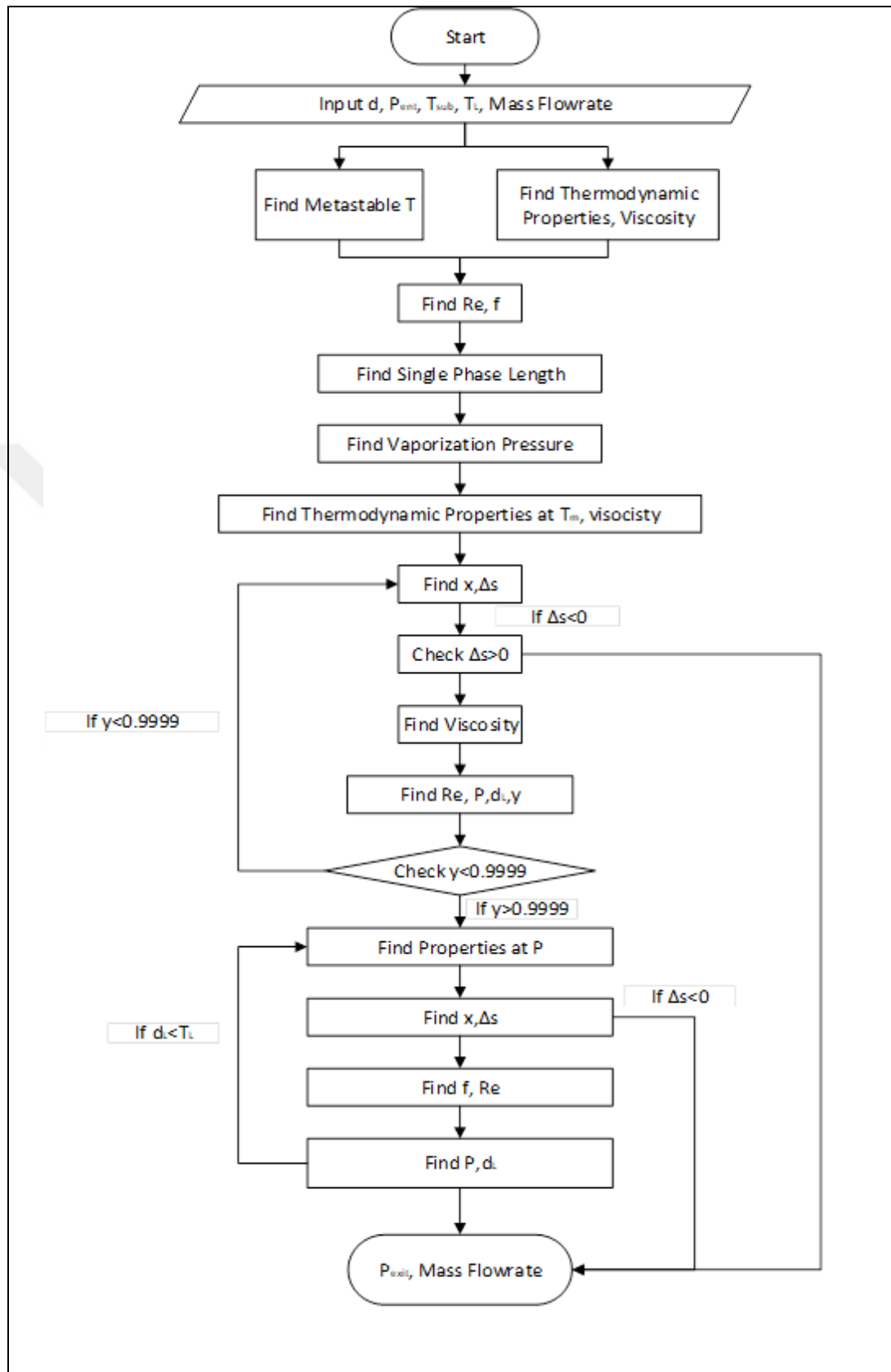


Figure 4.3: Flowchart of second numerical model



## 5. RESULTS AND DISCUSSION

### 5.1. EXPERIMENTAL RESULTS

Ten different tests performed and temperature data obtained. Difference between sets is subcooling temperatures. Temperature values are read from 56 different locations in total. Two sets that are indicated as “0” in the tables, are measured without working compressor to see if there is a variation on temperature readings through the system

Table 5.1: Test conditions

#	T (C)	Fan Freq (rpm)	Heater Location	Power (kW)	Pressure Dif (Cond-Evap) (kPa)	T sub (C)
0	23.62	3000	-	-	-	-
0	24.82	2200	-	-	-	-
1	66.21	3000	Air	0.30	845.64	15.99
2	37.08	2200	-	-	450.73	7.24
3	39.34	3000	-	--	404.68	12.01
4	75.32	3000	Air	0.37	1002.90	16.89
5	74.04	2200	Air	0.37	1212.80	11.55
6	61.06	2200	After Evaporator	0.30	881.44	10.32
7	65.88	2200	Between Evap & Cond	0.30	1060.11	7.55
8	39.18	2200	Before Condenser	0.10	491.41	8.723
9	45.29	2200	Before Condenser	0.20	606.48	9.603
10	49.73	2200	Before Condenser	0.28	706.28	10.34

Table 5.2: Condenser temperatures

Set/Channel	101 (C)	102 (C)	103 (C)	104 (C)	105 (C)	106 (C)	107 (C)	108 (C)	109 (C)	110 (C)	111 (C)
1	60.08	59.11	59.38	59.71	57.21	59.06	57.19	56.56	50.65	42.35	41.22
2	34.97	35.64	35.93	35.96	34.71	35.43	34.28	34.03	33.68	29.59	27.47
3	35.88	35.27	35.63	35.71	34.37	35.30	34.09	33.39	27.68	23.05	22.36
4	68.57	66.37	66.36	66.30	63.47	65.72	63.54	62.80	56.60	47.96	46.59
5	68.67	69.35	70.35	70.54	67.97	69.90	68.01	67.77	67.59	59.65	56.42
6	56.54	57.61	58.51	58.69	56.40	58.24	56.47	56.30	55.88	49.35	46.08
7	61.48	62.93	63.93	64.02	61.49	63.49	61.56	61.38	61.28	56.75	53.73
8	42.82	39.05	38.43	38.27	36.83	37.61	36.49	36.03	35.64	30.79	28.10
9	56.22	48.82	45.47	44.62	42.80	43.67	42.43	41.86	41.49	36.20	33.20
10	63.27	54.95	50.87	49.57	47.53	48.42	47.17	46.41	46.04	40.27	37.20

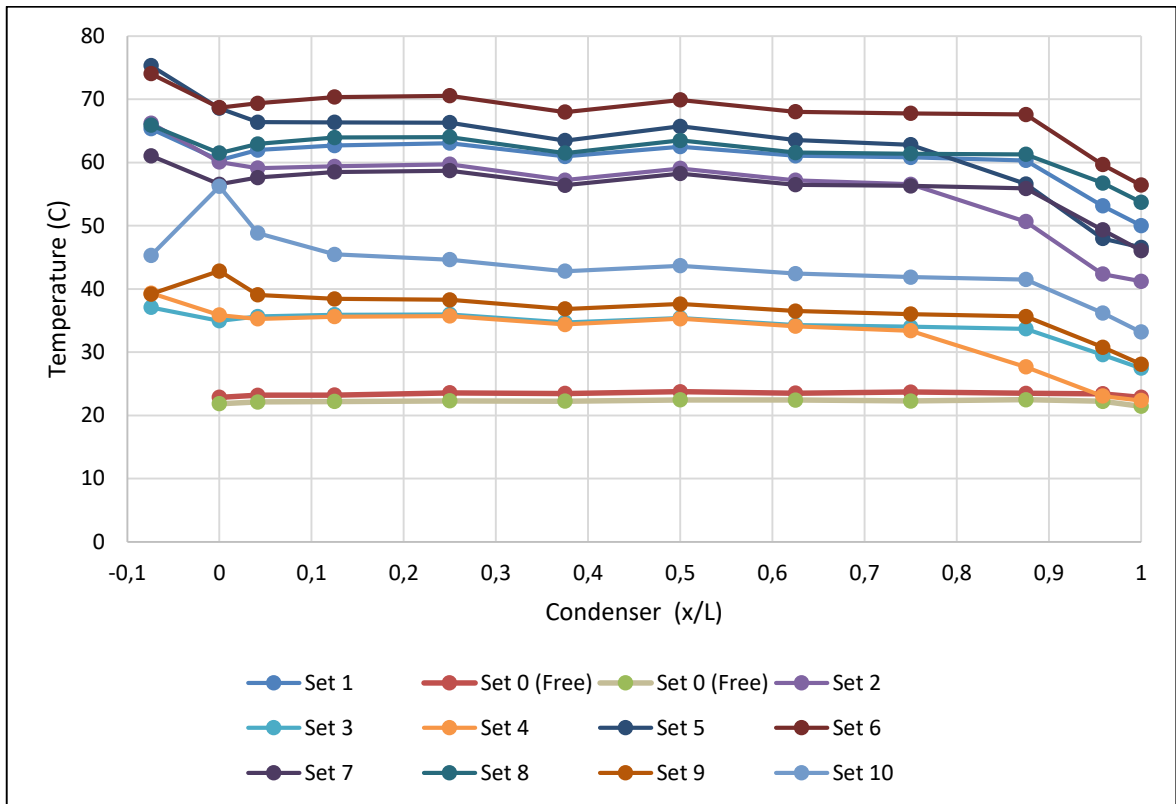


Figure 5.1: Condenser temperature distribution

As it can be seen from Figure 5.1 temperature of condenser is decreasing after a point due to condensation. Average of temperature values before decreasing point can be said as saturation temperature and first decreasing point can be named as saturation point for condenser. Saturation temperature is an important temperature to find out subcooling temperature. Subcooling is the main difference between saturation point and exit of the condenser temperature.

Table 5.3: Subcooling temperatures

Set	Tsub (C)
1	15.99
2	7.24
3	12.01
4	16.89
5	11.55
6	10.32
7	7.55
8	8.72
9	9.60
10	10.34

Twenty-five different temperature data are read on the surface of capillary tube.

Table 5.4: Capillary tube temperatures I

Set / Channel	112 (C)	113 (C)	114 (C)	115 (C)	116 (C)	117 (C)	118 (C)	119 (C)	120 (C)
0 (Free)	22.06	23.01	23.70	23.73	23.59	23.58	23.26	23.43	23.26
0 (Free)	20.05	19.42	19.70	19.96	20.03	20.04	20.04	19.95	19.87
1	40.79	38.91	41.31	41.16	40.80	41.03	39.13	39.92	39.65
2	27.17	26.49	27.30	27.27	27.06	27.11	26.41	26.63	26.51
3	22.26	22.04	22.25	22.28	22.09	22.10	21.96	21.96	21.90
4	45.84	45.06	46.70	46.47	46.06	46.39	44.01	45.29	44.60
5	55.74	53.94	56.47	56.15	55.71	56.07	52.59	54.38	53.93
6	44.80	44.40	45.96	45.86	45.62	45.87	44.10	45.00	44.60
7	51.94	50.63	53.98	53.47	53.14	53.48	50.54	52.10	53.13
8	27.76	27.34	28.16	28.03	27.86	27.95	27.11	27.44	27.48
9	32.84	31.95	36.45	33.17	32.97	33.12	31.94	32.40	32.47
10	36.73	35.61	37.42	37.18	36.90	37.11	35.63	36.23	36.30

Table 5.5: Capillary tube temperatures II

Set / Channel	201 (C)	202 (C)	204 (C)	205 (C)	206 (C)	207 (C)	208 (C)	209 (C)	210 (C)
0 (Free)	23.39	23.41	23.53	23.70	23.69	23.76	23.48	23.72	23.61
0 (Free)	20.38	20.53	20.66	20.73	20.86	20.79	20.86	20.86	21.14
1	40.32	39.63	39.82	40.52	39.97	40.94	39.79	40.56	39.97
2	26.97	26.79	26.77	27.16	27.04	27.22	26.77	27.11	27.16
3	22.08	22.16	22.32	22.38	22.41	22.28	22.25	22.23	22.11
4	45.73	44.55	45.15	45.73	45.06	46.17	45.09	45.88	45.93
5	55.07	53.61	52.85	54.92	54.15	55.61	53.55	54.24	55.25
6	44.30	43.69	43.53	45.18	44.61	45.74	44.53	45.59	45.79
7	51.88	51.09	52.43	52.48	51.57	52.93	51.31	52.35	51.82
8	27.61	27.20	27.15	27.80	27.68	27.97	27.51	27.81	27.78
9	32.50	31.86	31.72	32.72	32.54	33.02	32.36	32.75	32.74
10	36.34	35.47	35.32	36.69	36.43	36.97	36.17	36.64	36.66

Table 5.6: Capillary tube temperatures III

Set / Channel	211 (C)	212 (C)	213 (C)	214 (C)	215 (C)	216 (C)	217 (C)	218 (C)
0 (Free)	23.56	23.60	23.58	23.19	23.39	22.97	22.79	23.11
0 (Free)	20.81	21.04	21.17	21.33	21.22	21.17	21.34	21.50
1	40.64	40.60	41.08	40.28	41.00	39.73	36.64	31.43
2	27.09	26.80	27.24	26.93	27.08	26.36	21.81	14.21
3	22.18	22.18	22.11	22.27	21.90	21.63	20.33	16.28
4	45.77	45.34	46.24	44.90	46.22	44.59	41.13	35.86
5	54.05	52.47	52.52	50.35	50.82	48.29	44.40	36.80
6	45.33	44.78	45.44	43.53	42.54	39.40	36.08	29.22
7	48.87	47.31	47.75	46.05	45.82	43.27	39.31	30.50
8	27.57	27.37	27.42	26.51	25.53	23.08	19.68	14.62
9	32.45	32.02	32.25	30.95	29.87	27.05	23.70	18.27
10	36.42	35.84	36.36	35.19	33.81	30.65	27.24	21.35

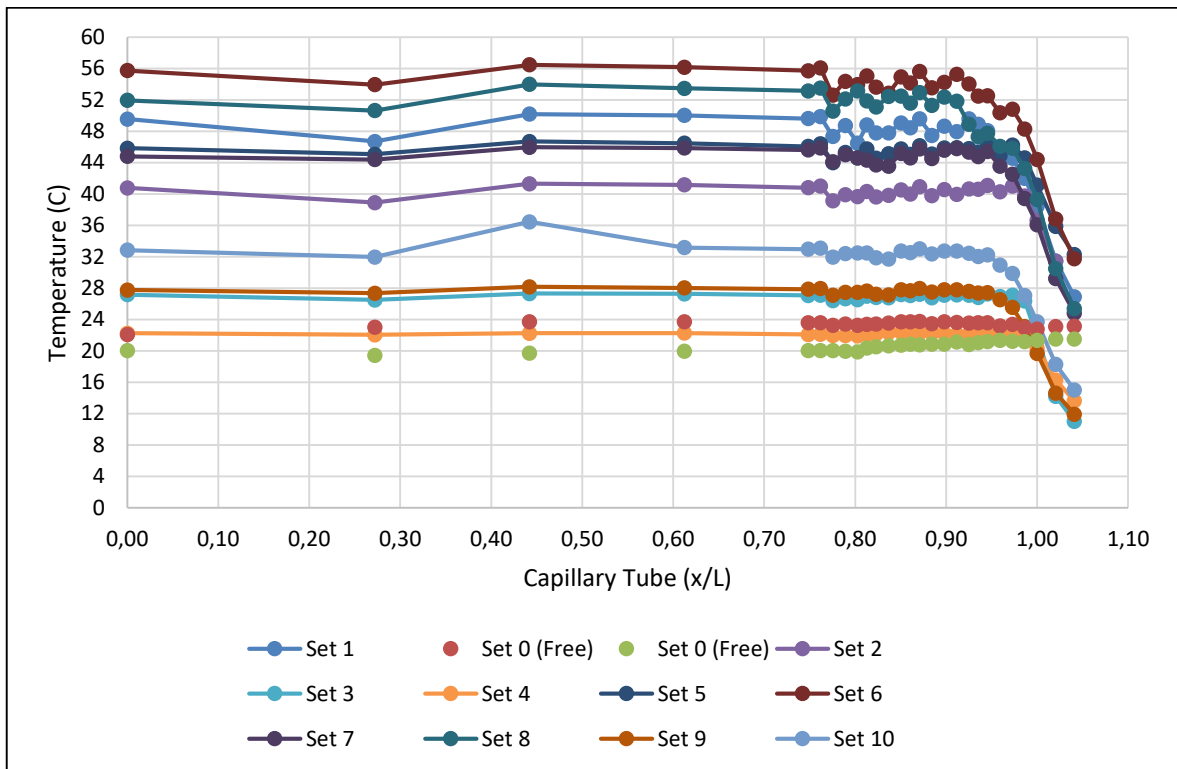


Figure 5.2: Capillary tube temperature distribution

In capillary tube, temperature is also decreased from entrance to exit due to pressure change as it can be seen from above graph. The temperature stays almost same until the rapid pressure drop that the flow changes its phase to two-phase mixture.

In single phase region fluid stays stable. After one phase region, temperature cannot stay stable due to pressure change and rapidly decreases towards to exit of capillary tube. Before rapid decrease of temperature, drops and ups can be seen from the graph. These instabilities of temperature shows that the flow becomes two-phase flow.

Temperature of evaporator is measured at five different points,

Table 5.7: Evaporator temperatures

Set/ Channel	219 (C)	220 (C)	301 (C)	302 (C)	303 (C)
0 (Free)	23.12	23.28	22.69	23.13	23.37
0 (Free)	21.52	21.80	21.42	21.83	21.93
1	28.06	28.21	27.60	28.80	28.86
2	11.04	10.69	10.25	11.56	11.66
3	13.61	13.36	12.75	14.07	14.25
4	32.26	32.55	31.95	33.78	34.16
5	31.74	31.81	31.14	32.87	32.76
6	24.81	24.59	24.22	25.38	25.54
7	25.40	25.37	24.89	26.24	26.38
8	11.91	11.57	11.25	12.44	12.80
9	15.02	14.75	14.41	15.70	16.02
10	17.68	17.45	17.12	18.47	18.75

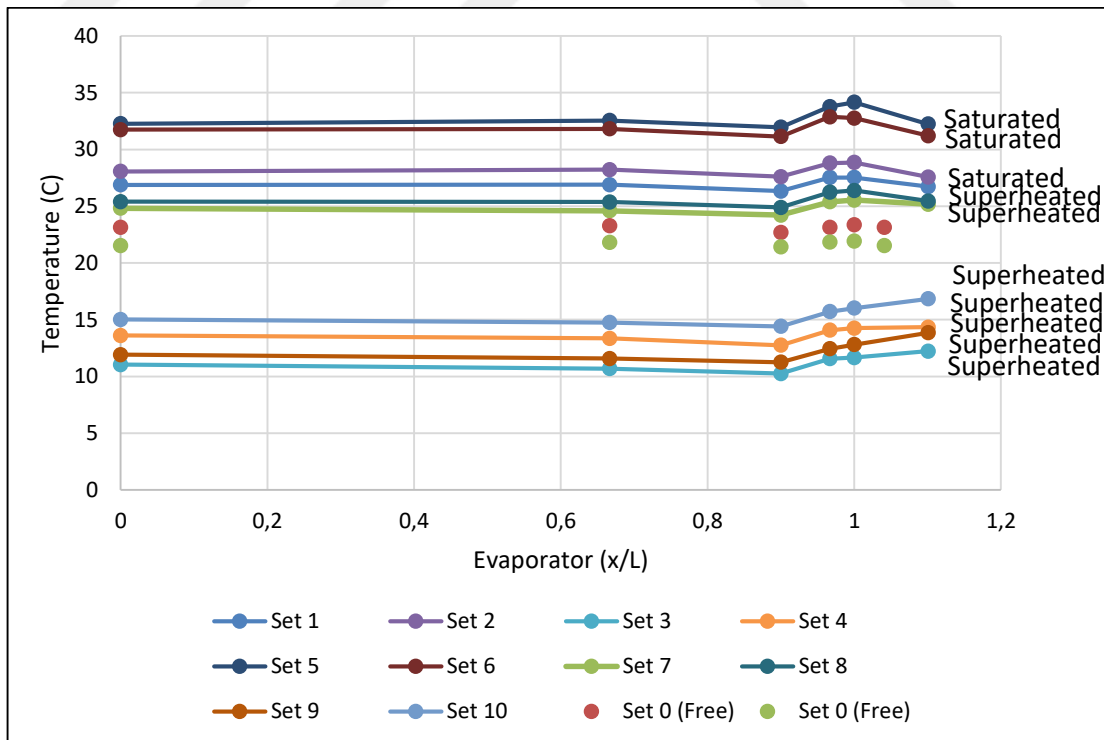


Figure 5.3: Evaporator Temperature Distribution

Evaporator temperature is same through the process till just before the exit. Fluid changes phase before exit of evaporator due to evaporation. After evaporation temperature increases.

Entrance and exit temperatures of compressor are measured.

Table 5.8: Compressor temperatures

Set	Entrance	Exit
0 (Free)	23.30	23.62
0 (Free)	21.73	24.82
1	27.57	66.21
2	12.23	37.08
3	14.34	39.34
4	32.24	75.32
5	31.20	74.04
6	25.18	61.06
7	25.46	65.88
8	13.85	39.18
9	16.84	45.29
10	18.77	49.73

Beside refrigerant temperature, air temperatures are measured and can be seen below:

Table 5.9: Air temperatures I

Set/ Channel	Air Befor Evap		Between Cond Evap		After Condenser			
	308 (C)	309 (C)	310 (C)	311 (C)	315 (C)	316 (C)	317 (C)	318 (C)
0 (Free)	24.04	24	23.7	23.53	23.38	23.25	23.22	23.01
0 (Free)	22.7	22.66	22.47	22.39	22.42	22.32	22.3	22.1
1	57.37	56.8	32.13	30.75	59.78	59.75	59.67	58.23
2	32.89	32.66	13.79	12.66	36.03	36	35.98	34.91
3	33.47	33.34	16.61	16.01	35.2	35.14	35.16	34.32
4	64.13	63.59	36.17	34.88	66.68	66.66	66.67	64.96
5	65.34	64.46	35.08	33.66	70.7	70.65	70.58	68.71
6	49.3	48.8	27.44	27.23	58.87	58.77	58.76	56.96
7	53.14	52.6	28.45	28.39	64.25	64.1	64.11	62.26
8	34.44	34.25	14.64	14.22	38.61	38.52	38.56	37.43
9	39.72	39.43	17.91	17.53	45.65	45.65	45.76	44.53
10	43.81	43.51	20.68	20.35	50.9	50.95	51.07	49.92

Table 5.10: Air temperatures II

	<b>Before Nozzle</b>	<b>Outside Air</b>
<b>Set/Channel</b>	<b>319 (C)</b>	<b>320 (C)</b>
0 (Free)	23.77	17.36
0 (Free)	22.34	17.78
1	55.83	18.2
2	33.96	17.76
3	34.19	18.19
4	61.99	18.79
5	62.75	18.09
6	52.87	17.66
7	57.31	17.93
8	35.96	17.01
9	41.97	17.19
10	46.58	17.36

Air is circulated by fan through system. Air temperature is cooled in evaporator although it is heated through condenser due to work input and output from component to and from air.

Besides temperature readings, one more thing needs to be measured. Air mass flow rate is found from pressure sensors through designed flow nozzle. Following current differences are read from sensor.



Table 5.11: Current differences of flow from flow nozzle

Set/Channel	321 (C)
0 (Free)	0.01276
0 (Free)	0.00830
1	0.01167
2	0.00810
3	0.01240
4	0.01142
5	0.00754
6	0.00774
7	0.00768
8	0.00807
9	0.00795
10	0.00788

Above currents are used to get air mass flowrate by converting current differences into pressure differences.

After gathering data from test setup, first step is to calculate mass flowrate of air. Secondly, to find out heat transfer from and to air with calculated mass flowrate of air. Using equation (3.1 and (3.2, the mass flowrate of air,  $Q_H$  at the condenser, and  $Q_L$  at the evaporator are obtained and the results can be seen from Table 5.12.

Table 5.12: Air cycle calculation results

Set	I (A)	P Diff (Pa)	T (C)	$\rho$ (kg/m <sup>3</sup> )	Q (m <sup>3</sup> /s)	$\dot{m}$ (kg/s)	Eva (kW)	Cond (kW)	Diff (kW)
1	0.0117	121.4	55.83	1.073	0.076	0.082	2.11	2.3	0.19
2	0.0081	65.7	33.96	1.149	0.054	0.062	1.22	1.41	0.18
3	0.0124	132.8	34.19	1.149	0.077	0.088	1.52	1.66	0.14
4	0.0114	117.4	61.99	1.053	0.076	0.08	2.27	2.46	0.19
5	0.0075	56.9	62.75	1.051	0.053	0.055	1.7	1.99	0.29
6	0.0077	60	52.87	1.083	0.053	0.058	1.26	1.8	0.54
7	0.0077	59.1	57.31	1.068	0.053	0.057	1.4	2.02	0.62
8	0.0081	65.1	35.96	1.142	0.054	0.062	1.24	1.48	0.24
9	0.008	63.4	41.97	1.12	0.054	0.06	1.33	1.68	0.35
10	0.0079	62.2	46.58	1.104	0.054	0.059	1.38	1.8	0.42

After performing calculations on the air cycle, the next step is to analyse the refrigerant cycle. Enthalpy values are found for the values of temperature and pressure at various locations: at the evaporator entrance and exit (see Table 5.13), at the condenser entrance and exit (see Table 5.14) and at the compressor entrance and exit (see Table 5.15).

Table 5.13: Enthalpy values at the evaporator

#	Evaporator Entrance			Evaporator Exit		
	T (C)	P (kPa)	h (kJ/kg)	T (C)	P (kPa)	h (kJ/kg)
1	28.06	728.18	258.24	28.86	728.18	414.70
2	11.04	429.38	238.08	11.66	429.38	405.48
3	13.61	467.06	230.80	14.25	467.06	406.93
4	32.26	821.57	266.37	34.16	821.57	417.93
5	31.74	809.55	281.73	32.76	809.55	416.74
6	24.81	661.84	265.59	25.54	661.84	412.97
7	25.40	673.54	277.46	26.38	673.54	413.53
8	11.91	441.73	238.98	12.80	441.73	406.22
9	15.02	488.88	246.37	16.02	488.88	408.04
10	17.68	531.91	252.25	18.75	531.91	409.56

Table 5.14: Enthalpy values at the condenser

#	Condenser Entrance			Condenser Exit		
	T (C)	P (kPa)	h (kJ/kg)	T (C)	P (kPa)	h (kJ/kg)
1	60.08	1573.82	429.57	41.22	1573.82	258.24
2	34.97	880.10	417.33	27.47	880.10	238.08
3	35.88	871.74	418.52	22.36	871.74	230.80
4	68.57	1824.47	434.53	46.59	1824.47	266.37
5	68.67	2022.35	429.39	56.42	2022.35	281.73
6	56.54	1543.28	425.77	46.08	1543.28	265.59
7	61.48	1733.64	427.22	53.73	1733.64	277.46
8	42.82	933.14	424.58	28.10	933.14	238.98
9	56.22	1095.36	435.63	33.20	1095.36	246.37
10	63.27	1238.19	440.66	37.20	1238.19	252.25

Table 5.15: Enthalpy values at the compressor

#	Compressor Entrance			Compressor Exit		
	T (C)	P (kPa)	h (kJ/kg)	T (C)	P (kPa)	h (kJ/kg)
1	27.57	728.18	413.63	66.21	1573.82	437.293
2	12.23	429.38	405.56	37.08	880.10	419.618
3	14.34	467.06	406.72	39.34	871.74	422.254
4	32.24	821.57	415.89	75.32	1824.47	443.352
5	31.20	809.55	415.40	74.04	2022.35	437.209
6	25.18	661.84	412.42	61.06	1543.28	431.539
7	25.46	673.54	412.57	65.88	1733.64	433.141
8	13.85	441.73	406.45	39.18	933.14	420.601
9	16.84	488.88	408.06	45.29	1095.36	423.419
10	18.77	531.91	409.10	49.73	1238.19	425.106

Now the refrigerant mass flowrate can be obtained from Eq. (3.7) and (3.8) using these enthalpy values. In addition, Eq. (3.6) is employed to obtain the flowrate directly from the compressor inner volume, the volumetric efficiency, the compressor rotational speed and the density at the compressor inlet. Mass flowrates obtained by three different methods are listed in Table 5.16 and plotted in Figure 5.4.

Table 5.16: Mass flow rates using three different methods

#	Evaporator	Condenser	Volumetric Compressor
	$\dot{m}$ (kg/s)	$\dot{m}$ (kg/s)	$\dot{m}$ (kg/s)
1	0.0135	0.0134	0.0102
2	0.0073	0.0079	0.0064
3	0.0086	0.0088	0.0068
4	0.0150	0.0146	0.0117
5	0.0126	0.0135	0.0114
6	0.0086	0.0112	0.0095
7	0.0103	0.0135	0.0096
8	0.0074	0.0080	0.0067
9	0.0082	0.0089	0.0074
10	0.0088	0.0096	0.0078

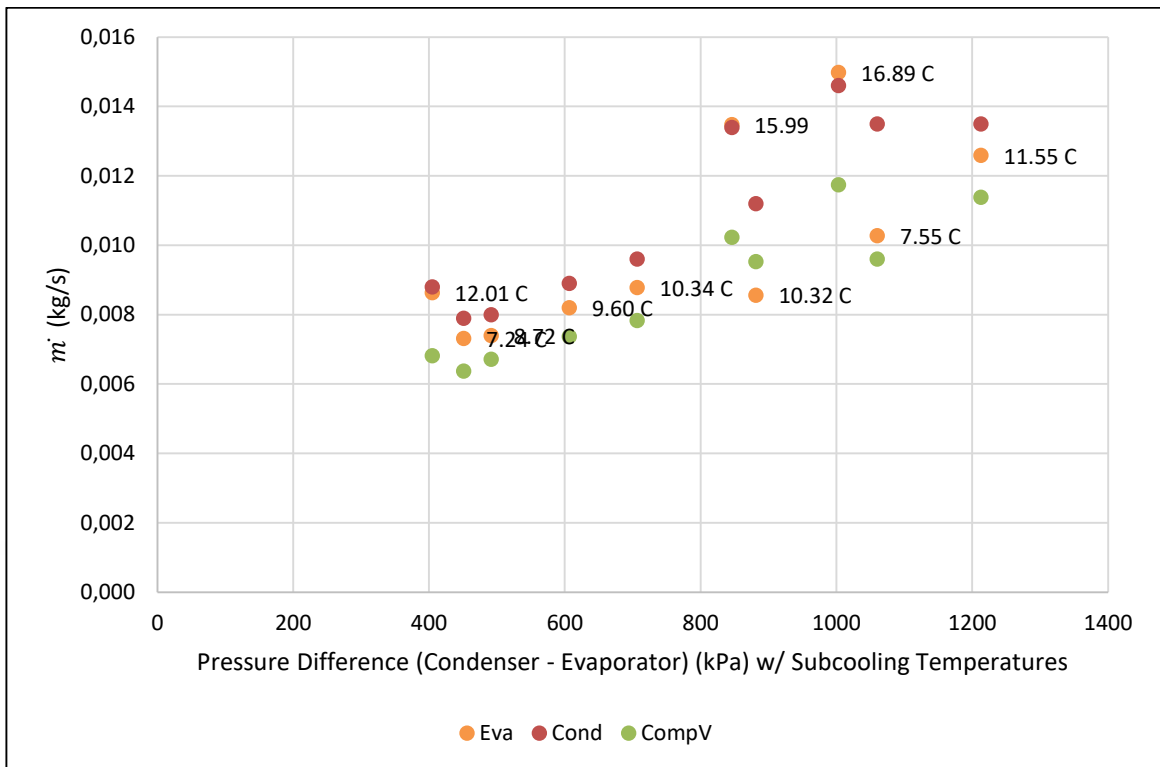


Figure 5.4: Mass flow rates versus pressure differences between the condenser and evaporator at given subcooling temperatures using three different methods

As it can be seen from Figure 5.4, volumetric compressor mass flowrates and evaporator mass flowrates are closer. However, condenser mass flowrates are higher than the others almost always. The reason for this may be that heat loss at the condenser is higher because its higher average refrigerant temperature, and that the higher heat loss affects the energy balance between air and refrigerant for the purpose of calculating the refrigerant mass flowrate.

At two tests (845 kPa and 1003 kPa pressure differences), mass flowrates obtained by the energy balances of evaporator and condenser are relatively high compared to the other data set trend. It is noted that the subcooling temperatures of the two data points (15.99°C and 16.89°C, respectively) are larger than the other data set. Therefore, it is believed that the single liquid-phase region in the capillary tube must be longer, resulting in higher mass flowrates.

In order to examine the effect of thermocouple measurement accuracy on calculating mass flowrates, temperature measurement values are varied by  $\pm 0.5^\circ\text{C}$  because the accuracy of

measurement by a thermocouple is believed to be about  $0.5^{\circ}\text{C}$ . As shown in Table 5.17, mass flowrate is not affected by more than 0.5%. Therefore, the present study assumes the thermocouple measurement error to be negligible in flowrate calculation.

Table 5.17: Sensitivity study of thermocouples on mass flowrates

Set	Evap	Cond	
	(-)0.5°C	(-)0.5°C	(+)0.5°C
1	0,52%	0,30%	-0,33%
2	0,46%	0,30%	-0,33%
3	0,49%	0,29%	-0,33%
4	0,44%	0,23%	-0,28%
5	0,40%	0,15%	-0,20%
6	0,45%	0,23%	-0,23%
7	0,52%	0,31%	-0,39%
8	0,52%	0,27%	-0,33%
9	0,44%	0,24%	-0,25%
10	0,48%	0,30%	-0,34%

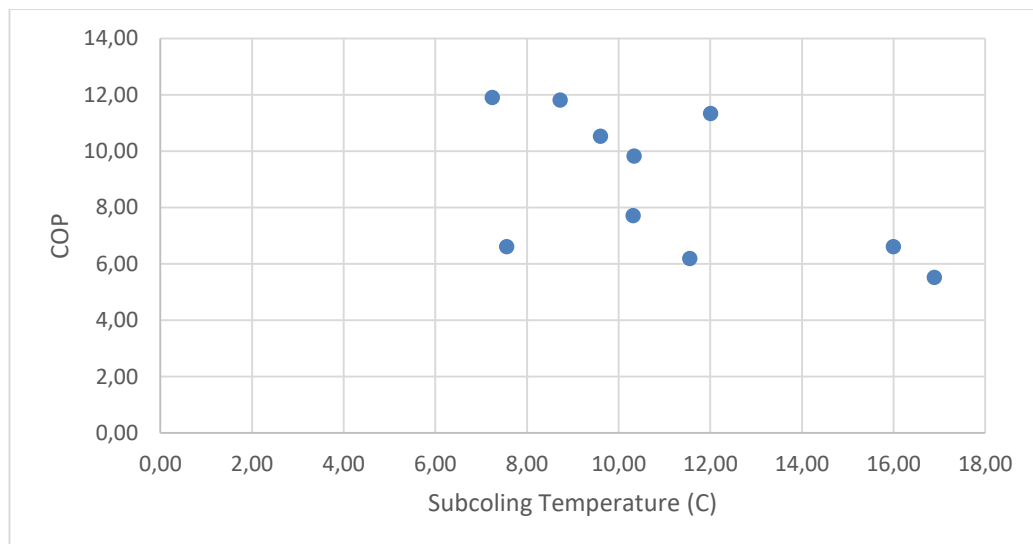


Figure 5.5: COP of experimental results

Table 5.5 examines the coefficient of performance (COP) of the present vapor compression refrigeration cycle as a function of subcooling temperature. As it can be seen from the figure, it seems that the COP of the cycle increases with decreasing subcooling, but the correlation between the subcooling temperature and COP appears to be very weak.

## **5.2. NUMERICAL RESULTS**

Two different numerical models have been developed as mentioned before to predict refrigerant mass flowrate and the exit pressure of the capillary tube. The first model divides the capillary tube into two regions (liquid phase and two-phase phase ) and does not consider metastable condition. On the other hand, the second model divides the tube into four regions (single-phase liquid, metastable liquid, mixture of metastable liquid and two-phase flow, and two-phase flow) by including the metastable phenomenon. Thus the main difference between two methods is whether to include the metastable phenomenon or not.

### **5.2.1. Numerical Model Without Considering Metastable Phenomenon**

The first approach considers two regions, single-phase liquid and two-phase liquid-vapor flow regions. This model includes the diameter, roughness and length of the capillary tube and the inlet condition (pressure and subcooling temperature) at the inlet of the tube as parameters. It calculates pressure decrease along the tube. The numerical step size of pressure is 1 Pa in the most calculations. At each 1 Pa decrease of pressure along the tube, the tube location and thermodynamic properties at the location are calculated. Viscosity effect of two-phase flow is also included. The tube is considered as adiabatic and the flow inside the tube is assumed to be homogenous two-phase flow. In the first model, metastable liquid is neglected and thermodynamic equilibrium through the tube is assumed. In order to find mass flowrate for a given exit pressure, initial guess is needed for mass flowrate. By trial and error, the mass flowrate is found for the given pressure at the exit of the tube. On the other hand, as calculation proceeds, it is checked to see whether the decrease of entropy takes place or not. If entropy at the location decreases, it means that choking must take place. If choking takes place before the end of the capillary tube (which is not possible physically), the mass flowrate has to be decreased in such a way that the choking may happen at the end

of the tube. In this case, the mass flowrate is found independent of the exit pressure. And the exit pressure is obtained for the maximum flowrate with choking at the exit.

Table 5.18: Mass flow rate results of non-metastable model

#	P (kPa)	T (C)	$\dot{m}$ (kg/s)
1	1573.81	41.22	0.01006
2	880.10	27.47	0.00601
3	871.73	22.36	0.00678
4	1824.46	46.59	0.01102
5	2022.35	56.42	0.01064
6	1543.28	46.08	0.00896
7	1733.64	53.73	0.00901
8	933.13	28.1	0.00650
9	1095.36	33.2	0.00728
10	1238.18	37.19	0.00794

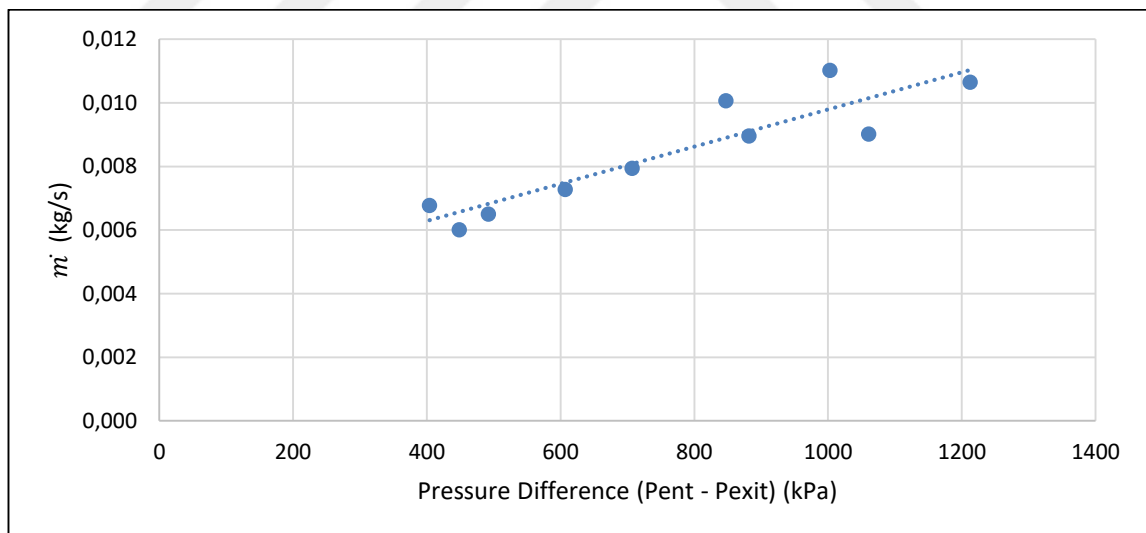
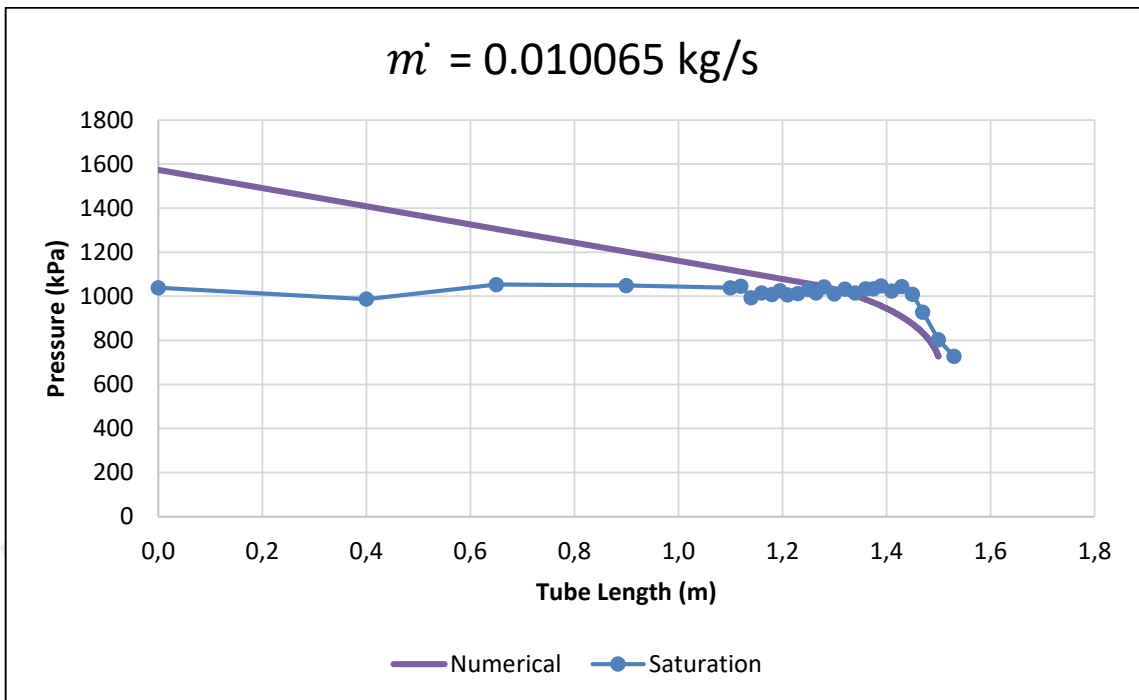
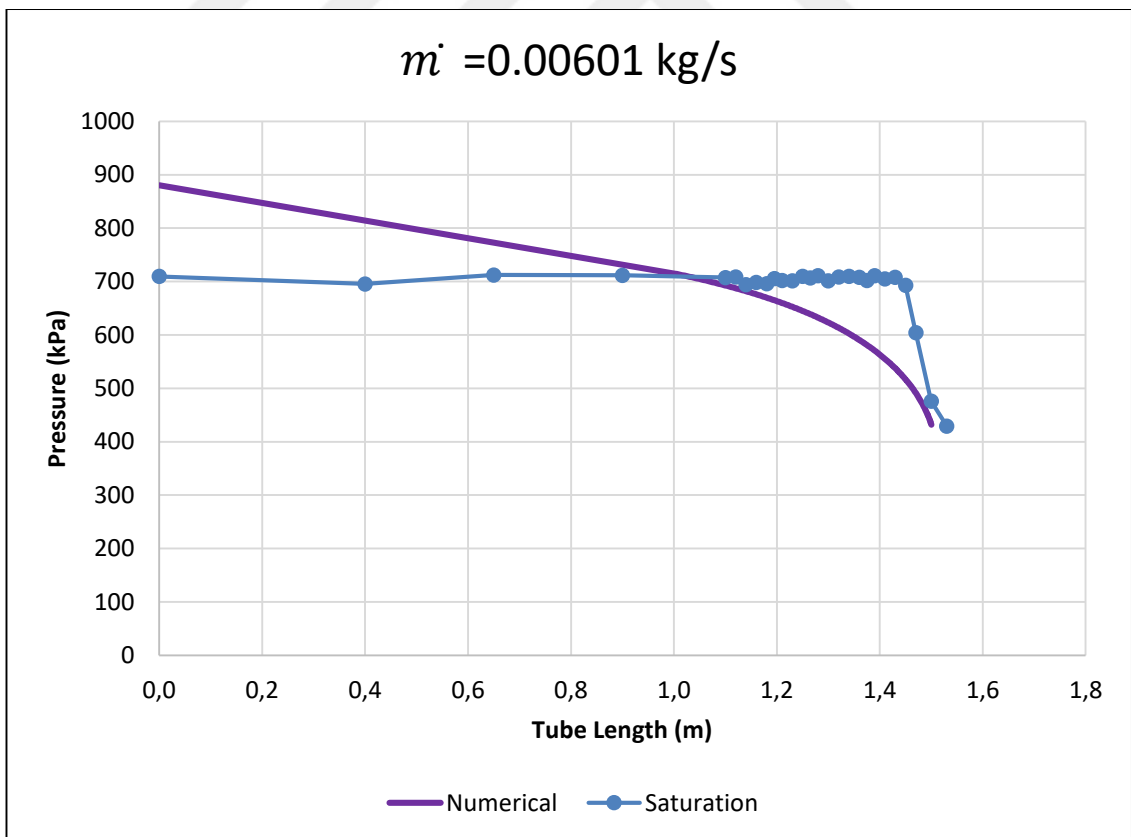


Figure 5.6: Mass flow rate vs pressure difference (inlet-exit) for the model without metastable condition

By employing the first numerical model without consideration of metastable condition, mass flowrates are calculated for given pressures at the tube exit. As it can be seen from Figure 5.6, mass flowrate increases as expected when the pressure difference between condenser and evaporator increases.

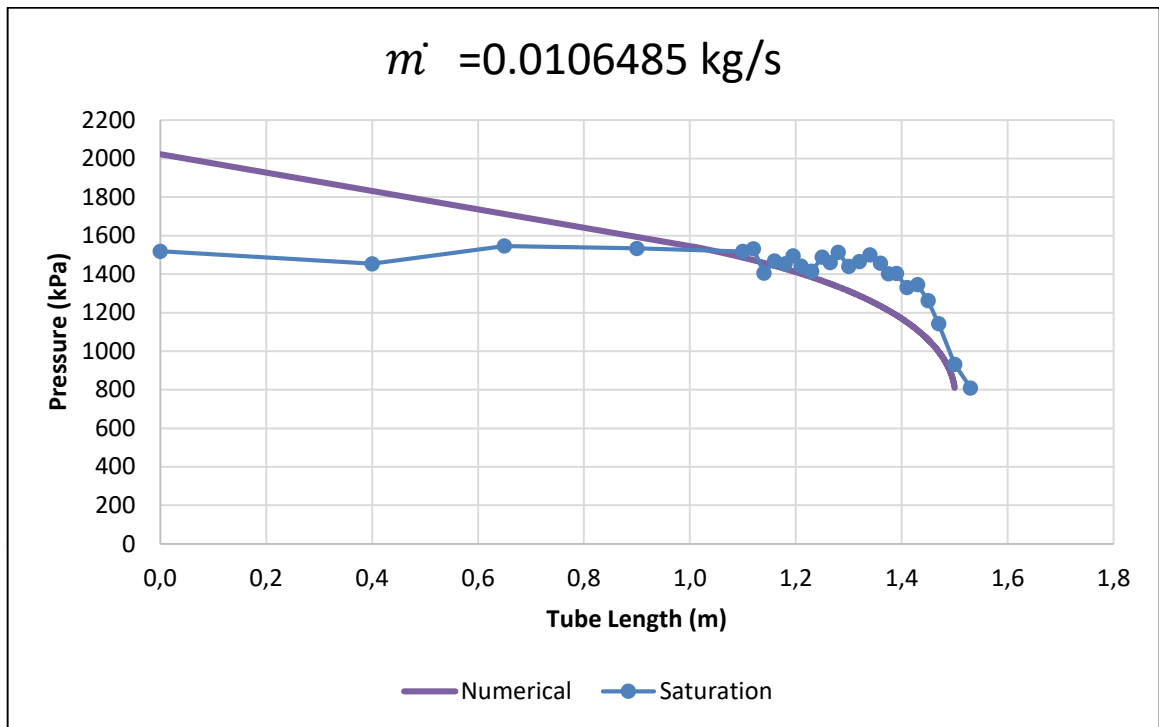


(a)

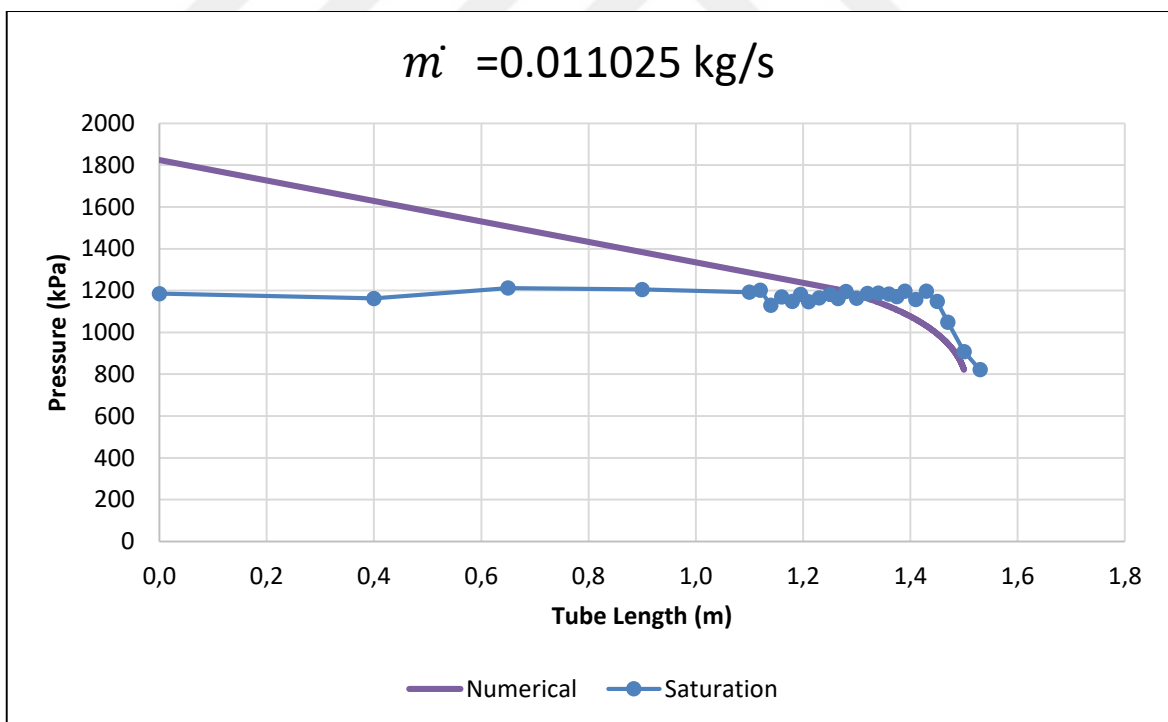


(b)





(c)



(d)

Figure 5.7: Pressure drops over capillary tube for different mass flowrates vs experimental results

When the expected pressure from model is compared with saturation pressure the difference can be seen. Pressure is a dynamic property that its change is quicker than temperature. Due to this rapid change, pressure decrease is affected more. Saturation pressure is found from the saturation temperature at related point that the difference occurs.

The graphs vary from each other by mass flowrate. When mass flowrate is increased the difference between saturation pressure and pressure of numerical model coincide with more in the two-phase region. In Figure 5.7, difference can be seen clearly between b and d graphs. On the other hand, as it can be seen from a and b graphs of Figure 5.7, when the mass flowrate increases single phase length of the flow increases. Numerical result of two-phase flow follows the saturation pressure after critical point.

Numerical model is also tested with change of capillary tube diameter and roughness affects. Change of roughness on mass flowrate has no effect. Difference between two situations mass flowrates are not larger than 0.03 percent at most. Even though roughness has no effects on calculations, copper roughness is considered and used as  $9 \times 10^{-8}$  m.

Table 5.19: Capillary tube roughness affect on numerical model with non-metastable approach

Set	$\dot{m}$ (kg/s)		Difference
	$\varepsilon = 0$	$\varepsilon = 9 \times 10^{-8}$	
1	0.010065	0.010064	0.01%
2	0.00601	0.006012	0.03%
3	0.00678	0.00678	0.01%
4	0.011025	0.011025	0.00%
5	0.010649	0.010649	0.00%
6	0.008965	0.008965	0.00%
7	0.009019	0.009019	0.00%
8	0.006501	0.006501	0.00%
9	0.007285	0.007285	0.00%
10	0.007941	0.007941	0.00%

Table 5.20: Capillary tube diameter affect on numerical model with non-metastable approach

Set	$\dot{m}$ (kg/s)		Difference
	d= 1.30 mm	d= 1.31 mm	
1	0.010065	0.010264	1.93%
2	0.00601	0.006131	1.97%
3	0.00678	0.006915	1.95%
4	0.011025	0.011243	1.93%
5	0.010649	0.010857	1.92%
6	0.008965	0.00914	1.92%
7	0.009019	0.009196	1.92%
8	0.006501	0.00663	1.94%
9	0.007285	0.007428	1.93%
10	0.007941	0.008097	1.93%

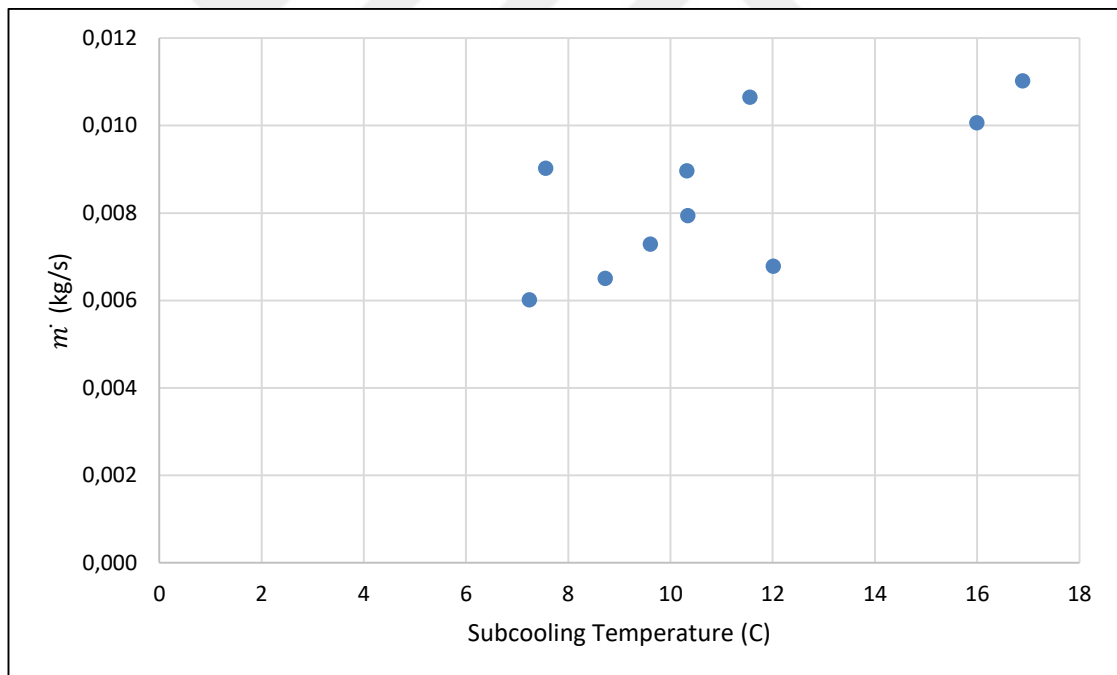


Figure 5.8: Mass flowrate vs subcooling temperature for numerical model without consideration of metastable condition

Subcooling temperature is another separator characteristic when mass flowrate is investigated. When subcooling temperature is increased, mass flowrate is also increased. Since the temperature difference between condenser saturation temperature and exit temperature is high, the pressure difference is also high, this pressure difference is a result of mass flowrate. It can be concluded as higher subcooling temperature can result in higher mass flowrate.

### **5.2.2. Numerical Model With Considering the Metastable Phenomenon**

Consideration of metastability in the model divides the flow into four regions as it is seen from

Figure 5.9 from Guobing Z, and Yufeng Z[2] study. The first region is assumed as single phase subcooled liquid region. After pressure decreases to saturation pressure, vaporization may be delayed that it occurs at some point below saturation pressure. From saturation point to vaporization occurring point is the second region as metastable liquid region. Flow becomes two-phase after vaporization and flow reaches and equilibrium at a point. This is the third region as metastable two-phase region where the metastable liquid and two-phase flow are mixed. The rest of the flow is considered as fourth region as equilibrium two-phase region.

The flow in the numerical model with metastable phenomenon is also considered as adiabatic flow. Length of tube is controlled and 0.00001 m is used as step size. After each step pressure decrease and thermodynamic properties are calculated for the pressure value. Entropy decrease is controlled and choking situation is checked. Viscosity effects of two-phase flow is included. Moreover, acceleration term of fluid in two-phase flow is also considered. Model requires initial guess for mass flowrate for given subcooling temperature and initial pressure, and pressure at the end of the capillary tube is obtained as output when choking takes place. When choking does not occur, the same iteration model is performed to obtain mass flowrate for a given exit pressure.

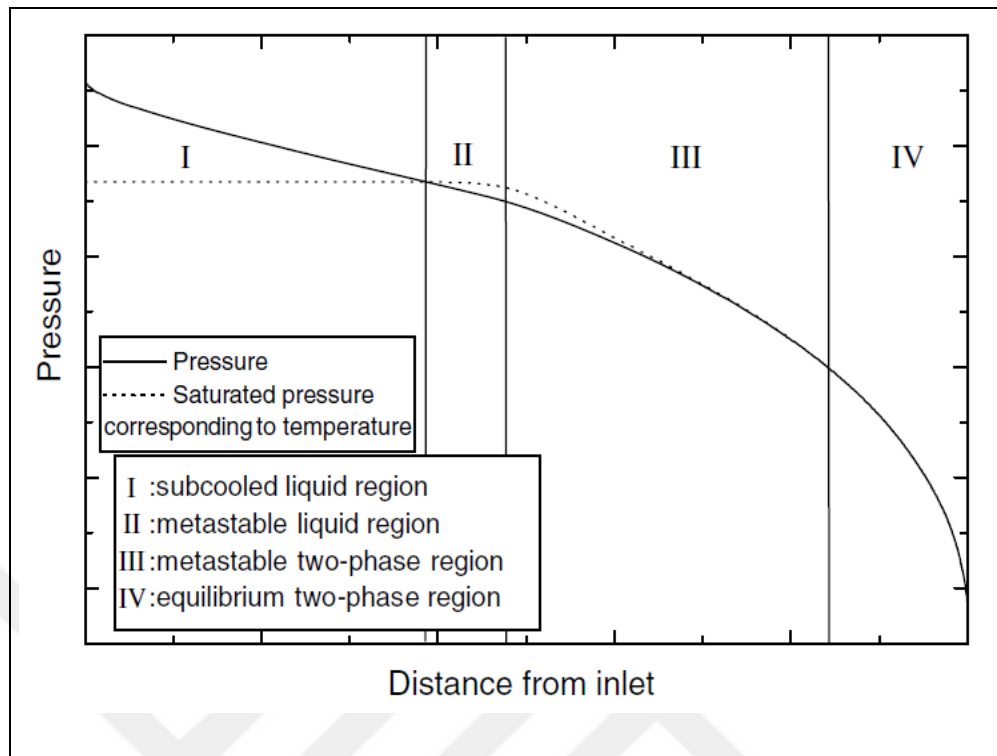


Figure 5.9: Regions of second numerical model with metastable phenomena

Table 5.21: Mass flowrates from the model considers metastable condition

Set	P (kPa)	T sub(C)	$\dot{m}$ (kg/s)
1	1573.817	15.99	0.01056150
2	880.103	7.24	0.00632260
3	871.736	12.01	0.00715430
4	1824.467	16.89	0.01155470
5	2022.350	11.55	0.01109555
6	1543.280	10.32	0.00936702
7	1733.640	7.55	0.00940280
8	933.139	8.72	0.00682930
9	1095.360	9.60	0.00763860
10	1238.189	10.34	0.00831522

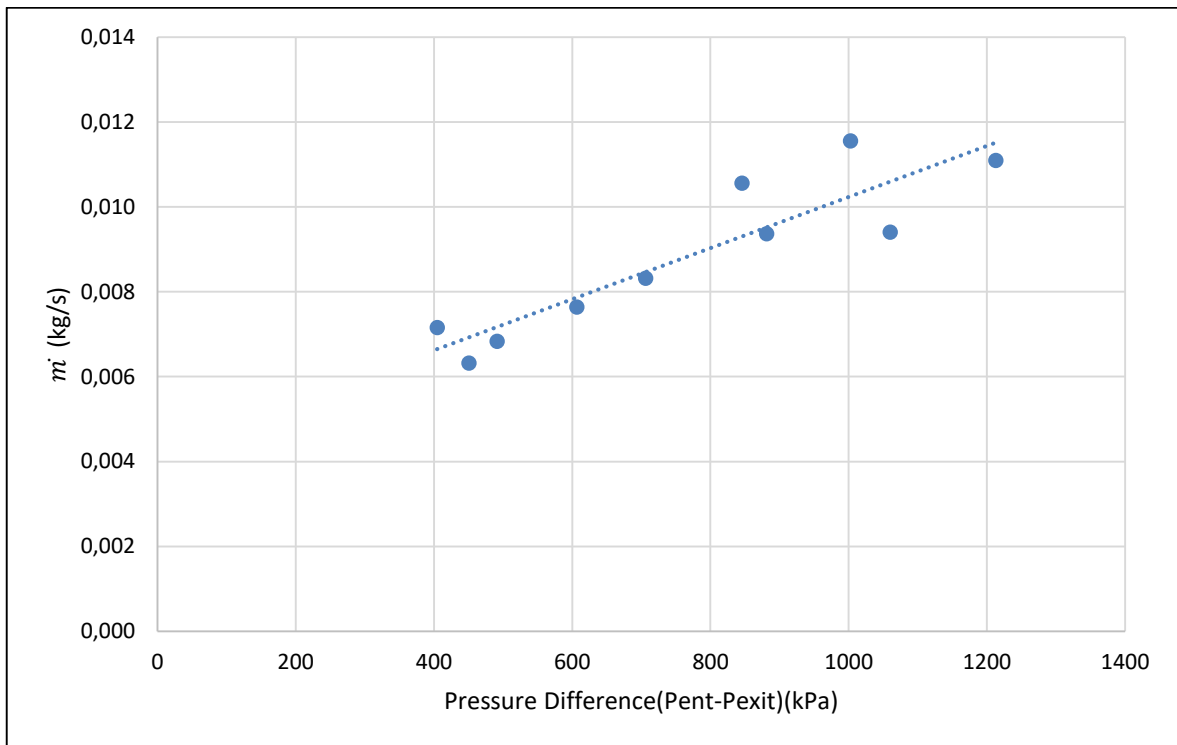


Figure 5.10: Mass flowrates vs pressure differences for the model with metastable condition

Results of the second model show that mass flowrate increases with higher pressure difference between the entrance and exit of the capillary tube. The mass flowrate seems to increase linearly with the pressure difference as shown in Table 5.10.

The effect of the roughness and diameter of the tube is investigated. Roughness has no considerable effect on mass flowrate calculations. The results with the completely smooth tube and with some rough tube show the maximum difference of 0.71% in mass flowrate.

Table 5.22: Capillary tube roughness affect on mass flowrate

#	$\dot{m}$ (kg/s)		Difference
	$\varepsilon = 0$	$\varepsilon = 0.00000009$	
1	0.01084100	0.010774	0.62%
2	0.00647400	0.006449	0.39%
3	0.00732700	0.0073	0.37%
4	0.01187000	0.011787	0.70%
5	0.01140500	0.0113153	0.79%
6	0.00961200	0.009553	0.61%
7	0.00965753	0.0095888	0.71%
8	0.00699400	0.006966	0.40%
9	0.00782630	0.007791	0.45%
10	0.00852400	0.0084808	0.51%

Capillary tube diameter has rather more effect on mass flowrate calculations. When the capillary tube diameter is increased by 0.01 mm, mass flowrate increases by around 2%. Table 5.23 shows mass flowrates that are calculated with two different diameters as 1.30 mm and 1.31 mm.

Table 5.23: Capillary tube diameter affect on mass flowrate

#	$\dot{m}$ (kg/s)		Difference
	d= 1.30 mm	d= 1.31 mm	
1	0.01056150	0.010774	2.01%
2	0.00632260	0.006449	2.00%
3	0.00715430	0.0073	2.04%
4	0.01155470	0.011787	2.01%
5	0.01109555	0.0113153	1.98%
6	0.00936702	0.009553	1.99%
7	0.00940280	0.0095888	1.98%
8	0.00682930	0.006966	2.00%
9	0.00763860	0.007791	2.00%
10	0.00831522	0.0084808	1.99%

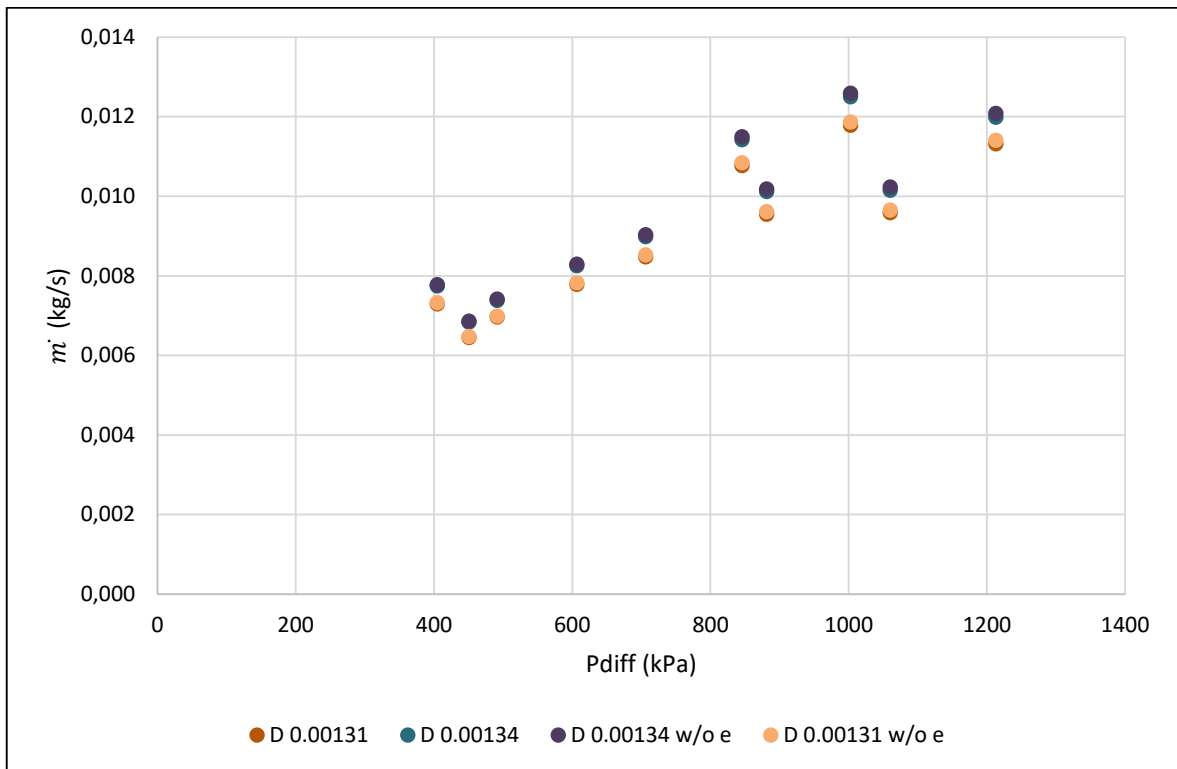


Figure 5.11: Mass flowrates for diameter and roughness changes



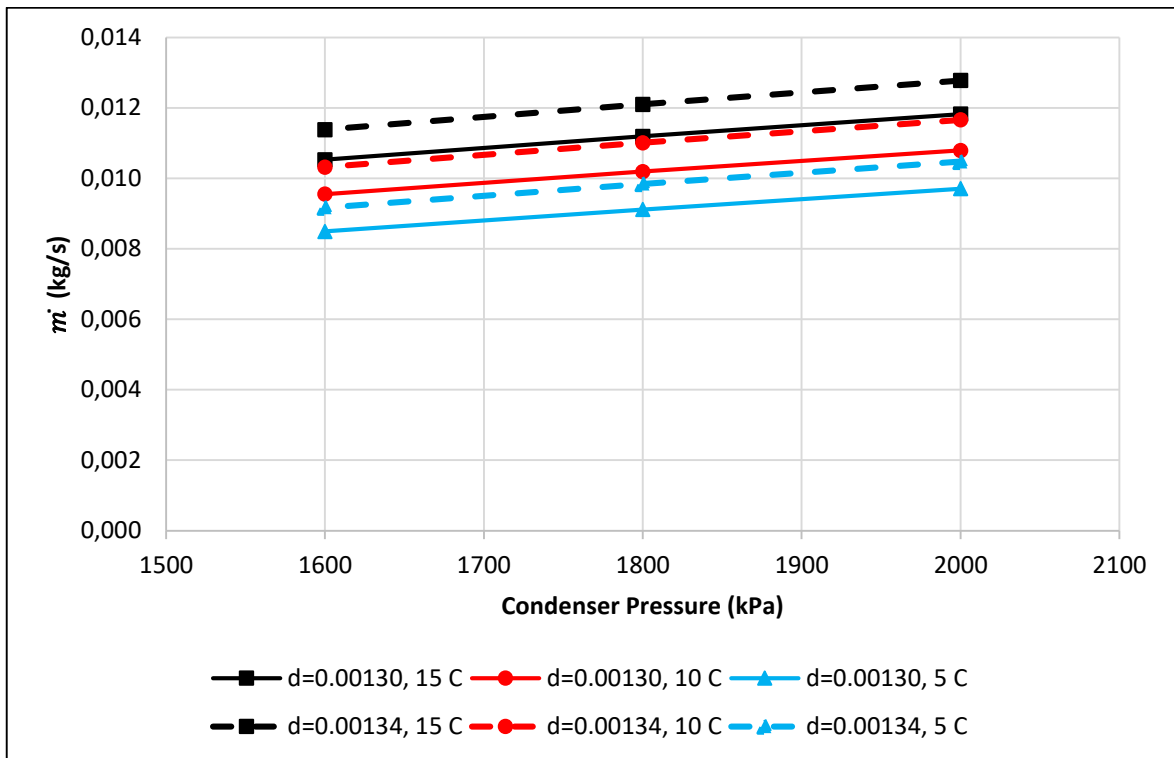


Figure 5.12: Mass flowrates vs entrance pressure of numerical model with metastable condition

Mass flowrate with subcooling temperature is also investigated with respect to the condenser pressure. Numerical results for various capillary tube diameters and subcooling temperatures at the capillary tube inlet can be seen from

Figure 5.12. It shows that mass flowrate increases with increasing tube entrance pressure which is assumed to be equal to the condenser pressure. When the subcooling temperature at the tube inlet increases, mass flowrate also increases with the same entrance pressures.

Choking phenomenon at the exit of the capillary tube is also investigated with the numerical model that includes the metastable phenomenon. The third column in Table 5.24 is the mass flow rate that is calculated numerically with the experimental inlet conditions and the capillary exit pressure data (which is in the second column of the table). Using the same experimental inlet conditions (total 10 data set), the maximum mass flowrate shown in the fourth column of the table is numerically calculated before choking occurs. The maximum mass flowrate with the given inlet conditions can be obtained as follows. When pressure is

calculated along a given tube length with a mass flowrate, the entropy increases downstream along the tube. With a higher mass flowrate, however, the maximum entropy may be achieved before the end of the tube and then the entropy starts decreasing, which is against the second law of thermodynamics, and the higher mass flowrate is not physically possible. Therefore, a lower flowrate is required for the maximum entropy to be achieved at the end of the tube. Thus there is a maximum mass flowrate at which the maximum entropy occurs at the end of the tube, and choking is said to occur at the end of the tube. When choking occurs at the end of the tube, the mass flowrate is independent of the exit pressure. The fifth column of the table shows the exit pressure calculated numerically at choking. When the exit pressures from the experimental data and the exit pressures at choking are compared, their differences are less than 50 kPa for all 10 data set. Therefore, it may be concluded that choking has occurred for all the data set.

Table 5.24: Choking pressures of numerical model with metastable condition

Set	$P_{\text{exit}}$ (kPa) from experimental data	$\dot{m}$ (kg/s) calculated numerically from experimental $P_{\text{exit}}$ data	$\dot{m}$ (kg/s) Maximum mass flowrate calculated numerically before choking occurs	$P_{\text{exit}}$ (kPa) capillary exit pressure at choking	Choking
1	728.480	0.010562	0.010571	687.284	Yes
2	429.598	0.006323	0.006335	390.494	Yes
3	467.654	0.007154	0.007184	415.947	Yes
4	821.915	0.011555	0.011565	770.395	Yes
5	809.634	0.011096	0.011096	794.679	Yes
6	661.695	0.009367	0.009369	651.023	Yes
7	676.550	0.009403	0.009403	671.018	Yes
8	441.944	0.006829	0.006835	415.023	Yes
9	488.681	0.007639	0.007640	473.156	Yes
10	531.741	0.008315	0.008315	531.741	Yes

Figure 5.13 shows comparisons between two cases where one considers the metastable phenomenon and the other does not. With the same inlet conditions and exit pressure, two models yield mass flowrates which differ by only 5 percent. When the metastable phenomenon is included in the model, liquid state is prolonged in the metastable form and

pressure decreases less, compared to two-phase flow when no metastable phenomenon is considered. Table 5.25 shows the comparisons in more detail.

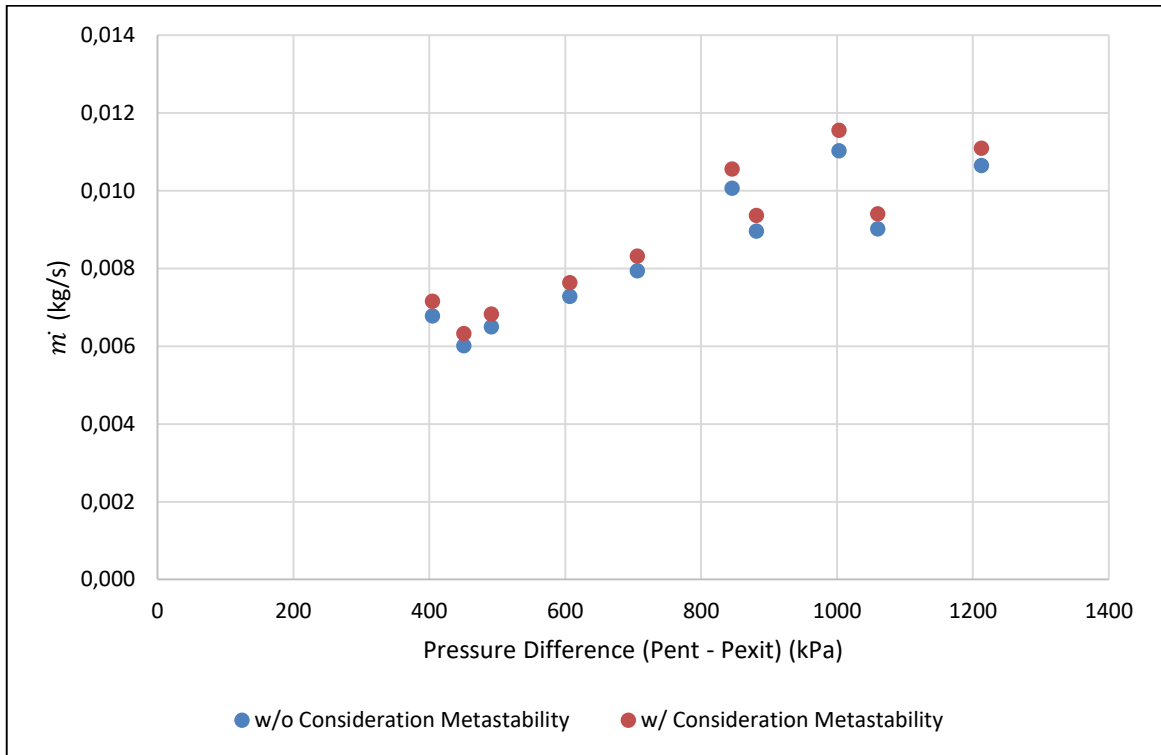
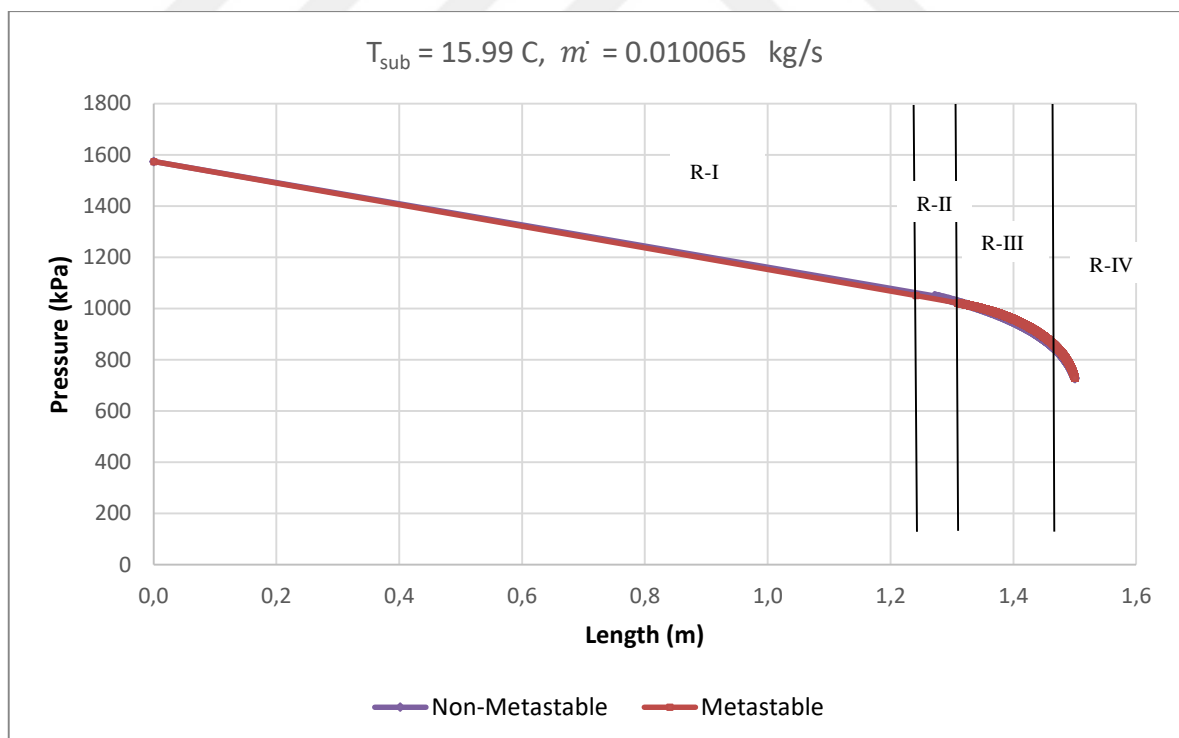


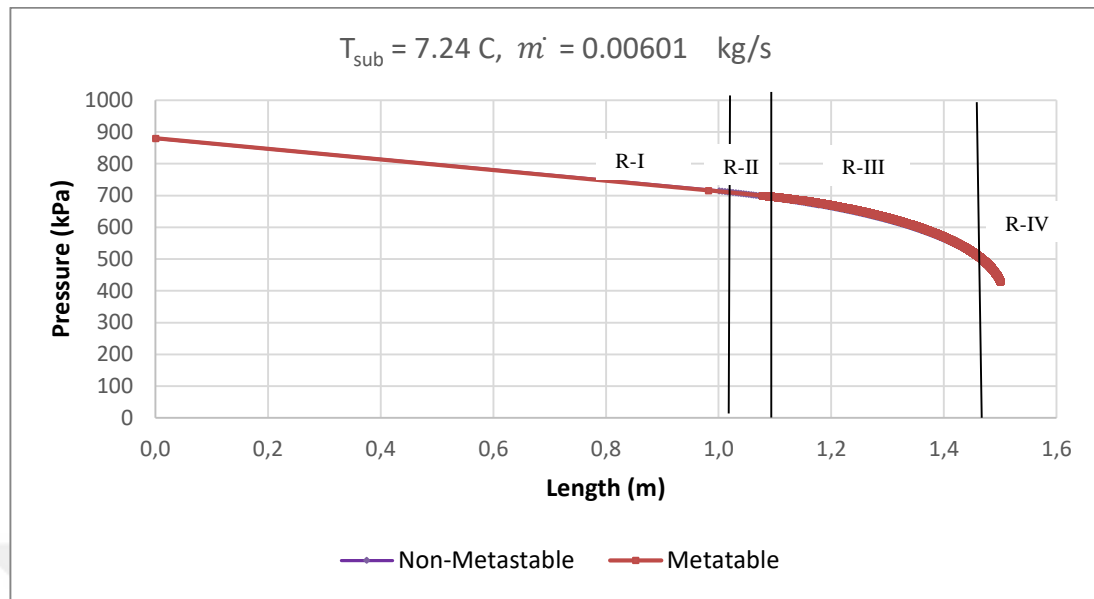
Figure 5.13: Mass flowrates of numerical model with and without consideration of metastable flow

Table 5.25: Mass flowrate results of numerical models

#	Pressure Diff (Cond-Evap) (kPa)	w/o Metastability Model $\dot{m}$ (kg/s)	w/ Metastability Model $\dot{m}$ (kg/s)	Difference (%)
1	845.64	0.0101	0.0106	5%
2	450.73	0.0060	0.0063	5%
3	404.68	0.0068	0.0072	5%
4	1002.90	0.0110	0.0116	5%
5	1212.80	0.0106	0.0111	4%
6	881.44	0.0090	0.0094	4%
7	1060.11	0.0090	0.0094	4%
8	491.41	0.0065	0.0068	5%
9	606.48	0.0073	0.0076	5%
10	706.28	0.0079	0.0083	5%



(a)



(b)

Figure 5.14: Numerical models' pressure results

Pressure distributions in capillary tube in both approaches to model slightly differ from each other although they are almost coinciding with each other. The difference is in the two-phase liquid and vapor region. Because of ignoring metastable phenomena in first numerical approach to model, decreasing of pressure is faster in almost same length in region III. On the other hand, in metastable numerical model, pressure decrease is faster in region II because of consideration of vaporization pressure.

Numerical models' pressure can also be compared with experimental method pressure in a way that the saturation pressure is almost same in region I of both models, after a point it has ups and downs, the pressure starts to change. The point is accurate with numerical models' two-phase region starting points. Phase of fluid starts to change that causes instabilities in flow, temperature starts to decrease and as a result of decrease pressure cannot stay stable anymore.

Using metastable numerical model, temperature of region III can be also calculated. Saturation pressure is found with calculated temperature and if they are compared with saturation pressures of experimental temperatures, it can be seen that they are accurate with each other. In region III of Figure 5.14. both saturation pressures can be seen.

### 5.3. COMPARISON OF NUMERICAL AND EXPERIMENTAL METHODS

This section discusses the comparison of the numerical results with the experimental data in the present study.

Figure 5.15 shows the experimental data of mass flowrate at the same subcooling temperatures and initial pressures with three different methods: two methods by energy balance at the evaporator and condenser between air and refrigerant flows, and the other method using the compressor volume with the volumetric efficiency. As discussed in Section 5.1, mass flowrates by the energy balance at the condenser and evaporator are higher than the compressor volume method. In addition, mass flowrates obtained by the numerical method are also plotted in Figure 5.15, and they appear to be very close to those of the compressor volume method. It is noted that both the compressor volume method and the numerical method do not involve heat transfer amount in calculating mass flowrates.

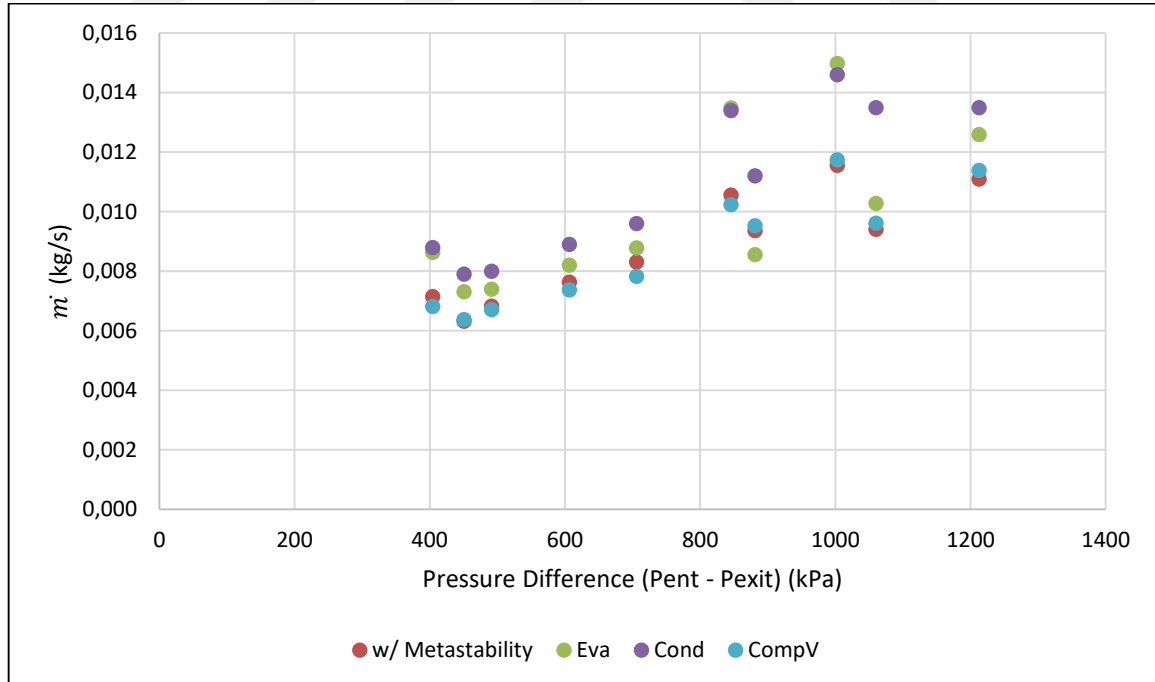


Figure 5.15: Mass flowrates comparison

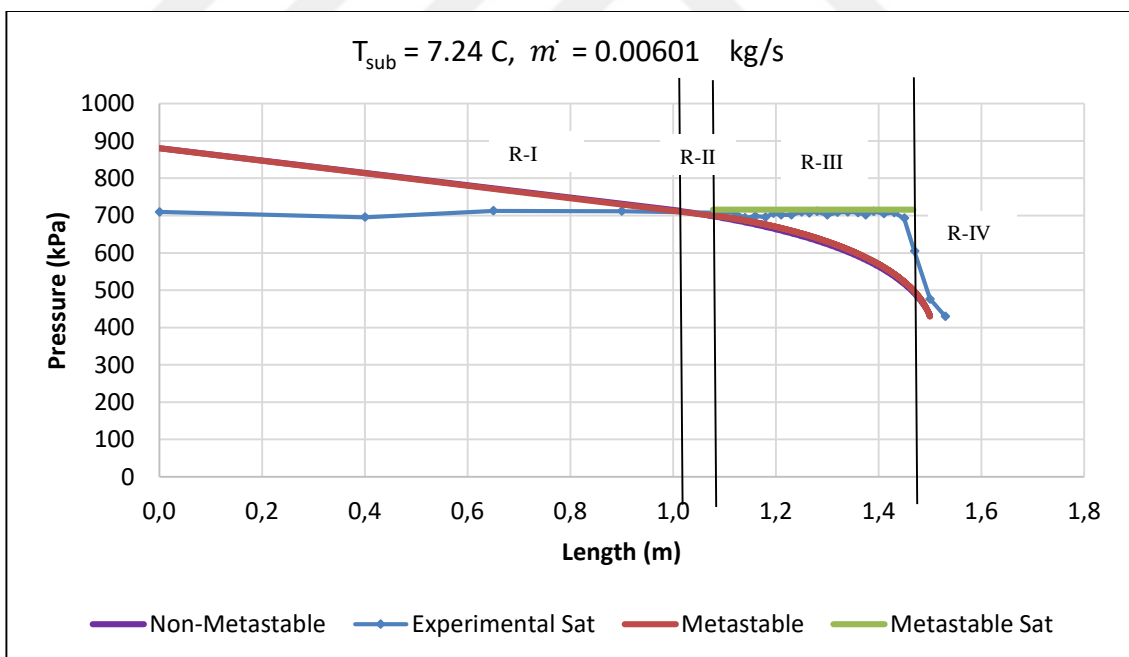
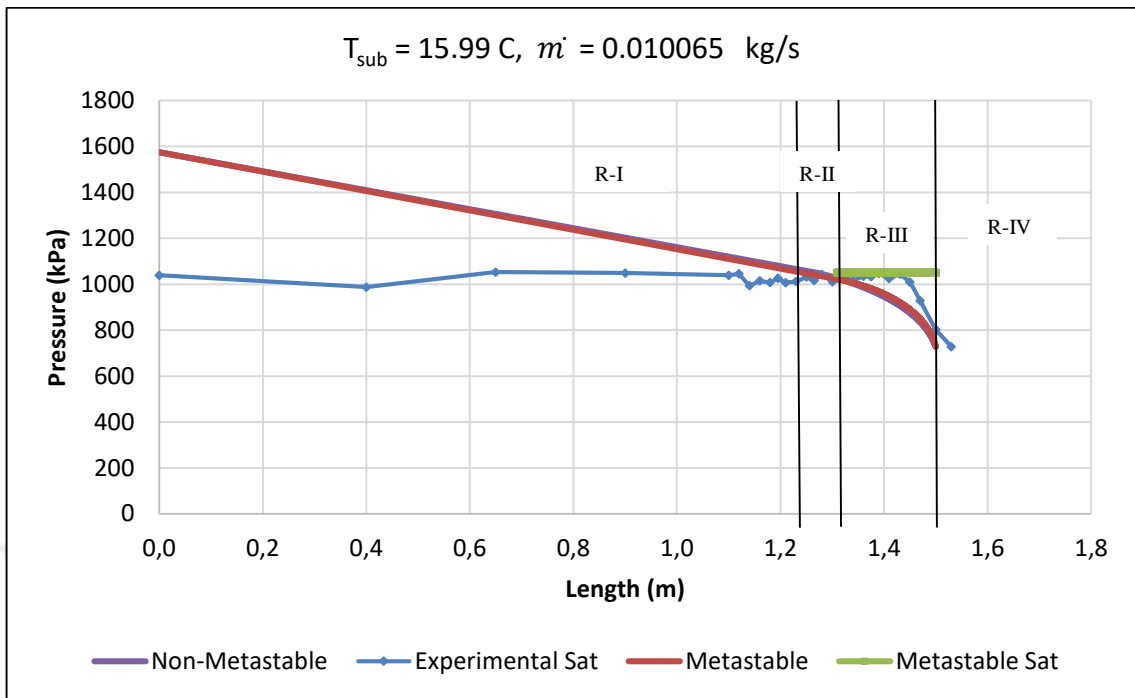


Figure 5.16: Experimental and numerical pressure results

Figure 5.16 shows the comparison of the experimental and numerical results. In experimental data, it is believed that the single-phase region ends at the location where the temperature measurement looks unstable. Thus the numerical model predicts the length of the single-phase region well compared to the result of Figure 5.16 (b) while Figure 5.16 (a) shows some discrepancy. On the other hand, Figure 5.16 (a) shows good agreement in the exit pressure between the experimental and numerical results while (b) shows rather large discrepancy between two results.

It is noted that the mass flowrate is higher with larger subcooling temperature, which ensures a longer single liquid-phase flow since pressure drop in two-phase flow is larger than that in liquid flow with the same flowrate.

Region boundaries of the Figure 5.16 are obtained from numerical results. Figure 5.16 also shows that a larger subcooling temperature results in a long Region I and a short Region III as shown in (a). On the other hand, as shown in Figure 5.16 (b), a smaller subcooling temperature results in a shorter single phase region due to a smaller pressure difference between the inlet pressure and the saturation pressure corresponding to the inlet temperature. For the given tube length of 1.5 m, therefore, the shorter single phase region leads to a longer metastable two-phase region which yields a lower mass flowrate due to higher pressure loss in two-phase flow.



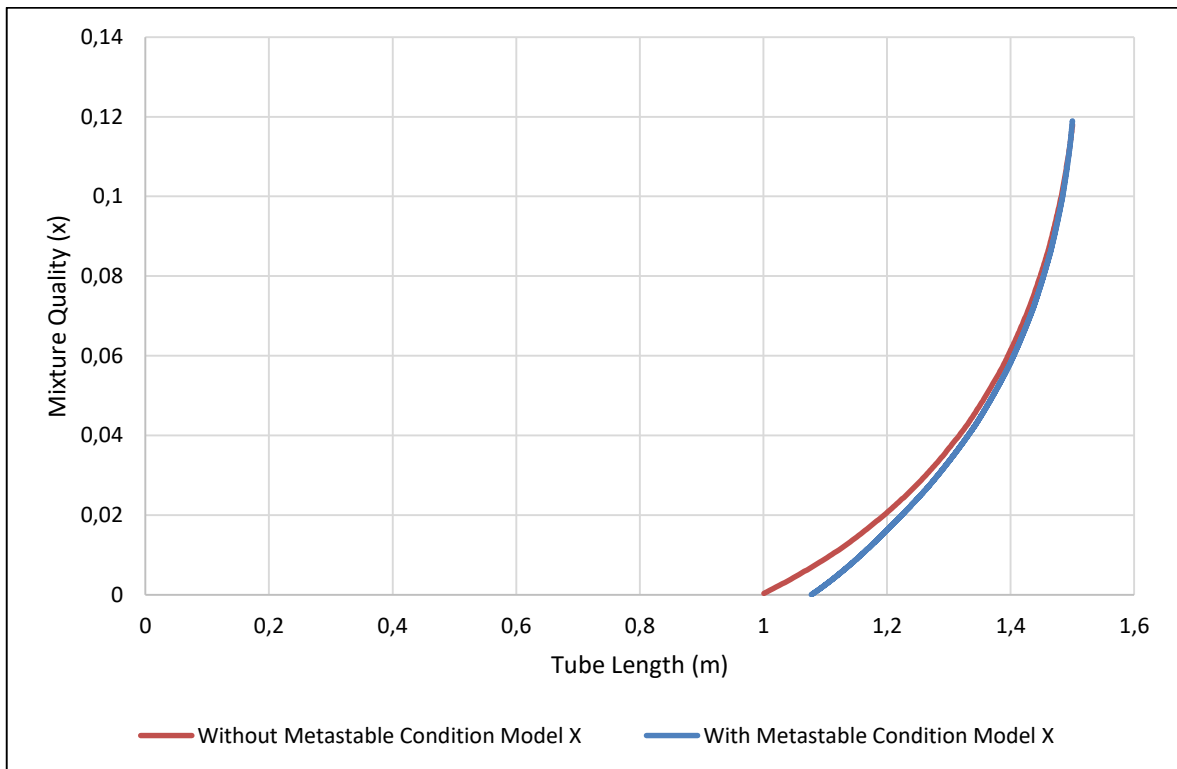


Figure 5.17: Mixture quality calculation from two numerical models

Figure 5.16 examines mixture quality along the tube using two different numerical models. When the metastable phenomenon is included in the model, the metastable liquid region causes the two-phase region to start later than the other model due to vaporization delay. However, both reach almost the same quality at the exit of the tube.

## 6. CONCLUSION

Characteristics of flow in a capillary tube are investigated both experimentally and numerically. The vapor compression refrigeration cycle in the present study includes the capillary tube, evaporator, compressor, and condenser. Total 10 data sets are obtained by measuring temperatures on various points at the refrigeration cycle. Furthermore, two different numerical models are developed where the first model does not consider the metastable condition while the second model includes the metastable phenomenon along the capillary tube.

The mass flowrate of the refrigerant are obtained in three different methods. Two methods use the energy conservation principle over the evaporator and condenser, and the third method employs the compressor displacement volume with the volumetric efficiency. Mass flowrates obtained by the first two methods are closer to each other, but mass flowrates obtained by the third method is lower than those of the first two methods by approximately 20 percent. On the other hand, the mass flowrate predicted by the second numerical model is closer to the third experimental method that uses the compressor displacement volume, and is higher than the result of the first numerical model by approximately 5 percent.

The sensitivity study of the effect of the capillary tube diameter and roughness on mass flowrate is conducted using the second numerical method, and shows that mass flowrate changes 2 percent with 0.01 mm change in diameter and increases by 0.7 percent with no roughness at all.

Pressure distributions along the capillary tube, which are not directly measured in the present study, can be deduced from temperature measurements on the tube. Until a point where temperature remains constant, the refrigerant is considered to be in liquid state. However, as the temperature decreases along the tube, the refrigerant is in the saturated state. If no metastable phenomenon is considered, the pressure in the tube must be saturation pressure corresponding to the temperature.

On the other hand, the numerical models make it possible to examine the regions of liquid, the metastable liquid, the mixture of metastable liquid and vapour, and two-phase flow. The model that includes the metastable phenomenon shows slower pressure decrease along the

tube than the model that does not consider the metastable phenomenon. But both models predict the exit pressure to be almost equal.

When the mass flowrate result of the numerical model is compared with the present experimental data, it is closer to that of the compressor displacement method than those of the other two experimental methods using the energy balance over the condenser and evaporator.

It is also investigated numerically whether choking has occurred or not at the end of the capillary tube with the inlet conditions of the present ten data set. Results show that flows of all data set become choked at the end of the tube.



## REFERENCES

1. S. Wongwises, and W. Pirompak. Flow Characteristics of Pure Refrigerants and Refrigerant Mixtures in Adiabatic Capillary Tubes. *Applied Thermal Engineering*, 21:845-861, 2001.
2. Z. Guobing, and Z. Yufeng. Numerical and Experimental Investigations on the Performance of Coiled Adiabatic Capillary Tubes. *Applied Thermal Engineering*, 21:1106-1141, 2006.
3. D. D. Subodh, B.K. Hardik, K. N. Iyer, and S. V. Prabhu. Experimental and Numerical Studies of Choked Flow Through Adiabatic and Diabatic Capillary Tubes. *Applied Thermal Engineering*, 90:879-894, 2015.
4. S. G. Kim, M. S. and Kim, S. T. Ro. Experimental Investigation of the Performance of R22, R407C, and R410A in Several Capillary Tubes for Air-Conditioners. *International Journal of Refrigeration*, 25:521-531, 2002.
5. C.Melo, R.T.S Ferreira, C. Boabaid Neto, J.M. Goncalves, and M. M. Mezavi. An Experimental Analysis of Adiabatic Capillary Tubes. *Applied Thermal Engineering*, 19:669-684, 1999.
6. V. Feburie, M. Giot, S. Granger, and J.M. Seynhaeve. A Model for Choked Flow Through Cracks with Inlet Subcooling. *Journal of Multiphase Flow*, 19:541-562, 1993.
7. F.A.S, Fiorelli, C. A .S. Silve, and A. A. S. Huerta. Metastable Flow of R-410A in Capillary Tubes. *Applied Thermal Engineering*, 51:1181-1190, 2013.
8. S. Chingulpitak, and S. Wongwises. Two-phase Flow Model of Refrigerants Flowing Through Helically Coiled Capillary Tubes. *Applied Thermal Engineering*, 30:1927-1936, 2010.

9. M. K. Khan, R. Kumar, and P. K. Sahoo. Flow Characteristics of Refrigerants Flowing Through Capillary Tubes – A Review. *Applied Thermal Engineering*, 29:1426-1439, 2009.
10. W.H McAdams, W.K. Wood, and R.L. Bryan. Vaporization Inside Horizontal Tubes. *II. Benzene-oil mixture Transaction ASME*, 64:193, 1942
11. Z.H. Chen, R.Y. Li, S. Lin, and Z.Y. Chen, A Correlation for Metastable Flow of Refrigerant R12 Through Capillary Tubes, *ASHRAE Transactions*, 96:550-554, 1990



## APPENDIX A: NON-METASTABLE NUMERICAL MODELLING APPROACH FORTRAN CODE

```

PROGRAM PRESDROPv2

IMPLICIT REAL*8(A-H,L,M,O-Z)

COMMON /BLKC/ LCAPILLARY,DCAPILLARY

OPEN(UNIT=9,FILE='two-region-pressure.TXT',STATUS='UNKNOWN')

CALL READTABLE

! TEST CASE OF WONGWISES & PIROMPAK [2001]

P1=1238.189

T1=37.19

MDOT=0.0080969

LCAPILLARY=1.5

DCAPILLARY=0.00131

ROUGHNESS= 0.00000009

!ROUGHNESS= 0

CALL CAPILLARY(P1,T1,MDOT,DP)

!WRITE(6,20) P1,DP

20 format(' P_entrance Pdrop ',2f9.2)

STOP

END

SUBROUTINE CAPILLARY(P1,T1,MDOT,DP)

IMPLICIT REAL*8(A-H,L,M,O-Z)

COMMON /BLKC/ LCAPILLARY,DCAPILLARY

```

```

OPEN(UNIT=39,FILE='TEST.TXT',STATUS='UNKNOWN')

PI=3.141593

!ROUGHNESS=0.8*1.5D-6/DCAPILLARY

AREA=PI/4*DCAPILLARY*DCAPILLARY

! SINGLE PHASE

LENGTH=0.

!WRITE(39,60) P1,LENGTH

CALL PROPSAT_T(T1,PSAT1,VF1,VG1,HF1,HG1,SF1,SG1)

G=MDOT/AREA

CALL PROPSATVISC(PSAT1,VISCF,VISCG)

RE=G*DCAPILLARY/VISCF

CALL HAALAND(RE,ROUGHNESS,FRICITIONFACTOR)

LENGTHSP=((P1-PSAT1)*2./VF1/G/G*1000.-1.5)*DCAPILLARY/FRICITIONFACTOR

!write(6,*) g,re,frictionfactor

!write(6,*) viscf,vf1

!write(6,*) p1,psat1

!WRITE(39,60) PSAT1,LENGTHSP

WRITE(9,62) LENGTH,P1

! TWO PHASE

DELTAP=1.

SMAX=0.

LENGTH=LENGTHSP

P=PSAT1

VTPOLD=VF1

100 CONTINUE

```

```

DO WHILE (LENGTH<LCAPILLARY)

P=P-DELTAP

CALL PROPSAT_P(P,TSAT,VF,VG,HF,HG,SF,SG)

HFG=HG-HF

VFG=VG-VF

DUM1=G*VFG

DUM2=G*VF

DUM3=DUM1*DUM2+HFG*1000.

DUM4=DUM2*DUM2/2.+(HF-HF1)*1000.

X=(-DUM3+DSQRT(DUM3*DUM3-2.*DUM1*DUM1*DUM4))/DUM1/DUM1

S=(1.-X)*SF+X*SG

VTP=(X*VG+(1.-X)*VF) ! TWO-PHASE SPECIFIC VOLUME

DVTP=VTP-VTPOLD

VTPAVE=(VTP+VTPOLD)/2.

VTPOLD=VTP

VEL=G*VTP

CALL PROPSATVISC(P,VISCF,VISCG)

VISCTP=1./(X/VISCG+(1.-X)/VISCF)

RE=VEL*DCAPILLARY/VISCTP/VTP

CALL HAALAND(RE,ROUGHNESS,FRICITIONFACTOR)

DL=2.*DCAPILLARY/FRICITIONFACTOR*(DELTAP*1000./G/G-DVTP)/VTPAVE

LENGTH=LENGTH+DL

DP=P1-P

PRINT *, P,LENGTH,LENGTHSP

WRITE(9,62) LENGTH,P

```



```

!WRITE(6,50) P,TSAT,LENGTH,S

!WRITE(39,60) P,LENGTH

50 FORMAT(F10.3,F9.2,F9.5,F12.7)

60 FORMAT(F10.3,F9.5)

62 FORMAT(F9.5,F10.3)

!IF(S.GT.SMAX) THEN

    SMAX=S

!IF(LENGTH.LT.LCAPILLARY) GOTO 100

!ENDIF

!write(6,*)

!WRITE(6,10) PSAT1,P,(PSAT1-P)

10 FORMAT(' PSAT P DP ',3F10.3)

!WRITE(6,20) LCAPILLARY,LENGTHSP,LENGTH

20 FORMAT(' LCAPILLARY LSP L',3F9.5)

!WRITE(6,30) SF1,SMAX,S

!30 FORMAT(' SF1 SMAX S',3F10.6)

!write(6,40) vel

40 format(' velocity at exit',f10.3)

END DO

RETURN

END

SUBROUTINE HAALAND(RE,ROUGHNESS,FRICITIONFACTOR)

IMPLICIT REAL*8(A-H,M,O-Z)

DUM=-1.8*DLOG10((0/3.7)**1.11+6.9/RE)

FRICITIONFACTOR=1./DUM/DUM

```

```

RETURN

END

!-----

! SUBROUTINES FOR PROPERTIES OF REFRIGERANT 134-A

!-----

SUBROUTINE READTABLE

IMPLICIT REAL*8(A-H,M,O-Z)

COMMON /BLK_SUPERHEATED/ P(26),T(26,80),V(26,80),H(26,80),S(26,80)

COMMON /BLK_SATURATED/
TSAT(71),PSAT(71),VF(71),VG(71),HF(71),HG(71),SF(71),SG(71)

COMMON /BLK_SATVISC/ PSATVISC(30),VISCF(30),VISCG(30)

COMMON /BLK_DATA/ NDATA(26)

! T          [degC]

! P          [kPa]

! V          [m3/kg]

! H          [kJ/kg]

! S          [kJ/kg/K]

! NUMBER OF ROWS IN THE TABLE

NSATVISCDATA=30      ! SATURATION VISCOSITY TABLE

NSATDATA=71         ! SATURATION TABLE

NDATA(1)=75         ! P=0.10 MPa

NDATA(2)=71         ! P=0.14 MPa

NDATA(3)=68         ! P=0.18 MPa

NDATA(4)=65         ! P=0.22 MPa

NDATA(5)=63         ! P=0.26 MPa

NDATA(6)=61         ! P=0.30 MPa

```

NDA(7)=59 ! P=0.34 MPa

NDA(8)=58 ! P=0.38 MPa

NDA(9)=56 ! P=0.42 MPa

NDA(10)=55 ! P=0.46 MPa

NDA(11)=54 ! P=0.5 MPa

NDA(12)=51 ! P=0.6 MPa

NDA(13)=48 ! P=0.7 MPa

NDA(14)=46 ! P=0.8 MPa

NDA(15)=44 ! P=0.9 MPa

NDA(16)=42 ! P=1.0 MPa

NDA(17)=38 ! P=1.2 MPa

NDA(18)=35 ! P=1.4 MPa

NDA(19)=33 ! P=1.6 MPa

NDA(20)=30 ! P=1.8 MPa

NDA(21)=28 ! P=2.0 MPa

NDA(22)=26 ! P=2.2 MPa

NDA(23)=24 ! P=2.4 MPa

NDA(24)=22 ! P=2.6 MPa

NDA(25)=20 ! P=2.8 MPa

NDA(26)=18 ! P=3.0 MPa

P(1)=100.

P(2)=140.

P(3)=180.

P(4)=220.

P(5)=260.

P(6)=300.

P(7)=340.

P(8)=380.

P(9)=420.

P(10)=460.

P(11)=500.

P(12)=600.

P(13)=700.

P(14)=800.

P(15)=900.

P(16)=1000.

P(17)=1200.

P(18)=1400.

P(19)=1600.

P(20)=1800.

P(21)=2000.

P(22)=2200.

P(23)=2400.

P(24)=2600.

P(25)=2800.

P(26)=3000.

OPEN(UNIT=19,FILE='r134a\_sat\_visc\_P.txt',STATUS='UNKNOWN')

OPEN(UNIT=20,FILE='r134a\_sat.txt',STATUS='UNKNOWN')

OPEN(UNIT=21,FILE='p0100.txt',STATUS='UNKNOWN')

OPEN(UNIT=22,FILE='p0140.txt',STATUS='UNKNOWN')

```
OPEN(UNIT=23,FILE='p0180.txt',STATUS='UNKNOWN')  
  
OPEN(UNIT=24,FILE='p0220.txt',STATUS='UNKNOWN')  
  
OPEN(UNIT=25,FILE='p0260.txt',STATUS='UNKNOWN')  
  
OPEN(UNIT=26,FILE='p0300.txt',STATUS='UNKNOWN')  
  
OPEN(UNIT=27,FILE='p0340.txt',STATUS='UNKNOWN')  
  
OPEN(UNIT=28,FILE='p0380.txt',STATUS='UNKNOWN')  
  
OPEN(UNIT=29,FILE='p0420.txt',STATUS='UNKNOWN')  
  
OPEN(UNIT=30,FILE='p0460.txt',STATUS='UNKNOWN')  
  
OPEN(UNIT=31,FILE='p0500.txt',STATUS='UNKNOWN')  
  
OPEN(UNIT=32,FILE='p0600.txt',STATUS='UNKNOWN')  
  
OPEN(UNIT=33,FILE='p0700.txt',STATUS='UNKNOWN')  
  
OPEN(UNIT=34,FILE='p0800.txt',STATUS='UNKNOWN')  
  
OPEN(UNIT=35,FILE='p0900.txt',STATUS='UNKNOWN')  
  
OPEN(UNIT=36,FILE='p1000.txt',STATUS='UNKNOWN')  
  
OPEN(UNIT=37,FILE='p1200.txt',STATUS='UNKNOWN')  
  
OPEN(UNIT=38,FILE='p1400.txt',STATUS='UNKNOWN')  
  
OPEN(UNIT=39,FILE='p1600.txt',STATUS='UNKNOWN')  
  
OPEN(UNIT=40,FILE='p1800.txt',STATUS='UNKNOWN')  
  
OPEN(UNIT=41,FILE='p2000.txt',STATUS='UNKNOWN')  
  
OPEN(UNIT=42,FILE='p2200.txt',STATUS='UNKNOWN')  
  
OPEN(UNIT=43,FILE='p2400.txt',STATUS='UNKNOWN')  
  
OPEN(UNIT=44,FILE='p2600.txt',STATUS='UNKNOWN')  
  
OPEN(UNIT=45,FILE='p2800.txt',STATUS='UNKNOWN')  
  
OPEN(UNIT=46,FILE='p3000.txt',STATUS='UNKNOWN')  
  
DO I=1,NSATVISCDATA
```

```

    READ(19,*) PSATVISC(I),VISCF(I),VISC(I)

ENDDO

DO I=1,NSATDATA

    READ(20,*) TSAT(I),PSAT(I),VF(I),VG(I),UF,UG,HF(I),HG(I),SF(I),SG(I)

ENDDO

DO I=1,26

    IFILE=20+I

    DO J=1,NDATA(I)

        READ(IFILE,*) T(I,J),V(I,J),H(I,J),S(I,J)

    ENDDO

ENDDO

DO I=19,46

    CLOSE(UNIT=I)

ENDDO

RETURN

END SUBROUTINE

SUBROUTINE PROP(T0,P0,V0,H0,S0,FLAG_SAT)

IMPLICIT REAL*8(A-H,M,O-Z)

LOGICAL FLAG_SAT

COMMON /BLK_SUPERHEATED/ P(26),T(26,80),V(26,80),H(26,80),S(26,80)

COMMON /BLK_DATA/ NDATA(26)

! PROPERTIES FOR SUPERHEATED R134A

FLAG_SAT=.FALSE.

IF(P0.LT.100.) THEN

```

```
WRITE(6,*) 'OUT OF RANGE: PRESSURE LESS THAN 100 kPa'  
  
STOP  
  
ELSEIF(P0.LT.500.) THEN  
  
    IP1=INT((P0-100.)/400.*10.)+1  
  
ELSEIF(P0.LT.1000.) THEN  
  
    IP1=INT((P0-500.)/500.*5.)+11  
  
ELSEIF(P0.LT.3000.) THEN  
  
    IP1=INT((P0-1000.)/2000.*10.)+16  
  
ELSE  
  
    WRITE(6,*) 'OUT OF RANGE: PRESSURE GREATER THAN 3000 kPa'  
  
    STOP  
  
ENDIF  
  
IP2=IP1+1  
  
IF(T0.LT.T(IP1,1)) THEN ! SATURATED  
  
    FLAG_SAT=.TRUE.  
  
    GOTO 100  
  
ELSEIF(T0.LT.T(IP1,2)) THEN  
  
    IT1=1  
  
ELSEIF(T0.LT.120.) THEN  
  
    IT1=INT((T0-T(IP1,2))/2.)+2  
  
ELSE  
  
    WRITE(6,*) 'OUT OF RANGE: TEMPERATURE GREATER THAN 120 degC'  
  
    STOP  
  
ENDIF  
  
IF(T0.LT.T(IP2,1)) THEN
```

```

CALL PROPSAT_P(P0,TSAT0,VF0,VG0,HF0,HG0,SF0,SG0)

IF(T0.LT.TSAT0) THEN ! SATURATED

    FLAG_SAT=.TRUE.

    GOTO 100

ENDIF

DO J=1,NDATA(IP1)

    IF(T(IP1,J).GT.T(IP2,1)) THEN

        IT2=J

        GOTO 200

    ENDIF

ENDDO

200 CONTINUE

IT1=IT2-1

RT=(T(IP2,1)-T(IP1,IT1))/(T(IP1,IT2)-T(IP1,IT1))

VIP1=V(IP1,IT1)+RT*(V(IP1,IT2)-V(IP1,IT1))

HIP1=H(IP1,IT1)+RT*(H(IP1,IT2)-H(IP1,IT1))

SIP1=S(IP1,IT1)+RT*(S(IP1,IT2)-S(IP1,IT1))

RP=(P0-P(IP1))/(P(IP2)-P(IP1))

VMID=VIP1+RP*(V(IP2,1)-VIP1)

HMID=HIP1+RP*(H(IP2,1)-HIP1)

SMID=SIP1+RP*(S(IP2,1)-SIP1)

RT=(T0-TSAT0)/(T(IP2,1)-TSAT0)

V0=VG0+RT*(VMID-VG0)

H0=HG0+RT*(HMID-HG0)

S0=SG0+RT*(SMID-SG0)

```



```

GOTO 100

ELSEIF(T0.LT.T(IP2,2)) THEN

    IT2=1

ELSEIF(T0.LT.120.) THEN

    IT2=INT((T0-T(IP2,2))/2.)+2

ELSE

    WRITE(6,*) 'OUT OF RANGE: TEMPERATURE GREATER THAN 120 degC'

    STOP

ENDIF

IT1P1=IT1+1

IT2P1=IT2+1

RT1=(T0-T(IP1,IT1))/(T(IP1,IT1P1)-T(IP1,IT1))

RT2=(T0-T(IP2,IT2))/(T(IP2,IT2P1)-T(IP2,IT2))

RT1M1=1.-RT1

RT2M1=1.-RT2

RP=(P0-P(IP1))/(P(IP2)-P(IP1))

V0=(RT1*V(IP1,IT1P1)+RT1M1*V(IP1,IT1))*(1.-
RP)+(RT2*V(IP2,IT2P1)+RT2M1*V(IP2,IT2))*RP

H0=(RT1*H(IP1,IT1P1)+RT1M1*H(IP1,IT1))*(1.-
RP)+(RT2*H(IP2,IT2P1)+RT2M1*H(IP2,IT2))*RP

S0=(RT1*S(IP1,IT1P1)+RT1M1*S(IP1,IT1))*(1.-
RP)+(RT2*S(IP2,IT2P1)+RT2M1*S(IP2,IT2))*RP

100 CONTINUE

RETURN

END

SUBROUTINE PROPSAT_T(TSAT0,PSAT0,VF0,VG0,HF0,HG0,SF0,SG0)

```

```

IMPLICIT REAL*8(A-H,M,O-Z)

COMMON                                /BLK_SATURATED/
TSAT(71),PSAT(71),VF(71),VG(71),HF(71),HG(71),SF(71),SG(71)

! PROPERTIES OF SATURATED R134A FOR GIVEN TEMPERATURE TSAT0

IF(TSAT0.LT.-40.) THEN

    WRITE(6,*) 'OUT OF RANGE: SAT. TEMP. LESS THAN -40 degC'

    STOP

ELSEIF(TSAT0.GT.120.) THEN

    WRITE(6,*) 'OUT OF RANGE: SAT. TEMP. GREATER THAN 120 degC'

    STOP

ELSE

    IT=INT((TSAT0+40.)/2.)+1

ENDIF

ITP1=IT+1

RT=(TSAT0-TSAT(IT))/2.

RTM1=1.-RT

PSAT0=PSAT(IT)*RTM1+PSAT(ITP1)*RT

VF0=VF(IT)*RTM1+VF(ITP1)*RT

VG0=VG(IT)*RTM1+VG(ITP1)*RT

HF0=HF(IT)*RTM1+HF(ITP1)*RT

HG0=HG(IT)*RTM1+HG(ITP1)*RT

SF0=SF(IT)*RTM1+SF(ITP1)*RT

SG0=SG(IT)*RTM1+SG(ITP1)*RT

ENDSUBROUTINE

SUBROUTINE PROPSAT_P(PSAT0,TSAT0,VF0,VG0,HF0,HG0,SF0,SG0)

```

```
IMPLICIT REAL*8(A-H,M,O-Z)

COMMON                               /BLK_SATURATED/
TSAT(71),PSAT(71),VF(71),VG(71),HF(71),HG(71),SF(71),SG(71)

!

! PROPERTIES OF SATURATED R134A FOR GIVEN PRESSURE PSAT0

!

IF(PSAT0.LT.51.209) THEN

    WRITE(6,*) 'OUT OF RANGE: SAT. PRESSURE LESS THAN 51.209 kPa'

    STOP

ELSEIF(PSAT0.GT.3972.4) THEN

    WRITE(6,*) 'OUT OF RANGE: SAT. PRESSURE GREATER THAN 3972.4 kPa'

    STOP

ENDIF

I=50

IF(PSAT0.GT.PSAT(I)) THEN

    20 CONTINUE

    I=I+1

    IF(PSAT(I).LT.PSAT0) GOTO 20

    IT=I-1

ELSE

    30 CONTINUE

    I=I-1

    IF(PSAT(I).GT.PSAT0) GOTO 30

    IT=I

ENDIF
```

```

ITP1=IT+1

RP=(PSAT0-PSAT(IT))/(PSAT(ITP1)-PSAT(IT))

RPM1=1.-RP

TSAT0=TSAT(IT)*RPM1+TSAT(ITP1)*RP

VF0=VF(IT)*RPM1+VF(ITP1)*RP

VG0=VG(IT)*RPM1+VG(ITP1)*RP

HF0=HF(IT)*RPM1+HF(ITP1)*RP

HG0=HG(IT)*RPM1+HG(ITP1)*RP

SF0=SF(IT)*RPM1+SF(ITP1)*RP

SG0=SG(IT)*RPM1+SG(ITP1)*RP

ENDSUBROUTINE

SUBROUTINE PROPSATVISC(PSAT0,VISCF0,VISCG0)

IMPLICIT REAL *8(A-H,M,O-Z)

COMMON /BLK_SATVISC/ PSATVISC(30),VISCF(30),VISCG(30)

!

! DYNAMIC VISCOSITY OF SATURATED R134A FOR GIVEN PRESSURE

!

IF(PSAT0.LT.0.1) THEN

WRITE(6,*) 'OUT OF RANGE: SAT. PRESSURE LESS THAN 100 KPA'

STOP

```

```

ELSEIF(PSAT0.GT.3000.) THEN

  WRITE(6,*) 'OUT OF RANGE: SAT. PRESSURE GREATER THAN 3000 KPA'

  STOP

ELSE

  I=INT(PSAT0/100.)+1

ENDIF

IP1=I+1

RP=(PSAT0-PSATVISC(I))/100.

RPM1=1.-RP

VISCF0=VISCF(I)*RPM1+VISCF(IP1)*RP

VISCG0=VISCG(I)*RPM1+VISCG(IP1)*RP

ENDSUBROUTINE

SUBROUTINE FIND_TSAT_FROM_HF(HF0,TSAT0)

IMPLICIT REAL *8(A-H,M,O-Z)

COMMON /BLK_SATURATED/
TSAT(71),PSAT(71),VF(71),VG(71),HF(71),HG(71),SF(71),SG(71)

! FIND TEMPERATURE OF SATURATED R134A FOR GIVEN HF

IF(HF0.LT.148.14) THEN

  WRITE(6,*) 'OUT OF RANGE: HF LESS THAN 148.14 KJ/KG'

  STOP

ELSEIF(HF0.GT.373.30) THEN

  WRITE(6,*) 'OUT OF RANGE: HF GREATER THAN 373.30 kPa'

  STOP

ENDIF

I=50

IF(HF0.GT.HF(I)) THEN

```

```
20 CONTINUE

  I=I+1

  IF(HF(I).LT.HF0) GOTO 20

  IT=I-1

ELSE

30 CONTINUE

  I=I-1

  IF(HF(I).GT.HF0) GOTO 30

  IT=I

ENDIF

ITP1=IT+1

R=(HF0-HF(IT))/(HF(ITP1)-HF(IT))

RM1=1.-R

TSAT0=TSAT(IT)*RM1+TSAT(ITP1)*R

ENDSUBROUTINE

SUBROUTINE PROP_ISENTROPIC(P0,SS,H,S)

IMPLICIT REAL*8(A-H,M,O-Z)

COMMON /BLK_SUPERHEATED/ P(26),T(26,80),V(26,80),H(26,80),S(26,80)

COMMON /BLK_DATA/ NDATA(26)

! FIND ENTHALPY AT CONSTANT ENTROPY

IF(P0.LT.100.) THEN

  WRITE(6,*) 'OUT OF RANGE: PRESSURE LESS THAN 100 kPa'

  STOP

ELSEIF(P0.LT.500.) THEN

  IP1=INT((P0-100.)/400.*10.)+1
```

```

ELSEIF(P0.LT.1000.) THEN

    IP1=INT((P0-500.)/500.*5.)+11

ELSEIF(P0.LT.3000.) THEN

    IP1=INT((P0-1000.)/2000.*10.)+16

ELSE

    WRITE(6,*) 'OUT OF RANGE: PRESSURE GREATER THAN 3000 kPa'

    STOP

ENDIF

IP2=IP1+1

DO I=1,NDATA(IP1)

    IF(SS.LT.S(IP1,I)) THEN

        IT2=I

        IF(I.EQ.1) THEN

            WRITE(6,*) 'OUT OF RANGE FOR ENTROPY: T < TSAT'

            H_S=0.

            GOTO 200

        ENDIF

        GOTO 100

    ENDIF

ENDDO

100 CONTINUE

IT1=IT2-1

RP=(P0-P(IP1))/(P(IP2)-P(IP1))

S1=(1.-RP)*S(IP1,IT1)+RP*S(IP2,IT1)

S2=(1.-RP)*S(IP1,IT2)+RP*S(IP2,IT2)

```

```

RT=(SS-S1)/(S2-S1)

H1=(1.-RP)*H(IP1,IT1)+RP*H(IP2,IT1)

H2=(1.-RP)*H(IP1,IT2)+RP*H(IP2,IT2)

H_S=(1.-RT)*H1+RT*H2

200 CONTINUE

ENDSUBROUTINE

SUBROUTINE FIND_P_FROM_H_AND_S(S,H,P)

IMPLICIT REAL *8(A-H,O-Z)

! FIND P FROM H AND S BY ITERATION

TOL=1.D-9

P=1700.          ! INITIAL GUESS

ICOUNT=0

10 CONTINUE

DIFFP=P*0.001

CALL PROP_ISENTROPIC(P,S,H1)

CALL PROP_ISENTROPIC(P+DIFFP,S,H2)

DHDP=(H2-H1)/DIFFP

F=H1-H          ! H IS CONSTANT; H1 IS VARIABLE.

DFDP=DHDP

DP=F/DFDP

P=P-DP

ICOUNT=ICOUNT+1

IF(ICOUNT.GT.50) THEN

WRITE(39,*) 'EXCESSIVE ITERATION IN FIND_P_FROM_H_AND_S'

```



```
WRITE(39,*) 'H S P',H,S,P

STOP

ENDIF

IF(ABS(DP/P).GT.TOL) GOTO 10

ENDSUBROUTINE

SUBROUTINE FIND_T_FROM_P_AND_H(P0,H0,TEMP)

IMPLICIT REAL*8(A-H,M,O-Z)

COMMON /BLK_SUPERHEATED/ P(26),T(26,80),V(26,80),H(26,80),S(26,80)

COMMON /BLK_DATA/ NDATA(26)

! FIND TEMPERATURE FROM P AND H

IF(P0.LT.100.) THEN

WRITE(6,*) 'OUT OF RANGE: PRESSURE LESS THAN 100 kPa'

STOP

ELSEIF(P0.LT.500.) THEN

IP1=INT((P0-100.)/400.*10.)+1

ELSEIF(P0.LT.1000.) THEN

IP1=INT((P0-500.)/500.*5.)+11

ELSEIF(P0.LT.3000.) THEN

IP1=INT((P0-1000.)/2000.*10.)+16

ELSE

WRITE(6,*) 'OUT OF RANGE: PRESSURE GREATER THAN 3000 kPa'

STOP

ENDIF

IP2=IP1+1

DO I=1,NDATA(IP1)
```

```
IF(H0.LT.H(IP1,I)) THEN

    IT2=I

    IF(I.EQ.1) THEN

        WRITE(6,*) 'OUT OF RANGE FOR ENTROPY: T < TSAT'

        H_S=0.

        GOTO 200

    ENDIF

    GOTO 100

ENDIF

ENDDO

100 CONTINUE

IT1=IT2-1

RP=(P0-P(IP1))/(P(IP2)-P(IP1))

H1=(1.-RP)*H(IP1,IT1)+RP*H(IP2,IT1)

H2=(1.-RP)*H(IP1,IT2)+RP*H(IP2,IT2)

RT=(H0-H1)/(H2-H1)

T1=(1.-RP)*T(IP1,IT1)+RP*T(IP2,IT1)

T2=(1.-RP)*T(IP1,IT2)+RP*T(IP2,IT2)

TEMP=(1.-RT)*T1+RT*T2

200 CONTINUE

RETURN

END
```

## APPENDIX B: WITH-METASTABLE NUMERICAL MODELLING APPROACH FORTRAN CODE

```

PROGRAM CAPIMETASTABLE

IMPLICIT REAL *8(A-H,L,M,O-Z)

REAL, PARAMETER::PI=3.1415926

CALL READTABLE

OPEN(UNIT=7,FILE='RESUTLS.TXT',STATUS='UNKNOWN')

OPEN(UNIT=8,FILE='RESUTLS2.TXT',STATUS='UNKNOWN')

OPEN(UNIT=9,FILE='RESUTLS-plot.TXT',STATUS='UNKNOWN')

OPEN(UNIT=21,FILE='TSAT-P.TXT',STATUS='UNKNOWN')

OPEN(UNIT=29,FILE='PRESSURES-3-CASE.TXT',STATUS='UNKNOWN')

!----- CONSTANTS -----

D=0.0013                                !Diameter of tube (m)

DX=1.D-5                                !Step size for length of tube

LTUBE=1.50                               !Length of tube

EP=0.00000009                            !Roughness

!EP=(0.8*1.5E-6)/D

U=PI*D

AREA=PI*D*D/4.                            !Area

Y=0.

BOLTZMANN=1.380662D-23

PC=4059.                                  !kPa,R134a Critical Pressure

TC=101.06+273.15                          !Critical Temperature, 134a

!SMAX=0.

```

```

!----- VARIABLES -----

MDOT=0.00940280      !kg/s, Average of condenser & evaporator mdots

DTSUB=7.55           !Subcooled temperature

!VISCOSITY=1.4367E-04      !Initial viscosity @ T

P1=1733.64           !Initial pressure of tube

!SIG=0.0040614       !Surface Tension

!-----REGION I-----

G=MDOT/AREA

LTOTAL=0

WRITE(9,99) LTOTAL,P1

99 FORMAT(F8.5,F10.3)

CALL PROPSAT_P(P1,TSAT,VF,VG,HF,HG,SF,SG)

T1=TSAT-DTSUB      !Inlet temperature

TLM=T1             !Superheated temperature at metastable condition = Inlet
temperature

HTOTAL=HF+G*G*VF*VF/2./1000.      ! TOTAL ENTHALPY AT THE
ENTRANCE OF CAPILLARY TUBE

CALL PROPSAT_T(T1,PSAT1,VF1,VG1,HF1,HG1,SF1,SG1) !Properties for liquid
phase(Region I) calculations

CALL PROPSATVISC(PSAT1,VISCF1,VISCG1)

RE=G*D/VISCF1

FRIC=(1./(-1.8*Dlog10(((EP/D)/3.7)**1.11)+(6.9/RE)))**2

L1=(2*D*(P1-PSAT1)*1000.)/(G*G*FRIC*VF1)      !REGION I LENGTH

LTOTAL=LTOTAL+L1

PRINT*, L1,FRIC

write(7,44) tsat,t1

```

```

44 format(' tsat t1 ',2f10.3)

write(7,48) RE,FRIC,VISCF1

write(8,48) RE,FRIC,VISCF1

48 format(' RE=',f9.1,' FRIC=',f10.6, ' VISC=',G12.4)

write(7,50) L1,PSAT1

50 format(' L1=',f9.4,' PSAT=',f12.4)

write(9,99) LTOTAL,PSAT1

PRINT *, LTOTAL,PSAT1

!-----REGION II-----

TSAT2=T1

TSATK=TSAT2+273.15

CALL SURFACETENSION(TSAT2,SIG)

DREF=SQRT(BOLTZMANN*TSATK/SIG)*10000. ! Reference length in Eq.6 of Guobing's
Journal

DPRES=0.679*VG/(VG-VF)*RE**0.914*(DTSUB/TC)**(-0.208)*((D/DREF)**(-
3.18))*SIG**1.5/SQRT(BOLTZMANN*TSATK)/1000.

P=PSAT1-DPRES ! P = PRESSURE IN TUBE AT THE END OF REGION II

L2=2.*D*DPRES*1000./(G*G*FRIC*VF1) !REGION II LENGTH

LTOTAL=LTOTAL+L2

write(7,52) L2,DPRES

52 format(' L2=',f9.4,' DPRES=',f12.4)

WRITE(9,99) LTOTAL,P

WRITE(29,*) LTOTAL,P

!-----REGION III-----

L3=0.

SMAX=0.

```

```

Y=0.D0

T=T1      ! SUPERHEATED TEMPERATURE OF FLUID IN TUBE AT THE BEGINNING
OF REGION III

      ! THIS TEMPERATURE IS ASSUMED TO BE CONSTANT.

CALL PROPSAT_T(T,PSATLM,VLM,VG,HLM,HG,SLM,SG)      !
PSATLM=PSAT1

CALL PROPSATVISC(PSATLM,VISCLM,VISCG) ! THIS IS VISCOSITY AT
SUPERHEATED TEMPERATURE

HTOTAL=HLM+G*G*VLM*VLM/2000.D0

DO WHILE (Y.LE.0.9999 .AND. LTOTAL.LE.LTUBE)

  DY=0.02*U/AREA*(1.-Y)*((PSATLM-P)/(PC-PSATLM))**0.25

  !CALL PROPSAT_T(T,PSAT,VLM,VG,HLM,HG,SLM,SG)

  CALL PROPSAT_P(P,TSAT,VF,VG,HF,HG,SF,SG)

  !CALL PROPSATVISC(PSAT,VISCLM,VISCG)

  CALL PROPSATVISC(P,VISCF,VISCG)

  !-----

  ! FIND X

  !-----

  VFG=VG-VF

  HFG=HG-HF

  VL=(1.-Y)*VLM+Y*VF

  HL=(1.-Y)*HLM+Y*HF

  A=0.5D0*G*G*VFG*VFG

  B=G*G*VL*VFG+HFG*1000.

  C=0.5D0*G*G*VL*VL+(HL-HTOTAL)*1000.

```

```

X=(-B+DSQRT(B*B-4.D0*A*C))/2.D0/A

DPSTAR=P*1.D-5

PSTAR=P+DPSTAR

CALL
PROPSAT_P(PSTAR,TSATSTAR,VFSTAR,VGSTAR,HFSTAR,HGSTAR,SFSTAR,SGSTAR)

HFGSTAR=HGSTAR-HFSTAR

VFGSTAR=VGSTAR-VFSTAR

VLSTAR=(1.-Y)*VLM+Y*VFSTAR

HLSTAR=(1.-Y)*HLM+Y*HFSTAR

A=0.5D0*G*G*VFGSTAR*VFGSTAR

B=G*G*VLSTAR*VFGSTAR+HFGSTAR*1000.

C=0.5D0*G*G*VLSTAR*VLSTAR+(HLSTAR-HTOTAL)*1000.

XSTAR=(-B+DSQRT(B*B-4.D0*A*C))/2.D0/A

DVFDP=(VFSTAR-VF)/DPSTAR

DVGDP=(VGSTAR-VG)/DPSTAR

DXDP=(XSTAR-X)/DPSTAR

!-----
! CHECK ENTROPY      TO SEE IF CHOKING
!-----

S=(1.-Y)*SLM+(Y-X)*SF+X*SG

IF(S.GT.SMAX) THEN

    SMAX=S

ELSE

    WRITE(6,*) 'ENTROPY DECREASES'

    STOP

```

```

ENDIF

!-----

! UPDATE P

!-----

VL0=(1.-Y)/(1.-X)*VLM+(Y-X)/(1.-X)*VF !Guobing Eq 13

VISCL=DEXP((1.-Y)/(1.-X)*DLOG(VISCLM)+(Y-X)/(1.-X)*DLOG(VISCF))

VISCOSITY=((1.-X)*VL0*VISCL+X*VG*VISC)/((1.-X)*VL0+X*VG)

V=(1.-Y)*VLM+(Y-X)*VF+X*VG

RE=G*D/VISCOSITY

write(8,74) vlm,vf,vg,vl0,v

74 format(5g15.4)

write(8,72) visclm,viscf,viscg,viscosity

72 format(4g15.4)

FRIC=(1./(-1.8*Dlog10(((EP/D)/3.7)**1.11)+(6.9/RE)))**2

DP=DX/(2.*D/FRIC/V*(1.D3/G/G+(Y-X)*DVFD+X*DVGDP+VFG*DXDP)) ! DP IS
DEFINED POSITIVE

! DP=FRIC*DX/D*0.5D0*G*G*V/1.D3 ! [kPa]

P=P-DP

write(8,70) RE,FRIC,DP

70 format(' RE FRIC DP',f10.1,f10.5,f10.4)

!-----

! UPDATE Y BY INTEGRATION

!-----

Y=Y+DX*DY

!-----

```



```

! UPDATE T

!-----

T=(1.-Y)*TLM+Y*TSAT

!-----

! UPDATE LENGTH

!-----

L3=L3+DX

LTOTAL=LTOTAL+DX

write(7,60) ltotal,t,PSATLM,p,y,x

60 format(' LTOTAL T PSAT P Y X',f10.6,F10.4,2f10.3,2f10.6)

WRITE(9,99) LTOTAL,P

WRITE(29,*) LTOTAL,P,PSATLM

ENDDO

LTR3=LTOTAL

!-----REGION IV-----

L4=0.

SMAX=0.

DUM=0.

DO WHILE (LTOTAL.LE.LTUBE)

CALL PROPSAT_P(P,TSAT,VF,VG,HF,HG,SF,SG)

HFG=HG-HF

VFG=VG-VF

DUM1=G*VFG

DUM2=G*VF

DUM3=DUM1*DUM2+HFG*1000.

```

```

DUM4=DUM2*DUM2/2.-DUM+(HF-HF1)*1000.

X=(-DUM3+DSQRT(DUM3*DUM3-2.*DUM1*DUM1*DUM4))/DUM1/DUM1

S=(1.-X)*SF+X*SG

VTP=(X*VG+(1.-X)*VF)      ! TWO-PHASE SPECIFIC VOLUME

DPSTAR=P*1.D-5

PSTAR=P+DPSTAR

CALL

PROPSAT_P(PSTAR,TSATSTAR,VFSTAR,VGSTAR,HFSTAR,HGSTAR,SFSTAR,SGSTAR)

R)

HFGSTAR=HGSTAR-HFSTAR

VFGSTAR=VGSTAR-VFSTAR

DUM1=G*VFGSTAR

DUM2=G*VFSTAR

DUM3=DUM1*DUM2+HFGSTAR*1000.

DUM4=DUM2*DUM2/2.-DUM+(HFSTAR-HF1)*1000.

XSTAR=(-DUM3+DSQRT(DUM3*DUM3-2.*DUM1*DUM1*DUM4))/DUM1/DUM1

DVFDp=(VFSTAR-VF)/DPSTAR

DVGDP=(VGSTAR-VG)/DPSTAR

DXDP=(XSTAR-X)/DPSTAR

CALL PROPSATVISC(P,VISCF,VISCG)

VISCTP=(X*VG*VISCG+(1.-X)*VF*VISCF)/(X*VG+(1.-X)*VF)

RE=G*D/VISCTP

FRIC=(1./(-1.8*Dlog10((((EP/D)/3.7)**1.11)+(6.9/RE))))**2

DP=DX/(2.*D/FRIC/VTP*(1.D3/G/G+(1.-X)*DVFDp+X*DVGDP+VFG*DXDP)) ! DP IS
DEFINED POSITIVE

! DP=DX/(2.*D/FRIC/VTP*(1.D3/G/G)) ! DP IS DEFINED POSITIVE

```

```

LTOTAL=LTOTAL+DX

P=P-DP

WRITE(9,99) LTOTAL,P

WRITE(7,80) LTOTAL,P,X,S

80 FORMAT(' LTOTAL P X S ',F10.6,F10.3,2F10.6)

IF(S.GT.SMAX) THEN

    SMAX=S

ELSE

    WRITE(6,*) 'ENTROPY DECREASES'

    STOP

ENDIF

WRITE(21,*) TSAT

WRITE(29,*) LTOTAL,P

END DO

PRINT *, LTR3, LTOTAL, P

END PROGRAM

#####
#####

SUBROUTINE READTABLE

IMPLICIT REAL *8(A-H,M,O-Z)

COMMON /BLK_SUPERHEATED/ P(26),T(26,80),V(26,80),H(26,80),S(26,80)

COMMON                               /BLK_SATURATED/
TSAT(71),PSAT(71),VF(71),VG(71),HF(71),HG(71),SF(71),SG(71)

COMMON /BLK_SATVISC/ PSATVISC(30),VISCF(30),VISC(30)

COMMON /BLK_DATA/ NDATA(26)

```

```
!  
  
! T          [degC]  
  
! P          [kPa]  
  
! V          [m3/kg]  
  
! H          [kJ/kg]  
  
! S          [kJ/kg/K]  
  
!  
  
! NUMBER OF ROWS IN THE TABLE  
  
NSATVISCDATA=30    ! SATURATION VISCOSITY TABLE  
  
NSATDATA=71        ! SATURATION TABLE  
  
NDATA(1)=75        ! P=0.10 MPa  
  
NDATA(2)=71        ! P=0.14 MPa  
  
NDATA(3)=68        ! P=0.18 MPa  
  
NDATA(4)=65        ! P=0.22 MPa  
  
NDATA(5)=63        ! P=0.26 MPa  
  
NDATA(6)=61        ! P=0.30 MPa  
  
NDATA(7)=59        ! P=0.34 MPa  
  
NDATA(8)=58        ! P=0.38 MPa  
  
NDATA(9)=56        ! P=0.42 MPa  
  
NDATA(10)=55      ! P=0.46 MPa  
  
NDATA(11)=54      ! P=0.5 MPa  
  
NDATA(12)=51      ! P=0.6 MPa  
  
NDATA(13)=48      ! P=0.7 MPa  
  
NDATA(14)=46      ! P=0.8 MPa  
  
NDATA(15)=44      ! P=0.9 MPa
```

NDATA(16)=42 ! P=1.0 MPa

NDATA(17)=38 ! P=1.2 MPa

NDATA(18)=35 ! P=1.4 MPa

NDATA(19)=33 ! P=1.6 MPa

NDATA(20)=30 ! P=1.8 MPa

NDATA(21)=28 ! P=2.0 MPa

NDATA(22)=26 ! P=2.2 MPa

NDATA(23)=24 ! P=2.4 MPa

NDATA(24)=22 ! P=2.6 MPa

NDATA(25)=20 ! P=2.8 MPa

NDATA(26)=18 ! P=3.0 MPa

P(1)=100.

P(2)=140.

P(3)=180.

P(4)=220.

P(5)=260.

P(6)=300.

P(7)=340.

P(8)=380.

P(9)=420.

P(10)=460.

P(11)=500.

P(12)=600.

P(13)=700.

P(14)=800.

P(15)=900.

P(16)=1000.

P(17)=1200.

P(18)=1400.

P(19)=1600.

P(20)=1800.

P(21)=2000.

P(22)=2200.

P(23)=2400.

P(24)=2600.

P(25)=2800.

P(26)=3000.

OPEN(UNIT=19,FILE='r134a\_sat\_visc\_P.txt',STATUS='UNKNOWN')

OPEN(UNIT=20,FILE='r134a\_sat.txt',STATUS='UNKNOWN')

OPEN(UNIT=21,FILE='p0100.txt',STATUS='UNKNOWN')

OPEN(UNIT=22,FILE='p0140.txt',STATUS='UNKNOWN')

OPEN(UNIT=23,FILE='p0180.txt',STATUS='UNKNOWN')

OPEN(UNIT=24,FILE='p0220.txt',STATUS='UNKNOWN')

OPEN(UNIT=25,FILE='p0260.txt',STATUS='UNKNOWN')

OPEN(UNIT=26,FILE='p0300.txt',STATUS='UNKNOWN')

OPEN(UNIT=27,FILE='p0340.txt',STATUS='UNKNOWN')

OPEN(UNIT=28,FILE='p0380.txt',STATUS='UNKNOWN')

OPEN(UNIT=29,FILE='p0420.txt',STATUS='UNKNOWN')

OPEN(UNIT=30,FILE='p0460.txt',STATUS='UNKNOWN')

OPEN(UNIT=31,FILE='p0500.txt',STATUS='UNKNOWN')

```
OPEN(UNIT=32,FILE='p0600.txt',STATUS='UNKNOWN')

OPEN(UNIT=33,FILE='p0700.txt',STATUS='UNKNOWN')

OPEN(UNIT=34,FILE='p0800.txt',STATUS='UNKNOWN')

OPEN(UNIT=35,FILE='p0900.txt',STATUS='UNKNOWN')

OPEN(UNIT=36,FILE='p1000.txt',STATUS='UNKNOWN')

OPEN(UNIT=37,FILE='p1200.txt',STATUS='UNKNOWN')

OPEN(UNIT=38,FILE='p1400.txt',STATUS='UNKNOWN')

OPEN(UNIT=39,FILE='p1600.txt',STATUS='UNKNOWN')

OPEN(UNIT=40,FILE='p1800.txt',STATUS='UNKNOWN')

OPEN(UNIT=41,FILE='p2000.txt',STATUS='UNKNOWN')

OPEN(UNIT=42,FILE='p2200.txt',STATUS='UNKNOWN')

OPEN(UNIT=43,FILE='p2400.txt',STATUS='UNKNOWN')

OPEN(UNIT=44,FILE='p2600.txt',STATUS='UNKNOWN')

OPEN(UNIT=45,FILE='p2800.txt',STATUS='UNKNOWN')

OPEN(UNIT=46,FILE='p3000.txt',STATUS='UNKNOWN')

DO I=1,NSATVISCDATA

  READ(19,*) PSATVISC(I),VISCF(I),VISCG(I)

ENDDO

DO I=1,NSATDATA

  READ(20,*) TSAT(I),PSAT(I),VF(I),VG(I),UF,UG,HF(I),HG(I),SF(I),SG(I)

ENDDO

DO I=1,26

  IFILE=20+I

  DO J=1,NDATA(I)

    READ(IFILE,*) T(I,J),V(I,J),H(I,J),S(I,J)
```

```

ENDDO

ENDDO

DO I=20,46

    CLOSE(UNIT=I)

ENDDO

END SUBROUTINE

SUBROUTINE PROPSAT_T(TSAT0,PSAT0,VF0,VG0,HF0,HG0,SF0,SG0)

IMPLICIT REAL*8(A-H,M,O-Z)

COMMON /BLK_SUPERHEATED/ P(26),T(26,80),V(26,80),H(26,80),S(26,80)

COMMON /BLK_SATURATED/
TSAT(71),PSAT(71),VF(71),VG(71),HF(71),HG(71),SF(71),SG(71)

! PROPERTIES FOR SUPERHEATED R134A

IF(TSAT0.LT.-40.) THEN

    WRITE(6,*) 'OUT OF RANGE: SAT. TEMP. LESS THAN -40 degC'

    STOP

ELSEIF(TSAT0.GT.120.) THEN

    WRITE(6,*) 'OUT OF RANGE: SAT. TEMP. GREATER THAN 120 degC'

    STOP

ELSE

    IT=INT((TSAT0+40.)/2.)+1

ENDIF

ITP1=IT+1

RT=(TSAT0-TSAT(IT))/2.

RTM1=1.-RT

PSAT0=PSAT(IT)*RTM1+PSAT(ITP1)*RT

VF0=VF(IT)*RTM1+VF(ITP1)*RT

```



```
VG0=VG(IT)*RTM1+VG(ITP1)*RT
HF0=HF(IT)*RTM1+HF(ITP1)*RT
HG0=HG(IT)*RTM1+HG(ITP1)*RT
SF0=SF(IT)*RTM1+SF(ITP1)*RT
SG0=SG(IT)*RTM1+SG(ITP1)*RT

RETURN

END

SUBROUTINE PROPSAT_P(PSAT0,TSAT0,VF0,VG0,HF0,HG0,SF0,SG0)
IMPLICIT REAL *8(A-H,M,O-Z)

COMMON /BLK_SATURATED/
TSAT(71),PSAT(71),VF(71),VG(71),HF(71),HG(71),SF(71),SG(71)

! PROPERTIES OF SATURATED R134A FOR GIVEN PRESSURE PSAT0

IF(PSAT0.LT.51.209) THEN

    WRITE(6,*) 'OUT OF RANGE: SAT. PRESSURE LESS THAN 51.209 kPa'

    STOP

ELSEIF(PSAT0.GT.3972.4) THEN

    WRITE(6,*) 'OUT OF RANGE: SAT. PRESSURE GREATER THAN 3972.4 kPa'

    STOP

ENDIF

I=50

IF(PSAT0.GT.PSAT(I)) THEN

20 CONTINUE

    I=I+1

    IF(PSAT(I).LT.PSAT0) GOTO 20

    IT=I-1
```

```
ELSE

30 CONTINUE

  I=I-1

  IF(PSAT(I).GT.PSAT0) GOTO 30

  IT=IENDIF

ITP1=IT+1

RP=(PSAT0-PSAT(IT))/(PSAT(ITP1)-PSAT(IT))

RPM1=1.-RP

TSAT0=TSAT(IT)*RPM1+TSAT(ITP1)*RP

VF0=VF(IT)*RPM1+VF(ITP1)*RP

VG0=VG(IT)*RPM1+VG(ITP1)*RP

HF0=HF(IT)*RPM1+HF(ITP1)*RP

HG0=HG(IT)*RPM1+HG(ITP1)*RP

SF0=SF(IT)*RPM1+SF(ITP1)*RP

SG0=SG(IT)*RPM1+SG(ITP1)*RP

ENDSUBROUTINE

SUBROUTINE PROPSATVISC(PSAT0,VISCF0,VISCG0)

IMPLICIT REAL *8(A-H,M,O-Z)

COMMON /BLK_SATVISC/ PSATVISC(30),VISCF(30),VISCG(30)

! DYNAMIC VISCOSITY OF SATURATED R134A FOR GIVEN PRESSURE

IF(PSAT0.LT.0.1) THEN

  WRITE(6,*) 'OUT OF RANGE: SAT. PRESSURE LESS THAN 100 KPA'

  STOP

ELSEIF(PSAT0.GT.3000.) THEN

  WRITE(6,*) 'OUT OF RANGE: SAT. PRESSURE GREATER THAN 3000 KPA'
```

```
STOP

ELSE

  I=INT(PSAT0/100.)+1

ENDIF

IP1=I+1

RP=(PSAT0-PSATVISC(I))/100.

RPM1=1.-RP

VISCF0=VISCF(I)*RPM1+VISCF(IP1)*RP

VISCG0=VISCG(I)*RPM1+VISCG(IP1)*RP

ENDSUBROUTINE

SUBROUTINE SURFACETENSION(T,SIG)

IMPLICIT REAL*8(A-H,M,O-Z)

! SURFACE TENSION OF SATURATED LIQUID AS A FUNCTION OF TEMPERATURE

! T [degC]

! SIG [N/m]

SIG=((9.5997D-10*T+1.7737D-07)*T-1.4476D-04)*T+1.1564D-02

ENDSUBROUTINE
```